

A STRUCTURAL-METAMORPHIC  
AND GEOCHEMICAL STUDY OF  
THE HUNT RIVER  
SUPRACRUSTAL BELT, NAIN  
PROVINCE, LABRADOR

CENTRE FOR NEWFOUNDLAND STUDIES

**TOTAL OF 10 PAGES ONLY  
MAY BE XEROXED**

(Without Author's Permission)

CONRAD WAYNE JESSEAU

33768



National Library of Canada

Cataloguing Branch  
Canadian Theses Division

Ottawa, Canada  
K1A 0N4

Bibliothèque nationale du Canada

Direction du catalogage  
Division des thèses canadiennes

## NOTICE

The quality of this microfiche is heavily dependent upon the quality of the original thesis submitted for microfilming. Every effort has been made to ensure the highest quality of reproduction possible.

If pages are missing, contact the university which granted the degree.

Some pages may have indistinct print especially if the original pages were typed with a poor typewriter ribbon or if the university sent us a poor photocopy.

Previously copyrighted materials (journal articles, published tests, etc.) are not filmed.

Reproduction in full or in part of this film is governed by the Canadian Copyright Act, R.S.C. 1970, c. C-30. Please read the authorization forms which accompany this thesis.

THIS DISSERTATION  
HAS BEEN MICROFILMED  
EXACTLY AS RECEIVED

## AVIS

La qualité de cette microfiche dépend grandement de la qualité de la thèse soumise au microfilmage. Nous avons tout fait pour assurer une qualité supérieure de reproduction.

S'il manque des pages, veuillez communiquer avec l'université qui a conféré le grade.

La qualité d'impression de certaines pages peut laisser à désirer, surtout si les pages originales ont été dactylographiées à l'aide d'un ruban usé ou si l'université nous a fait parvenir une photocopie de mauvaise qualité.

Les documents qui font déjà l'objet d'un droit d'auteur (articles de revue, examens publiés, etc.) ne sont pas microfilmés.

La reproduction, même partielle, de ce microfilm est soumise à la Loi canadienne sur le droit d'auteur, SRC 1970, c. C-30. Veuillez prendre connaissance des formules d'autorisation qui accompagnent cette thèse.

LA THÈSE A ÉTÉ  
MICROFILMÉE TELLE QUE  
NOUS L'AVONS REÇUE

A STRUCTURAL-METAMORPHIC AND GEOCHEMICAL STUDY OF THE  
HUNT RIVER SUPRACRUSTAL BELT, MAIN PROVINCE, LABRADOR

by



Conrad Wayne Jesseau, B.Sc. (Hon.), B.Ed.

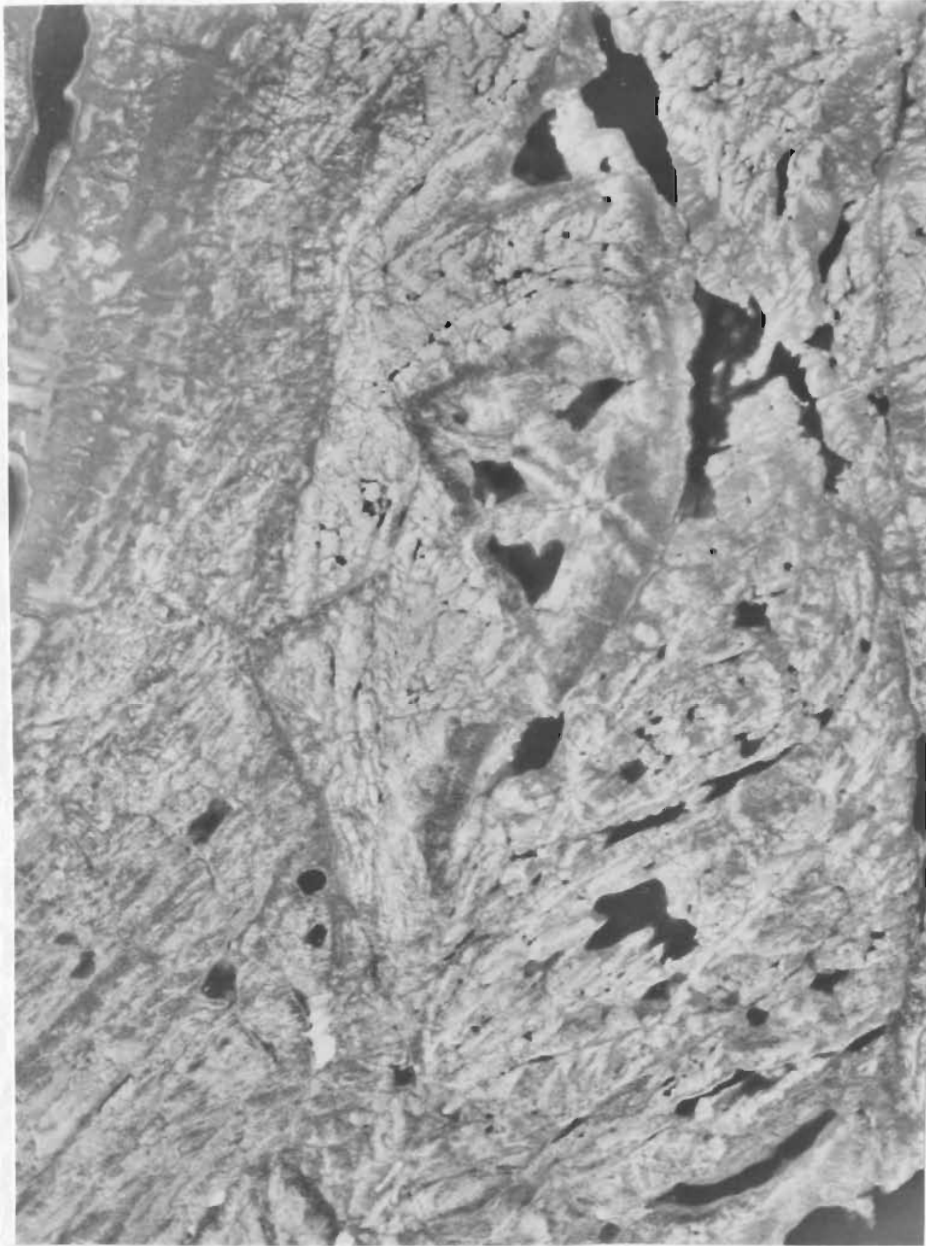
A Thesis submitted in partial fulfillment  
of the requirements for the degree of  
Master of Science

Department of Geology  
Memorial University of Newfoundland

June 1976

St. John's

Newfoundland



Frontispiece: Aerial photograph of the northern half  
of the Hunt River amphibolite belt.



Frontispiece: Aerial photograph of the northern half of the Hunt River amphibolite belt.

ABSTRACT

The southern Nain Province is characterized by several north-easterly trending supracrustal belts, Archean in age, which are infolded into a complex of polygenetic quartzofeldspathic gneisses. This thesis describes a petrological, geochemical and structural-metamorphic study of one of these belts, the Hunt River Belt, a predominantly mafic supracrustal sequence.

The Hunt River Belt consists of a series of amphibolite schists (meta-volcanics), ultramafic lenses, and minor meta-sediments. The chemistry of the meta-volcanics displays close similarities to tholeiites found in the lowermost cycles of Archean greenstone belts. The ultramafics, containing preserved igneous textures, are considered to have intruded early into a developing volcanic pile.

The thesis area has undergone a complex history of structural and igneous development. The earliest recognized widespread event ( $D_1$ ) produced a strong tectonic fabric in the Hunt River Belt, and produced banded gneisses in the quartzofeldspathic rocks through thrusting and transposition.  $D_2$  reflects a period of pure shear deformation and overprinted the area with a pronounced planar fabric.  $D_3$  represents a period of tectonically active crustal uplift associated with magma upwelling and gave rise to heterogeneous deformation.  $D_4$ , a period of shallow level upright open folding, closed out the periods of folding and was followed by the development of megascopic faulting and diabase dyke intrusion.

Each of the deformational episodes was accompanied by periods of plutonic activity which led to the development of distinct gneiss types.

Mineralogical and microstructural evidence in the amphibolite schists and the quartzofeldspathic gneisses indicates that  $D_1$ ,  $D_2$  and  $D_3$  all occurred within the amphibolite facies of metamorphism.  $D_4$  and subsequent faulting occurred under greenschist facies conditions.

TABLE OF CONTENTS

ABSTRACT .....	i
CHAPTER 1 - INTRODUCTION .....	1
1.1 AIM AND SCOPE OF THESIS .....	2
1.2 LOCATION AND ACCESS .....	2
1.3 TOPOGRAPHY AND EXPOSURE .....	4
1.4 FIELD WORK .....	5
1.5 REGIONAL GEOLOGICAL SETTING AND PREVIOUS INVESTIGATIONS..	5
1.6 GENERAL GEOLOGY .....	9
1.7 ACKNOWLEDGMENTS .....	13
CHAPTER 2 - LITHOLOGY AND PETROLOGY .....	15
2.1 INTRODUCTION .....	16
2.1.1 Mineral Assemblages .....	16
2.1.2 Plagioclase Determinations .....	16
2.1.3 Fabrics .....	16
2.1.4 Scale .....	17
2.2 HUNT RIVER BELT .....	17
2.2.1 Meta-volcanics .....	19
2.2.1.1 Normal Amphibolite .....	20
2.2.1.2 Garnet-bearing Amphibolite .....	23
2.2.1.3 Diopside-bearing Amphibolite .....	25
2.2.2 Ultramafics .....	28
2.2.2.1 Hornblende Schist .....	29
2.2.2.2 Tremolite Schist .....	32
2.2.2.3 Serpentinite Schist .....	33

2.2.3	Meta-sediments .....	37
2.2.3.1	Pelitic Schist .....	38
2.2.3.2	Grey Schist .....	42
2.2.3.3	Rusty Zones .....	46
2.3	QUARTZOFELDSPATHIC GNEISS COMPLEX .....	49
2.3.1	Banded Gneiss .....	51
2.3.2	Homogeneous Gneiss .....	53
2.3.3	Mixed Gneiss .....	56
2.3.4	Agmatite .....	57
2.3.5	Anorthositic Gabbro .....	59
2.4	BORDER ZONE .....	61
2.4.1	Pink Muscovite Gneiss .....	62
2.4.2	Variable Quartzofeldspathic Gneiss .....	65
2.5	INTRUSIVES .....	68
2.5.1	Meta-quartz-monzodiorite .....	68
2.5.2	Granodiorite .....	70
2.5.3	Mafic Dykes .....	72
2.5.3.1	Deformed Dykes .....	72
2.5.3.2	Post-tectonic Dykes .....	73
2.5.4	Pegmatites .....	78
CHAPTER 3 - GEOCHEMISTRY .....		80
3.1	INTRODUCTION .....	81
3.1.1	Analytical Methods .....	81
3.2	HUNT RIVER BELT .....	82
3.2.1	Ultramafics .....	84
3.2.1.1	Serpentinite Schist .....	84

3.2.2	Meta-volcanics (amphibolites)	93
3.2.2.1	Chemical Control on Mineralogy	94
3.2.2.2	Major Element Chemistry	97
3.2.2.3	Trace Element Chemistry	100
3.2.2.4	Tectonic Setting	104
3.2.2.5	Discussion	105
3.2.3	Meta-sediments	108
3.2.3.1	Pelitic Schist	108
3.2.3.2	Grey Schist	112
3.3	BORDER ZONE	113
3.4	QUARTZOFELDSPATHIC GNEISS COMPLEX	115
3.4.1	Chemical Character of the Banded, Homogeneous and Mixed Gneisses	118
3.4.2	Geochemical Interpretation of Polygenetic gneisses	120
3.4.3	Significance of Crustal Fractionation Processes	123
3.5	INTRUSIVES	124
3.5.1	Granites (s.l.)	124
3.5.2	Post Tectonic Diabase Dykes	128
CHAPTER 4	STRUCTURE AND METAMORPHISM	130
4.1	INTRODUCTION	131
4.1.1	Nomenclature	133
4.1.1.1	Deformation	133
4.1.1.2	Fold Geometry	134
4.1.2	Outline of the Structural History	134
4.1.3	Metamorphism	137

4.2	PRE - D <sub>1</sub> DEFORMATION .....	138
4.2.1	Pre - D <sub>1</sub> Metamorphism .....	141
4.3	D <sub>1</sub> DEFORMATION .....	143
4.3.1	Folds .....	143
4.3.2	Homogeneous Gneiss .....	146
4.3.3	D <sub>1</sub> Metamorphism .....	147
4.4	D <sub>2</sub> DEFORMATION .....	149
4.4.1	Folds .....	149
4.4.2	Discordant Veins .....	152
4.4.3	Boudinage .....	152
4.4.4	Quartz-monzodiorite .....	155
4.4.5	Interpretation of the D <sub>2</sub> Deformation .....	155
4.4.6	D <sub>2</sub> Metamorphism .....	156
4.5	DISTINCTION BETWEEN D <sub>3</sub> AND D <sub>4</sub> MEGASCOPIC FOLDS .....	157
4.6	D <sub>3</sub> DEFORMATION .....	159
4.6.1	Megascopic Folds .....	159
4.6.2	Mesoscopic F <sub>3</sub> Folds .....	160
4.6.3	Granodiorite .....	163
4.6.4	Heterogeneous Nature of D <sub>3</sub> Deformation .....	163
4.6.5	D <sub>3</sub> Metamorphism .....	167
4.7	D <sub>4</sub> DEFORMATION .....	170
4.7.1	Megascopic Folds .....	170
4.7.2	Mesoscopic Structures .....	172
4.8	FAULTING AND MAFIC DYKE EMPLACEMENT .....	172
4.8.1	NW-SE Trending Faults .....	174
4.8.2	NE-SW Trending Faults .....	176

4.9 POST-D <sub>3</sub> METAMORPHISM .....	176
CHAPTER 5 - DISCUSSION AND SUMMARY .....	180
5.1 DISCUSSION .....	181
5.2 SUMMARY .....	188
REFERENCES .....	192

LIST OF FIGURES

FIGURES	PAGE
1.1 Location map showing the geological setting of the Nain Province in relation to the North Atlantic Craton.....	3
1.2 Solid geology map of the Hunt River Belt.....	8
2.1 Typical outcrop weathered surface of normal amphibolite.....	21
2.2 Photomicrograph of normal amphibolite in plane light.....	22
2.3 Thin layer of garnet-bearing amphibolite in an outcrop of normal amphibolite.....	26
2.4 Photomicrograph of garnet-bearing amphibolite from the southern area in plane light.....	26
2.5 Outcrop of small lense of hornblende schist from southern area.....	30
2.6 Outcrop surface of finely crenulated tremolite schist from the northern area.....	30
2.7 Serpentinite schist showing elongate olivine texture.....	35
2.8 Serpentinite schist showing etched weathered surface of elongate olivine texture.....	35
2.9 Serpentinite schist showing a completely random network of very coarse olivine crystals.....	37
2.10 Photomicrograph of pelitic schist showing the disequilibrium reaction between staurolite and cordierite.....	43
2.11 Photomicrograph of pelitic schist showing sillimanite needles growing at a garnet-cordierite contact.....	43
2.12 Photograph of grey schist.....	45

2.13	Rounded white pyrite crystals growing in a matrix of grey, massive pyrrhotite.....	48
2.14	Contact between the Hunt River Belt and the pink muscovite gneiss in the northern part of the thesis area..	63
2.15	Contact between the variable quartzofeldspathic gneiss and the meta-volcanic amphibolite of the Hunt River Belt..	66
2.16	Glacial polished surface of quartz-monzodiorite showing the anastomosing planar fabric.....	69
2.17	Exposed outcrop of weakly-banded hornblende-bearing gneiss in the banded gneiss terrain.....	74
2.18	Photomicrograph of post tectonic diabase dyke showing fresh ophitic texture.....	75
2.19	Diabase dyke - quartzofeldspathic gneiss contact showing remobilized zone.....	75
2.20	Diabase dyke showing a sheared contact with a foliated amphibolite.....	77
2.21	Post tectonic diabase dyke exhibiting hexagonal columnar jointing.....	77
3.0	Localities of geochemical samples.....	83a
3.1	Major element variations vs. $SiO_2$ in wt.% for the mafic and ultramafic rocks from the Hunt River Belt.....	86
3.2	$MgO - CaO - Al_2O_3$ ternary diagram comparing Hunt River serpentinite schist to spinifex-bearing ultramafics from Canada, Australia and South Africa.....	88
3.3A	$Na_2 + K_2O - SiO_2$ variation diagram for the Hunt River Belt amphibolites.....	99
3.3B	AFM ternary diagram for the Hunt River Belt amphibolites..	99

3.4	Trace element variations vs. $\text{SiO}_2$ in wt% for the mafic and ultramafic rocks from the Hunt River Belt.....	101
3.5	Ti:Zr variation diagram of the Hunt River Belt amphibolite.	106
3.6	Cr:Ni variation diagram comparing meta-volcanic and met-sedimentary schists from the Hunt River Belt to rocks from Saglek, Labrador.....	111
3.7A	Normative or - ab - an for quartzofeldspathic gneisses.....	119
3.7B	Normative or - ab - an for Nuk gneisses, Godthab district West Greenland.....	119
3.8	Normative qtz -or - plag for quartzofeldspathic gneisses...	121
3.9	AFM ternary diagram of the quartzofeldspathic gneisses.....	122
3.10	Log : log plot of K and Rb for quartzofeldspathic gneisses.	126
4.1	Structural geology map of the Hunt River Belt.....	136
4.2	Typical gneissic banding in banded gneiss terrain.....	140
4.3	Detail of an $F_1$ intrafolial fold.....	145
4.4	Steeply plunging $L_1$ lineations defined by elongation of feldspars in a banded gneiss.....	145
4.5	Isoclinal Z-shaped $F_2$ fold in banded gneiss.....	150
4.6	Isoclinal $F_2$ fold in amphibolite from the Hunt River Belt..	151
4.7	$F_2$ parasitic fold in banded gneiss.....	151
4.8	Thin quartz veins isoclinally folded during $D_2$ .....	153
4.9	Discordant pegmatite vein ptlygmatically folded during $D_2$ ...	153
4.10	Isolated boudinaged remnant of pegmatite vein.....	154
4.11	Schematic of megascopic synform-antiform couples showing the geometrical relationship of small scale folds and lineations.....	158

4.12	Stereographic plot of structural elements of the megascopic synform-antiform couple in the south.....	161
4.13	Tight mesoscopic folds occurring in an ultramafic lense in the $F_3$ megascopic synform.....	162
4.14	Broad open mesoscopic fold in an ultramafic lense in the $F_3$ megascopic antiform.....	162
4.15	Outcrop of agmatite in banded gneiss terrain.....	166
4.16	Outcrop of agmatite in amphibolite unit of the Hunt River Belt.....	166
4.17	Stereographic plot of structural elements of the megascopic synform-antiform in the north.....	171
4.18	Mesoscopic $F_4$ fold on eastern limb of the megascopic $F_4$ antiform in the north.....	173
4.19	Small scale elliptical dome and basin interference patterns developed in the nose of the $F_4$ antiform.....	173
4.20	Photograph of exposure of large fault which cuts $F_3$ synform in the northern part of the Hunt River Belt.....	175
4.21	Schematic of major fault orientations with their relative sense of displacement.....	177
5.1	Schematic cross-section through the North Atlantic Craton..	184
5.2	Diagrammatic representation of the distribution of forces resulting from the crustal wedge attaining isostatic equilibrium.....	186

LIST OF TABLES

TABLES	PAGE
3.1 Precision and accuracy of analytical data.....	83
3.2 Chemical analyses and C.I.P.W. Norms of the ultramafic rocks from the Hunt River Belt.....	85
3.3 Microprobe analysis of olivine from ultramafic rock.....	90
3.4 Comparison of $\text{CaO}_{(\text{host rock})} / \text{CaO}_{(\text{olivine})}$ ratios.....	91
3.5 Chemical analyses and C.I.P.W. Norms of the normal amphibolite from the Hunt River Belt.....	95
3.6 Chemical analyses and C.I.P.W. Norms of garnet-bearing amphibolite and diopside-bearing amphibolite from the Hunt River Belt.....	96
3.7 Trace element comparison of Labrador meta-volcanics with modern volcanic environments and other Archean terrains...	103
3.8 Chemical analyses and C.I.P.W. Norms of the meta-sedimentary schists from the Hunt River Belt.....	109
3.9 Chemical analyses and C.I.P.W. Norms of the pink muscovite gneiss and the variable quartzofeldspathic gneiss from the border zone.....	114
3.10 Chemical analyses and C.I.P.W. Norms of the banded and homogeneous gneiss from the quartzofeldspathic gneiss complex.....	116
3.11 Chemical analyses and C.I.P.W. Norms of the amphibolite and mixed gneisses of the quartzofeldspathic gneiss complex.....	117

3.12	A chemical comparison of granulite facies rocks and equivalent amphibolite facies rocks with average chemical values of the crust, the Canadian Shield and the Hunt River Belt gneisses.....	125
3.13	Chemical analyses and C.I.P.W. Norms of the intrusives...	127
4.1	Summary of the geological development of the Hunt River Belt and the surrounding gneiss terrain.....	135

#### MAPS

The following maps may be found in the pocket at the end of the thesis:

Figure 1.2 Solid geology of the Hunt River Belt.

Figure 4.1 Structural geology of the Hunt River Belt.

CHAPTER 1  
INTRODUCTION

## 1.1 AIM AND SCOPE OF THESIS

The aim of this thesis is to provide some insight into the hitherto relatively unknown Archean supracrustal rocks of the Nain Province in the Canadian Shield. A comprehensive geological investigation was carried out on a small ( $\leq 4$  km X 20 km), predominantly mafic supracrustal sequence (the Hunt River Belt) and the surrounding quartzofeldspathic gneiss complex. The Hunt River Belt is located in the southern part of the Nain Province, inland from Hopedale, just south of the Hunt River. This thesis is concerned with the field relations, petrology, geochemistry, structure and metamorphism of the rocks, with emphasis on the Hunt River Belt.

The data is discussed in terms of the crustal evolution of the southern part of the Nain Province. Comparisons are made with geological studies of other high-grade Archean gneiss terrains, and certain aspects (geochemistry, for example) are compared and contrasted with low-grade Archean greenstone belts.

The thesis concludes with a discussion on the relevance of the geology of the thesis area to present day theories for the evolution of the earth's early crust.

## 1.2 LOCATION AND ACCESS

The thesis area, located 30 km west-southwest of Hopedale in eastern Labrador, (latitude  $55^{\circ}19'$ ; longitude  $60^{\circ}45'$ ), covers an area of approximately 100 square km (Figure 1.1). There are no navigable waterways from the coast into the area, and channels between lakes are generally very shallow rocky creeks. However, the numerous small lakes

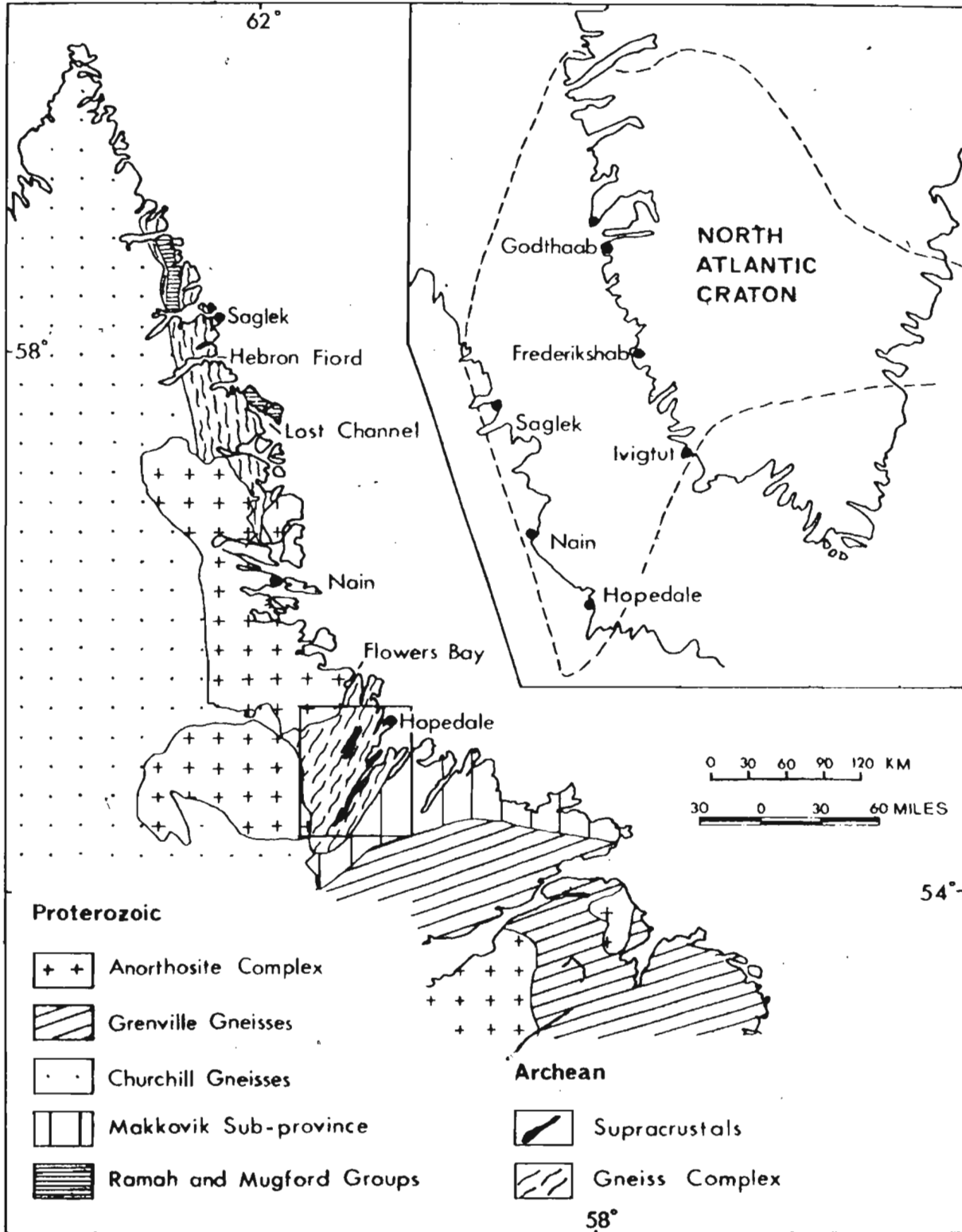


FIGURE 1.1: Location map showing the geological setting of the Main Province in relation to the North Atlantic Craton. Geological map of Labrador after Greene, 1974. Insert of North Atlantic Craton after Bridgwater et al., 1973c.

allow good access by small aircraft.

Although there are several coastal communities such as Hopedale, Davis Inlet and Makkovik much closer to the study area, Goose Bay, 224 km to the south is the most reliable logistical support centre.

### 1.3 TOPOGRAPHY AND EXPOSURE

The highest elevation in the map area is 400 m above sea level. The relief, ranging from 100 m to 200 m, roughly outlines the north-northeasterly trending ridges and valleys. The topographic trends are parallel to and are greatly influenced by the regional structural trends of the underlying bedrock.

The Hunt River Belt forms a topographic 'high' and is bordered to the west by a flat, low-lying valley about 7 km wide. Bedrock exposure throughout most of the thesis area averages approximately 50 percent.

Forest vegetation occurs in some of the valleys which are bottomed by streams and elongate lakes, however, for the most part the land is quite barren with minor low-lying bushes and moss. In places the bedrock is covered by a coarse boulder till. The extreme degree of sorting and the coarse nature of the till is apparently the result of strong aeolian action.

Outcrop surfaces have generally been rounded by glaciation and are commonly lichen covered. There are numerous creek beds which do, however, provide fresh, lichen-free surfaces.

#### 1.4 FIELD WORK

Due to unforeseen logistic delays only 7 weeks were spent in the field during the summer of 1973. On July 11 the field party was flown into Hab Lake where the main base camp was established. The northern half of the area was covered by making use of backpacking fly camps. Special light-weight equipment and freeze-dried food allowed regional traverses lasting 2 to 4 days. On August 15 a traverse was made to the southern end of Snake Lake where a second base camp was established. Extra equipment had been previously cached there by aircraft. The field party left for Goose Bay on September 2.

The weather was very good for most of the field season with only 8 days lost to inclement conditions. Throughout the last 2 weeks of August freezing temperatures at night and much rain and intermittent hail during the day was experienced.

Topographic map coverage of the thesis area was at a scale of 1:250,000 (13N Edition 1 MCE Series A501). Mapping was carried out at a scale of 1:25,000 using enlarged 1:50,000 aerial photographs. The airphotos were purchased from the NAPL Reproduction Centre, Dept. of Energy, Mines and Resources, Ottawa. Flight line numbers A20576-11, A21899-20, A21899-21, and A21901-243 gave complete coverage of the area.

#### 1.5 REGIONAL GEOLOGICAL SETTING AND PREVIOUS INVESTIGATIONS

The map area lies within the Nain Province of the Canadian Shield (Stockwell, 1963, 1964; Taylor, 1971), a relatively thin wedge of Archean gneisses and migmatites which parallels the Labrador seaboard. The Nain Province is bordered to the west and north by

the Churchill Province made up of reworked Archean gneisses and deformed Proterozoic sediments and volcanics. To the south the Nain Province is bordered by the Makkovik Sub-Province (Taylor, 1971) which is also composed of reworked basement Archean gneisses and Proterozoic sedimentary-volcanic cover rocks.

In a broader geological context, the Nain Province is considered to form the westernmost extension of the North Atlantic Craton (Bridgwater et al., 1973c). This Archean block extends through south central Greenland and includes the Lewisian rocks of north-western Scotland. The Churchill Province and the Makkovik Sub-Province are generally equated to the Nagssugtoqidian and Ketilidian mobile belts in Greenland (Bridgwater et al., 1973b).

The south-western extension of the North Atlantic Craton in eastern Labrador is dominated by three separate north-easterly trending linear belts of schistose mafic and ultramafic rocks and meta-sediments infolded within highly deformed quartzofeldspathic banded to migmatitic gneisses. Relatively little detailed mapping has been carried out in this part of Labrador. The two most northerly belts were visited by F.C. Taylor during 1:250,000 reconnaissance mapping of north-eastern Quebec and northern Labrador in 1971. Taylor (1972, p.2) describes the middle belt as consisting "chiefly of limy argillite and siltstone with small amounts of amphibolite. In places the banding can be determined to be primary bedding", while the northernmost belt consists of "amphibolite and smaller amounts of meta-sedimentary rocks ... primary bedding is locally discernable ... dolomite is present in the central part." The southernmost belt, the Ugjoktok Bay supracrustals, is

described by Sutton (1972, p.1691) as "complexly deformed and metamorphosed hornblende schist and associated mica schists and limestones."

The quartzofeldspathic gneisses in Labrador also lack extensive detailed investigation. Kranck (1953), in his mapping of the seaboard of Labrador from Hopedale to points south, coined the term "Hopedale Gneiss" for the basement gneisses north of Kaipokok Bay. According to Kranck (1953, p.33), "The main constituent of the bedrock is a light grey, comparatively homogeneous biotite gneiss, with slightly lenticular structure, interbedded with schlierly of banded gneiss consisting of alternating basic hornblende and granitic layers. Both are interwoven by pegmatitic and aplitic material."

Taylor (1971) recognized a great diversity of gneissic rock types and uses the term "migmatite" as an all-encompassing description at the regional scale of mapping.

Sutton (1972, p.1679) describes the gneiss from the western shore of Kaipokok Bay as a "heterogeneous unit of banded gneiss and migmatite with associated acid intrusions." He attributes the heterogeneity to both original lithologic variation and to heterogeneous polydeformation, and introduces the term "Hopedale Complex" to reflect the marked heterogeneity.

The equivalent Archean terrain which outcrops along the southwestern coast of Greenland has by comparison received fairly extensive geological investigation. Supracrustal rocks of at least three different ages have been recognized (Bridgwater et al., 1973a). These include the 3.75 by rocks of the Isua Region (Moorbath et al., 1973) the Malene

**LEGEND**

**Intrusives**

-  DIABASE DYKES
-  GRANODIORITE
-  PEGMATITE
-  META-QUARTZMONZODIORITE

**Hunt River Belt**

-  AMPHIBOLITE SCHIST
-  SERPENTINITE SCHIST
-  HORNBLENDITE SCHIST
-  TREMOLITE SCHIST
-  RUSTY ZONES
-  PELITIC SCHIST
-  GREY SCHIST

**Border Zone**

-  VARIABLE QUARTZOFELDSPATHIC GNEISS
-  PINK MUSCOVITE GNEISS

**Quartzofeldspathic Gneiss Complex**

-  AGMATITE
-  HOMOGENEOUS GNEISS
-  MIXED GNEISS
-  BANDED GNEISS
-  ANORTHOSITIC GABBRO
-  AMPHIBOLITE GNEISS

**Key**

-  LIMIT OF OUTCROP
-  SWAMPY LOWLANDS
-  GLACIAL DRIFT
-  FAULT
-  GEOLOGICAL BOUNDARY (defined, approximate, transitional)

**Index Map**

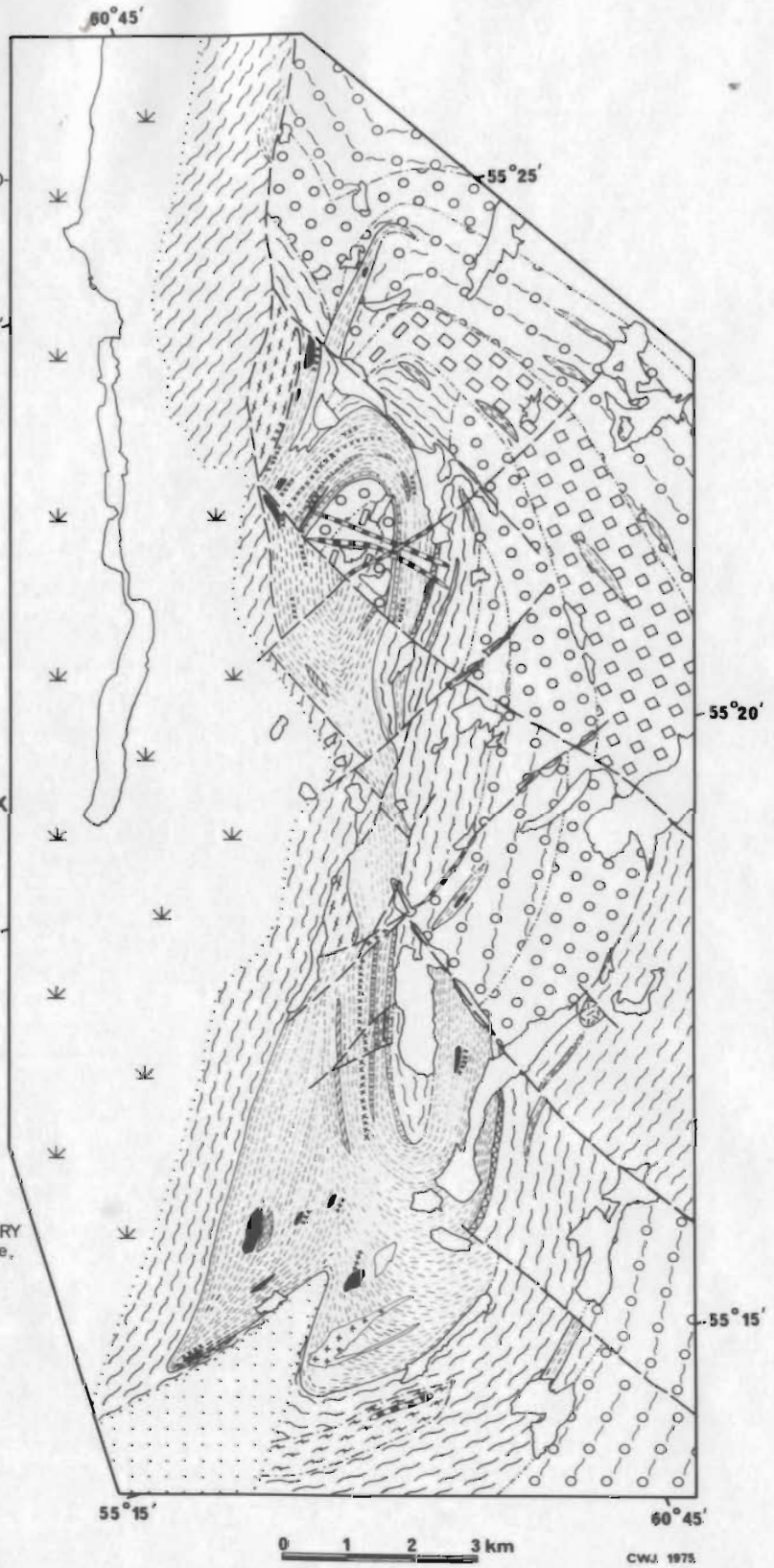
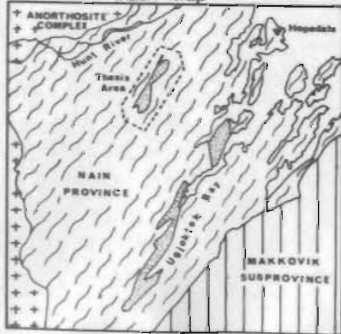


Figure 1.2: Solid Geology of the Hunt River Amphibolite Belt

supracrustals (McGregor, 1973), and the Tartoq Group in the south (Higgins, 1968; Higgins and Bondsen, 1966). Supracrustal rocks from the southern Nain Province (the Uqjoktok supracrustals) have been equated with the Tartoq Group (Sutton et al., 1972; Sutton, 1972).

## 1.6 GENERAL GEOLOGY

The thesis area is made up of two rock complexes; the Hunt River Belt, and a sequence of quartzofeldspathic gneisses (Figure 1.2). The Hunt River Belt crops out as a NNE trending linear sequence up to 4 km wide and 20 km long. It may be subdivided geographically into two areas; a northern area comprising a large antiform-synform couple plunging to the northeast, and a southern area comprising a large antiform-synform couple plunging to the southwest. The sequence is predominantly composed of mafic and ultramafic rocks. Three distinct groups of rocks have been recognized including meta-volcanics, meta-ultramafics and meta-sediments.

The meta-volcanics are now represented by amphibolites including garnet amphibolite, pyroxene amphibolite and thinly banded felsic-enriched varieties. They are chiefly fine- to medium-grained, massive to schistose and commonly display compositional variation (involving hornblende, plagioclase, garnet, pyroxene and quartz). This mineralogical layering varies from discontinuous bands less than 1 cm in thickness to major mappable units tens of metres in thickness.

Meta-ultramafic rocks include units ( $\leq 4$  km long) of hornblende schist and tremolite schist, and a series of lenses ( $\leq 1$  km long) of serpentinite. The hornblende and tremolite schists

crop out as fairly extensive conformable units, although at one locality the hornblendite was observed to be distinctly discordant to the adjacent amphibolite schist. The serpentinite occurs as distinct lenses and pods which have been transposed axial planar to late stage folds. In certain of the serpentinite lenses preserved harzburgitic patches retain coarse textures characterized by elongate olivine and interstitial enstatite. These textures may well represent igneous cumulate textures.

Minor meta-sediments crop out as a series of garnet-Stauroilite-cordierite-bearing pelitic schist, biotite-garnet-bearing rusty units and grey feldspar-biotite schist.

The garnetiferous and clinopyroxene-bearing amphibolites are chemically distinctive units. The garnetiferous amphibolite in particular shows anomalous trace element contents. Generally there are no transitional rock types between the basic volcanics and the ultramafics. The pelitic schist shows very similar nickel-chromium contents as the amphibolites, indicating a close spatial relationship in their formation.

The amphibolites from Labrador have been compared to other volcanics, and they correlate most favourably with basalts associated with ultramafics in the lower parts of volcanic cycles from Archean greenstone belts.

The Hunt River Belt is infolded into a complex of polygenetic quartzofeldspathic gneisses. A well-banded tonalitic gneiss is the most extensive gneiss type. The strong compositional banding developed during a period of intense deformation, which included reworking of the supracrustals. The mafic component of the banded gneiss varies in

scale from small semi-continuous alternating bands enriched in hornblende several centimetres thick, to relatively large amphibolite lenses up to 250 m across. The larger amphibolitic lenses, some with ultramafic pods, are regarded as schlieren of meta-volcanics related to the supracrustals. Intrafolial folds within the dominant gneissic banding provide evidence of an even earlier gneissic terrain. Rare zones of low intensity deformation within the banded gneiss expose a weakly-banded to homogeneous hornblende-bearing quartzofeldspathic gneiss containing deformed amphibolite pods which are clearly discordant to the gneissic foliation. Locally, these mafic pods closely resemble deformed dykes.

Homogeneous trondhjemitic to granitic gneiss forms a fairly extensive rock unit intrusive into the banded gneiss. A strong planar schistosity defined mainly by biotite is present throughout the homogeneous gneiss. Locally, a weakly developed gneissic banding is also discernable.

The mixed gneiss forms a transitional zone between the banded and the homogeneous gneisses. It is characterized by relatively well-banded tonalitic units and hornblende-biotite banded units which are intercalated with the banded and homogeneous gneisses on a scale of tens of metres.

The development of agmatite gneiss coincided with a major phase of folding. Large amounts of coarse pegmatitic leucosome were injected syntectonically and axial planar to megascopic folds. In Figure 1.2, the area of extensive leucosome emplacement is represented as a single, well-defined linear unit. However, the regional effects are widespread.

A small area of gabbroic anorthosit<sup>o</sup> was discovered south of the Hunt River Belt. The rock, composed of anorthite-rich plagioclase and hornblende, is strongly deformed and is conformable to the surrounding banded gneiss.

The contacts between the Hunt River Belt and the gneissic terrain are to a great extent fault bounded. Very coarse-grained pink pegmatites are commonly found in the fault zones. Elsewhere, the gneisses are separated from the Hunt River Belt by a rock unit approximately 5 m thick. It is variable in composition along strike, becoming enriched in potassium feldspar and pink in colour. In other places hornblende is present in sufficient amounts to form a well-banded pink gneissic rock. This unit may represent an intrusive rock emplaced along the margins of the Belt, but the highly variable nature of the unit makes its origin uncertain.

Igneous intrusions of several ages have been recognized, including small granitic plutons and plugs as well as ubiquitous pegmatitic and mafic dyke swarms. These igneous rocks range from highly foliated largely concordant bodies to undeformed post-tectonic intrusions.

The structural development of the area is polydeformational and heterogeneous. Major rock units show evidence of both flattening and intense rotational shearing. The regional intercalation of units is interpreted to be the result of thrusting accompanied by folding and transposition of layering parallel to the axial planes of the folds. Later stages of folding were accompanied by extensive syntectonic formation of granite resulting in the development of agmatite in the

gneisses. Late stage regional fold patterns are the salient structural features and strongly influence the outcrop pattern of the Hunt River Belt.

Mineral assemblages in the mafic and pelitic rock units indicate that at least medium to high grade amphibolite facies metamorphism was reached. Common mineral phases include:

1. biotite, garnet, staurolite, cordierite and sillimanite in pelitic and semi-pelitic schists,
2. blue-green hornblende, actinolite, cummingtonite, diopside, garnet, biotite and plagioclase ( $An_{35-45}$ ) in amphibolites,
3. olivine, anthophyllite, tremolite, hornblende, brucite, calcite and talc in ultramafics, and
4. quartz, plagioclase, microcline, biotite, muscovite, garnet and hornblende in the quartzofeldspathic gneisses.

Widespread partial retrogression to greenschist facies is present throughout the study area.

#### 1.7 ACKNOWLEDGMENTS

I am sincerely grateful to Dr. K.D. Collerson who suggested the project, provided encouragement and guidance throughout the study, and suggested valuable improvements to the manuscript. Financial assistance was provided by a Department of Regional and Economic Expansion grant from the Newfoundland Department of Mines and Energy to Dr. Collerson, and by National Research Council of Canada Grants A-3694 and A-8694. The School of Graduate Studies, Memorial University of Newfoundland also provided financial assistance.

I would also like to thank Mrs. G.R. Andrews for completing the major element chemistry of the serpentinite schists, Mr. J. Vahtra and Mr. D. Press for assistance with the X.R.F. analyses, Dr. C. Klein for providing microprobe analyses, Mr. W. Marsh for photographic help and Mr. T. Green for assistance in the field. Fellow graduate students shared an interest in the Labrador research and I am particularly grateful to Mr. Bruce Ryan for sound advice and stimulating discussions.

This work would not have been possible without the enthusiastic support and encouragement of my wife, Sharon, who also assisted in the geochemical analyses and drafting, and I am very grateful for her patient and excellent typing of the manuscript.

CHAPTER 2  
LITHOLOGY AND PETROLOGY

## 2.1 INTRODUCTION

### 2.1.1 Mineral Assemblages

Throughout this chapter the component minerals of a particular lithology are listed as 'mineral assemblages'. The prerequisite for minerals belonging to a single mineral assemblage is that they are in physical contact with one another (Winkler, 1967). Following Chatterjee (1971), further restrictions on minerals in an assemblage include absence of reactions along contacts or alterations of individual minerals, and contemporaneous growth of minerals based on correlation of deformation and crystallization during polymetamorphism. This latter restriction is very important in polydeformed rocks, as it would be misleading to combine two minerals in a single assemblage based only on chemical criteria, if microstructural evidence clearly indicates that the two minerals are spatially unrelated.

### 2.1.2 Plagioclase Determinations

Plagioclase determinations were made following the Michel-Levy Method described by Moorhouse (1959). At least ten determinations were made in each thin section in order to make the anorthite content values of the plagioclases as accurate as possible.

### 2.1.3 Fabrics

Penetrative tectonic fabrics are classified as:

S-fabrics - those which define a planar surface such as a parallel alignment of platy micas,

L-fabrics - those which define a linear trend such as a linear parallel

alignment of acicular hornblende crystals, and L-S-fabrics - those which display components of both L-fabrics and S-fabrics which have formed during a single deformation. The formation of these fabrics is discussed following theories of homogeneous deformation originally proposed by Flinn (1962), and more recently as applied to practical field work by Watterson (1968).

#### 2.1.4 Scale

Throughout the chapter the structural elements are scaled according to the terminology suggested by Turner and Weiss (1963).

Microscopic scale covers bodies such as thin sections that can be conveniently studied with a microscope. In describing microscopic grain relationships the term 'microstructure' is used following the usage of Vernon (1968) and Collerson (1974). Descriptive microstructural terminology for the metamorphic rocks is that of Spry (1969).

Mesoscopic scale covers bodies that can be effectively examined in three dimensions by direct observation in the field.

Megascopic scale (this term is preferable to macroscopic used by Turner and Weiss, 1963) covers bodies too large to be examined directly in their entirety in the field.

## 2.2 HUNT RIVER BELT

The Hunt River Belt is a relatively thin, folded, tabular body, bounded on both sides by quartzofeldspathic gneisses. Its widest outcrop (approximately 4 km) occurs in the south (Figure 1.2).

The strike length of the Belt, when measured around major folds, is approximately 45 km. These measurements are in no way related to the original size of the Belt as it has been extensively modified by successive tectonic deformations of varying magnitudes.

There is considerable small scale lateral and vertical variation in mineralogy and texture within the Belt, yet it is remarkable that such a relatively slender rock unit retains a complex and consistent stratigraphy throughout most of its strike length. In the following discussion the individual lithologic units are described with emphasis placed on field relations, mineralogy and microstructural features.

In Chapter 1 the Hunt River Belt was referred to as a meta-volcanic supracrustal belt. It is appropriate at this time to define the terms "meta-volcanic" and "supracrustal" and to justify their usage here. The term supracrustal as defined by Windley *et al.* (1966, p.1) refers to "all forms of sedimentary and volcanic rocks which are sufficiently untransformed for them to be recognizable as such." In southwestern Greenland supracrustal rocks make up less than 20% of the Archean terrain (Bridgwater, 1970) yet linear supracrustal belts are widespread. The main occurrences are found at Isua (Keto and Allaart, 1975), Godthaab (McGregor, 1973), Fiskenaesset (Myers, 1973), Ravens Storo (Andersen and Friend, 1973), Frederikshabs Isblink (Dawes, 1970), Frederikshåb (Jensen, 1969) and Ivigtut (Higgins, 1968). All of these occurrences are considered to be meta-volcanic supracrustal rocks, even though primary structures are rarely preserved. In the Frederikshåbs Isblink area, for example, Dawes (1970) reports

that although it is likely that other amphibolites in the complex may represent meta-volcanic rocks, preserved primary volcanic structures in amphibolites are found in only one location (the northern nunatak 1340 m). It is the preserved volcanic structures occurring throughout southwestern Greenland which indicate that the amphibolites are meta-volcanic rather than meta-sedimentary in origin (Blank, 1972).

In Labrador large amphibolitic units found at Saglek Bay (Bridgwater et al., 1975), Hunt River (this thesis) and Ugjoktok Bay (Sutton, 1972) are very similar in size, distribution, field relations and associated rock types (pelitic schists and ultrabasics) to the supracrustal belts in Greenland. Therefore, although primary volcanic structures have not yet been found in Labrador, it is reasonable to use the term meta-volcanic supracrustal to describe the rocks.

#### 2.2.1 Meta-volcanics

Amphibolite is by far the most abundant rock type in the Hunt River Belt. The term amphibolite applies to a homogeneous, fine- to coarse-grained, dark, schistose rock composed predominantly of equal amounts of hornblende and plagioclase. In the field it was not possible to subdivide the amphibolites into discrete mappable units. Thin section studies however revealed three distinct varieties. In this section the terms normal amphibolite, garnet-bearing amphibolite and diopside-bearing amphibolite are introduced for the purpose of petrographic description, following the terminology used by Kalsbeek and Leake (1970) in southwestern Greenland studies.

#### 2.2.1.1 Normal Amphibolite

In the field the normal amphibolite ranges in colour from dark grey and dark green to black, and it is generally fine- to medium-grained. It possesses a strong penetrative tectonic fabric usually defined as a schistosity in amphibole-enriched rocks or, less commonly, as a small scale banding ( $\leq 1$  cm wide) formed by alternating amphibole-enriched and quartzofeldspathic-enriched layers (Figure 2.1). A lineation defined by the parallel alignment of elongate hornblende crystals is also locally developed.

The following mineral assemblages were observed in thin section:

1. hornblende + plagioclase
2. hornblende + plagioclase + quartz.

Sphene, zircon and opaque oxides are accessory phases, whereas epidote, sericite and carbonate represent retrograde alteration products of the dominant mineral constituents.

On a microscopic to mesoscopic scale the normal amphibolites exhibit a wide variety of microstructures, depending largely upon their structural position. For example, rocks occurring in the cores of megascopic tight synforms displayed a strong nematoblastic texture whereas rocks occurring in the open antiformal structures displayed a more equigranular crystalloblastic texture.

Hornblende commonly forms 50% to 80% of the rocks and varies from xenoblastic grains .1 mm across to hypidioblastic crystals as large as 1 mm across and 2 - 4 mm in length (Figure 2.2). The hornblendes display the following pleochroic schemes: X green to

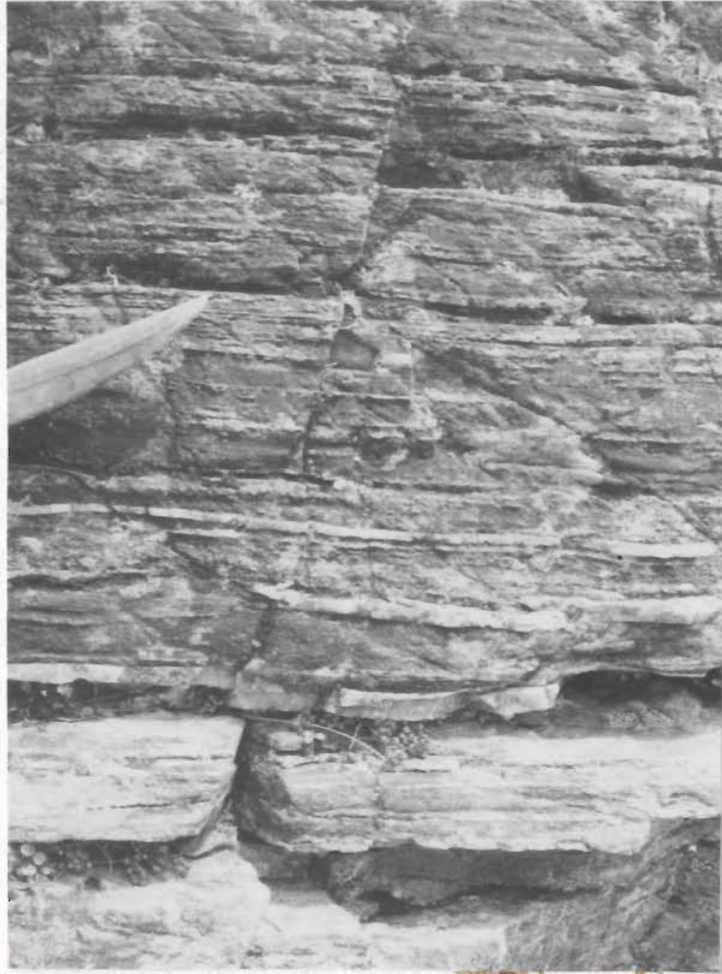


FIGURE 2.1: Typical outcrop weathered surface of normal amphibolite. Bands enriched in quartz-plagioclase stand out in relief. The lower third of the photograph is a portion of a light buff coloured rusty zone.

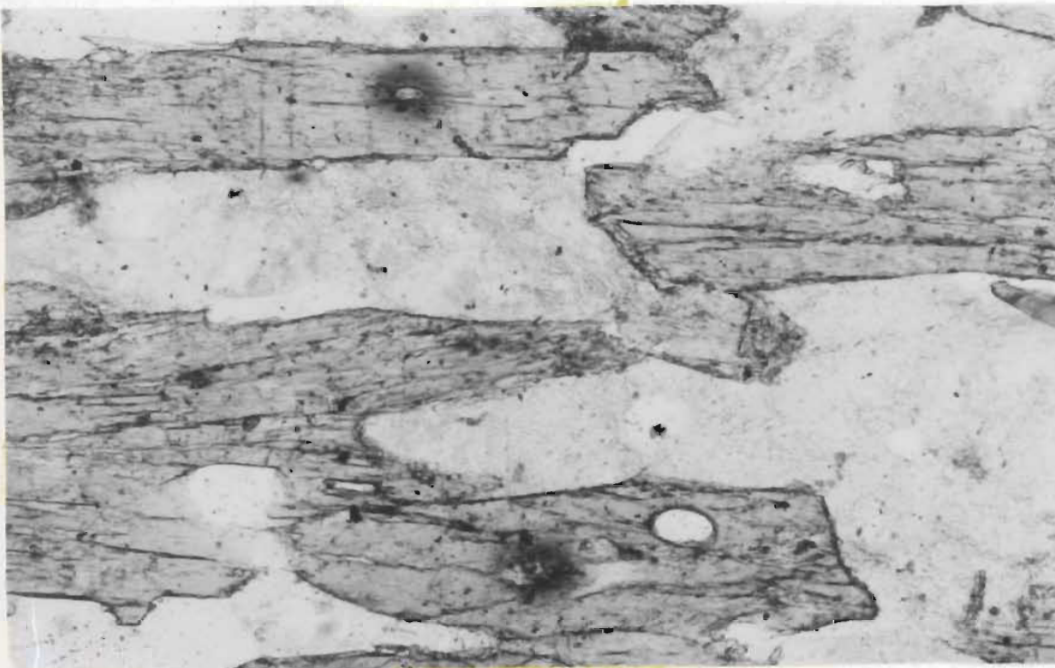


FIGURE 2.2: Photomicrograph of normal amphibolite in plane light (scale X 120). Lepidoblastic texture is defined by aligned subidioblastic laths of hornblende (dark grey) in a matrix of colourless granoblastic polygonal quartz and plagioclase crystals. Note the dark pleochroic halos surrounding tiny zircon crystals in the hornblende.

blue green, Y green to pale green, and Z pale brown to colourless ( $X > Y > Z$ ). They develop rational or irrational grain boundaries in monomineralic aggregates and curved and embayed boundaries when in contact with quartz and feldspar. There was no evidence in thin section that any hornblende formed as a regressive alteration of orthopyroxene.

Undulose quartz and twinned feldspar ( $An_{45-53}$ ) usually occur as xenoblastic crystals and are generally of slightly smaller grain size than the hornblende. The plagioclase is well-twinned according to Albite and Pericline twin laws, appears to be largely unaltered in the northern part of the thesis area, but is commonly highly saussuritized in the south. The felsic minerals are generally interstitial to the amphibole and their xenoblastic crystal shapes are largely controlled by the enclosing hornblende. Textures of the felsic minerals in hornblende-free layers or aggregates tend to be more polygonal.

#### 2.2.1.2 Garnet-bearing Amphibolite

Thin zones (from 1 - 4 m in width) of amphibolite containing abundant bright red garnets form a distinctive lithology within the Hunt River Belt. The zones are very local in nature, however, and do not constitute mappable units. The largest outcrop (4 m in width and 50 m in length) occurs in the northeastern part of the Belt.

In the field the outcrops of garnet-bearing amphibolite display sharp or transitional to diffuse boundaries with the adjacent garnet-free amphibolites (normal amphibolite and diopside-bearing

amphibolite), a feature generally related to the modal abundance of garnet in the rock. The rock exhibits a strong anastomosing schistosity defined by the hornblende and plagioclase which surrounds the subidioblastic garnet porphyroblasts. Locally, thin layers of garnet-bearing amphibolite are intensely folded or boudinaged (Figure 2.3). In general the garnet-bearing amphibolite appears to be more silicic than the other amphibolites.

The mineral assemblages identified in this rock type include:

1. hornblende + quartz + garnet + plagioclase
2. hornblende + quartz + garnet + plagioclase + biotite
3. cummingtonite + quartz + garnet + plagioclase + biotite
4. hornblende + biotite + quartz + plagioclase.

Accessories include opaques, carbonate, sphene and apatite.

In thin section a pronounced schistosity is defined by elongate mineral constituents and by a poorly developed discontinuous banding of alternate layers of felsic and mafic-enriched layers (approximately 1 mm in thickness). In places the schistosity wraps around porphyroblasts of garnet, forming augen structures.

The quartz and plagioclase ( $An_{35-42}$ ) occurs as a fine-grained polygonal granoblastic mosaic. A minor percentage of grains are elongate to platy and lie parallel to the main schistosity. The thin section length:width ratio of these grains averages 2:1.

The hornblende, similar to that found in the normal amphibolite, is of the common green variety and displays a blue green to green (X), green to pale green (Y) and pale brown to colourless (Z) pleochroism. It occurs in two habits. The majority is fine- to medium-grained,

xenoblastic to subidioblastic, and generally elongate parallel to the banding. Less commonly the hornblende occurs as coarse (1 - 2 mm across), extremely poikiloblastic crystals overgrowing the dominant fabric of the rock.

The garnets, which average 1 - 2 mm in diameter, are much coarser than the average grain size of the rock, and are xenoblastic and very poikiloblastic. They are characterized by a corona-like development of quartz around their outer edge.

Cummingtonite, an alteration product of the hornblende, occurs in the same habit and form as the hornblende. It is pale green to colourless, has higher birefringence than hornblende, and commonly exhibits polysynthetic twinning. Found only in the southern part of the Hunt River Belt, it appears to be chemically controlled (low Ca in host rock) rather than a reflection of regional metamorphic zoning. Where cummingtonite is present, the hornblende appears to be in disequilibrium with the garnet. Hornblende in contact with garnet or in proximity to garnet is altered to cummingtonite (Figure 2.4).

Biotite displays the following pleochroic scheme: X = yellow, Y = Z = red-brown. It occurs mainly as discrete, fine-grained, thin, sub-idioblastic flakes which parallel and help define the schistosity. In the northern part of the Hunt River Belt small amounts of biotite were seen to be replacing hornblende.

#### 2.2.1.3 Diopside-bearing Amphibolite

The diopside-bearing amphibolite is generally inconspicuous because it is similar in colour to the other amphibolites and because



FIGURE 2.3: Thin layer of garnet-bearing amphibolite in an outcrop of normal amphibolite. The garnet-bearing layers, bounded by felsic-enriched layers, are strongly boudinaged.



FIGURE 2.4: Photomicrograph of garnet-bearing amphibolite from the southern area in plane light (scale X 120). Poikiloblastic garnet (high relief) is surrounded by colourless quartz and plagioclase. The dark grey hornblende is altered to cummingtonite (colourless) where in proximal contact with garnet.

there is only a small amount of pyroxene present ( $\leq 5\%$ ). However, the diopside is readily apparent in thin section. The rock also has a very distinctive chemical composition ( $\text{CaO} \approx 14\%$ ). In the field the relationship of the diopside-bearing amphibolite to the other rock types is obscure, but it appears to crop out in thin ( $\leq 10$  cm in thickness) discontinuous lenses which are transitional with the adjacent rock types.

The mineral assemblages observed are as follows:

1. hornblende + diopside + quartz + plagioclase
2. hornblende + diopside + plagioclase
3. hornblende + diopside + plagioclase + trace garnet.

Interstitial carbonate and very fine epidote crystals are common accessory minerals.

The diopside is unaltered, pale green to colourless and characteristically occurs in widely spaced layers (4 - 5 mm thick). The amount of diopside in these layers varies from less than 50% to almost 100%. In the latter case, the diopside usually forms large hypidioblastic crystals 1 - 6 mm in length. Less commonly, single very large diopside crystals from 5 - 10 mm in length occur. These large isolated crystals are very poikiloblastic and appear to overgrow the main schistosity.

The petrographic characteristics of the remaining mineral species (hornblende, quartz, feldspar and trace garnet) are much the same as the descriptions outlined in the normal and garnet-bearing amphibolites.

### 2.2.2 Ultramafics

The ultramafic rocks are always found in contact with the meta-volcanics. Only one small lens is not completely enclosed by amphibolite but crops out along an amphibolite-quartzofeldspathic gneiss contact. Three types of ultramafic rocks have been discerned including hornblende schist, tremolite schist and serpentinite schist.

Unlike ultramafic lenses occurring elsewhere in the North Atlantic Craton, the Hunt River Belt ultramafic lenses are not mineralogically zoned. Zoned ultramafic lenses described from Faeringehaven in southwestern Greenland (Windley, 1972) formed under conditions varying from granulite to greenschist facies. Farther to the south in the Frederikshåb district (Misar, 1973) and also in the Lewisian of northeast Scotland in Skye (Matthews, 1967) zoned ultramafic lenses are found in amphibolite facies rocks. In general the mineralogical zoning is interpreted to have resulted from migration of elements during regional metamorphism.

For the most part the ultramafic lenses in the thesis area have been tectonically remobilized during late stage folding and therefore the contacts would not be expected to retain any symmetrical mineralogical zoning which may have developed during an earlier high grade metamorphic event. Certain lenses, especially the thin concordant layers near the grey schist unit, do not appear to be allochthonous with respect to the adjacent amphibolite. Even in these bodies the contacts between the ultramafic and amphibolite rock are quite sharp with no evidence of diffusion between the chemically distinct rock types. These relationships seem to indicate that the early metamorphism

of the Hunt River Belt proceeded under essentially isochemical conditions.

#### 2.2.2.1 Hornblende Schist

Units of hornblende schist occur either as small scale lenses (5 m long X 2 m wide) or as large traceable units up to 50 m in width. They are found in both the northern and southern areas. Contacts with the amphibolites are normally quite distinct but in places the hornblende schist becomes interbanded with the amphibolite on a scale of up to several metres over tens of metres.

The main hornblende schist units occur as structurally conformable bodies within the amphibolite. However, just north of the faulted termination of the hornblende schist in the southern area, a small unit of dark green hornblende schist approximately 1 m thick is definitely discordant to the schistosity in the amphibolite (Figure 2.5). In the field the rock is generally dark green in colour and fine-grained. Although it contains a strong tectonic fabric, at times it appears to be rather massive, due to its monomineralic nature.

The mineral assemblages include:

1. hornblende + carbonate + opaques
2. hornblende + anthophyllite + carbonate + opaques.

In thin section the rock is fine-grained. The average grain size is about .5 mm and ranges up to 1 mm in length. Textures observed in thin sections cut perpendicular to the schistosity vary from a mosaic of hypidioblastic, slightly elongate crystals to a nematoblastic



FIGURE 2.5: Outcrop of small lense of hornblende schist from southern area. The hornblende is the dark unit running diagonally from lower left to upper right of the photograph. Discordant contact is particularly irregular along the right side.



FIGURE 2.6: Outcrop surface of finely crenulated tremolite schist from the northern area.

texture defined by elongated subidioblastic to xenoblastic hornblende. Sections cut parallel to the schistosity show a poorly defined lineation. There is no evidence to suggest an over-printing of the schistosity and the fabric appears to be an S-L fabric as defined by Flynn (1962).

The hornblende occurs mainly as interlocking, hypidioblastic crystals averaging .5 mm across. Less commonly it is found as xenoblastic, elongated, lath-like crystals up to 1.2 mm in length. It is strongly pleochroic (X = dark green, Y = green, Z = colourless) and displays a 2V of about  $90^{\circ}$ .

The anthophyllite is distinguished from the hornblende by its parallel extinction. It is very fine-grained ( $\approx .2$  mm in length) and occurs as thin, lath-like, subidioblastic crystals which for the most part are oriented subparallel to the main schistosity. The crystals are also found lying at a high angle to the schistosity.

The carbonate (calcite?) occurs as small ( $\leq .5$  mm) xenoblastic crystals completely interstitial to the hornblende. The carbonate crystals make up as much as 5% of the total rock and are unevenly distributed throughout it. They tend to be concentrated along irregular linear zones which commonly lie at a high angle to the main schistosity.

The opaques occur predominantly as very fine ( $< .1$  mm) xenoblastic grains irregularly disseminated throughout the rock. Rarely they are found as aggregates which appear to be interstitial to hypidioblastic hornblende crystals.

#### 2.2.2.2 Tremolite Schist

Tremolite schist crops out in two places. In the northern area an isolated lense less than 500 m in length was found in the core of a megascopic synform. In the southern area the rock crops out as a rather extensive unit about 40 m in thickness. It can be traced continuously for approximately 3 km along strike. In the field the tremolite schist is green to pale green, very fine-grained and in places displays a very fine, crenulated fabric (Figure 2.6).

In thin section the tremolite schist appears to be a monominerallic rock composed essentially of tremolite with minor opaques, a trace of talc and secondary epidote. The rock generally has a crenulated schistosity which is defined by a planar alignment of very fine-grained, acicular tremolite. A fine layering is defined by reddish-brown discolouration in certain lamellae. In places, on a scale of up to 5 mm in width, the fine schistose texture alternates with discontinuous lenses in which tremolite occurs as coarser, xenoblastic, equidimensional to elongate decussate aggregates of crystals up to 1 mm in length.

The tremolite is colourless and generally has an acicular habit with an extinction angle (ZVc) of  $12^{\circ}$ . In the finely laminated schistose rock approximately .5% of the tremolite is coarser ( $\approx .5$  mm) than the average grain size. Where they intersect a hinge of a crenulation fold, some tremolite crystals cut across the schistosity. However, rather than representing a secondary overgrowth of a previous fabric, these coarser tremolite crystals were not affected (deformed) by the crenulation folding. In places the schistosity appears to be

distorted around these coarser crystals, and in one area a coarse-bladed tremolite crystal was found broken into three pieces with each fragment rotated around a small crenulation fold.

The epidote occurs as an alteration product of the tremolite. It is concentrated in the cores of the crenulation folds.

#### 2.2.2.3 Serpentinite Swist

Fourteen ultrabasic lenses, which are in large part serpentinite, were discovered ranging in size from 20 m X 5 m to 600 m X 50 m. They are conspicuous in the field, as weathering surfaces are highly coloured in varying shades of green, orange and red.

Two of the bodies occur as thin (1 m wide) layers in the amphibolite near the grey schist contact in the northern and the southern part of the map area. They are predominantly serpentinite with an extremely flattened, well-developed schistosity. The serpentinite appears to be talcose in places.

Two other lenses, also occurring in the northern and the southern parts of the map area, outcrop on the eastern limbs of the major antiforms. The lense in the northern area is actually at the contact of the Hunt River Belt with the adjacent quartzofeldspathic gneiss. These lenses are highly schistose and are predominantly composed of fibrous anthophyllite with approximately 10% highly sheared olivine or its serpentine derivative. Minor carbonate, talc and magnetite are also present.

The remaining ten serpentinite lenses are associated with

the synforms of the late stage folding. The lenses are variably deformed and transposed with an elongate orientation parallel to the axial planes of the late stage megascopic folds. Contacts with the surrounding amphibolites are generally sharp and locally appear intrusive due to tectonic remobilization. In three of these lenses from the northern area unusual coarse, interlocking growths of elongate olivine crystals are preserved in isolated, blocky patches surrounded by schistose serpentinite.

There is considerable variation in the texture of these three ultramafic lenses. In general the texture is characterized by random intergrowths of fine to very coarse plates of olivine crystals ranging up to 1 m in length. In places the texture consists of random intergrowths of large platy olivine with inter-plate regions composed of smaller, closely spaced parallel plates of olivine crystals (Figures 2.7 and 2.8). In another variation of this texture, a completely random network of crystals grows in fan-shaped configurations with a number of crystals extending out from a common nucleus (Figure 2.9). Less commonly, individual olivine crystals appear to branch out in the same manner.

Although the ultramafic lenses, in general, have been almost completely serpentinitized, relics of the original mineralogy are preserved in certain of the zones exhibiting the elongate olivine textures. Olivine shows alteration to aggregates of decussate serpentine and granular magnetite, with partial preservation of some crystals. The olivines are massive in nature with fairly straight crystal boundaries. The inter-plate regions are commonly



FIGURE 2.7: Serpentinite schist showing elongate olivine texture composed of random network of crystals. Interplate regions are filled with smaller, closely spaced, parallel plates of olivine. Outcrop from northern area.



FIGURE 2.8: Serpentinite schist showing etched weathered surface of elongate olivine texture, occurring in same outcrop as Figure 2.7.



FIGURE 2.9: Serpentinite schist showing a completely random network of very coarse olivine crystals, in fan-shaped configuration, with open triangular interplate regions. Outcrop from northern area near location of Figures 2.7 and 2.8.

infilled with large, often single crystals of interstitial enstatite, which displays exsolution lamellae of clinopyroxene. The enstatite is largely altered to bastite and fine-grained talc, minor opaque oxide and traces of carbonate. Platy brucite intimately intergrown with magnetite occurs as small patches up to 5 mm in diameter, replacing both olivine and enstatite. Tremolite, the only other essential mineral constituent, is abundant locally, but is commonly entirely absent in thin section. It occurs as idioblastic to sub-idioblastic, elongate, decussate patches in the inter-plate regions or as radiating fibrous to prismatic crystals up to 4 mm long which overgrow olivine - enstatite grain boundaries. The tremolite appears to be a late stage metamorphic crystallization product associated with the last major phase of folding.

There is no evidence in thin section of a tectonic fabric pre-dating the olivine crystals. The fabric that is observed in thin section is a result of late stage shearing and recrystallization. Olivine crystals oriented at a high angle to the shearing commonly develop serrated boundaries indicative of intracrystalline slip.

### 2.2.3 Meta-sediments

The meta-sediments are a minor, although significant component of the Hunt River Belt. The pelitic schist offers the best opportunity for establishing the relationships between the various phases of deformation. The grey schist is one of the few lithologies which exhibits a vertical mineralogical zonation. While the mineral assemblages are obviously a result of metamorphic growth

or recrystallization, the zonation coincides with a bulk chemical variation, which may reflect a primary lithologic control. The grey schist is interpreted to be a meta-sediment because of its similarity with meta-sedimentary grey schists described from south western Greenland (Higgins, 1968). Of the various types of rusty zones described, only the larger mappable units of garnet-biotite-enriched layers are considered to be of meta-sedimentary derivation. It is possible that the smaller sulphide-bearing lenses are local zones of secondary enrichment, or they may represent small pockets of volcanic exhalative sulphides which are commonly found in Archean greenstone belts (Ridler, 1970; Goodwin and Ridler, 1972).

Taylor (1972) reported observing primary bedding and dolomite in the Hunt River Belt, however, during field work studies for this thesis no primary sedimentary depositional features were found.

#### 2.2.3.1 Pelitic Schist

The pelitic schist offers a good opportunity for determining relationships between mineral growth and phases of deformation. Unfortunately the rock type is rather limited in extent, and this restricts any regional correlation which may have been possible from quantitative analyses.

One outcrop of this rock type occurs in the core of the megascopic synform in the southern area. Differential weathering of the minerals has caused the idioblastic garnets to stand out in relief on the surface, giving the rock a hobnailed appearance.

This weathering process appears to have been fairly rapid since many of the cracks and crevices in the outcrop are nearly filled with garnets.

The rock is a medium- to coarse-grained porphyroblastic schist. In the field the weathered surface may reveal up to 30% fresh-looking purple garnet. The schistose groundmass is a nondescript grey to dirty (rusty) light brown. A discontinuous layering is defined by alternate layers several centimetres thick enriched in garnet.

In thin section the pelitic schist displays exceptionally fresh-looking mineralogy. A strong anastomosing schistosity is defined by elongated flakes of biotite. The layering observed in the field is also apparent in thin section, with alternate layers enriched in garnet, staurolite or quartz-feldspar. Coarse-grained porphyroblastic crystals of garnet and staurolite show evidence of multiple stages of growth prior to and after the formation of the biotite which defines the main schistosity.

There are two microstructural characteristics which seem to indicate that the pelitic schist was highly sensitive to temperature and/or pressure fluctuations brought about by the various phases of deformation. Intercrystalline cross-cutting relationships and discordant helicitic inclusion trails in porphyroblastic minerals indicate that there were several stages of mineral growth. Disequilibrium contacts between various mineral phases are also indicative of possible fluctuations in the temperature-pressure conditions.

The significant mineral assemblages include:

1. quartz + plagioclase + cordierite + biotite
2. quartz + plagioclase + staurolite + garnet
3. quartz + biotite + sillimanite.

These mineral assemblages are intended to represent the last stages of mineral growth. There is evidence from helicitic inclusion trails that staurolite and garnet were present before the formation of cordierite. However, a much more detailed petrographic study of the pelitic schist is necessary before the complex chronology of mineral growth can be established with certainty. For the present, only general observations based on a few thin sections may be stated.

The quartz and plagioclase for the most part form a fine-grained, xenoblastic, irregular, interlocking groundmass. The quartz is much more abundant than the plagioclase and also occurs as coarser ( $\approx 1$  mm) crystals in quartz-rich aggregates which form discontinuous lenses throughout the rock, parallel to the weak schistosity. The plagioclase is unzoned and poorly twinned according to Albite and Pericline twin laws. It was not possible to approximate the composition of the plagioclase optically. The quartz aggregates may or may not represent primary sedimentary features, however, they do appear to be very early constituents which have undergone considerable deformation and recrystallization.

The biotite is fine- to coarse-grained and occurs as subidioblastic flakes. The pleochroic scheme is X = pale brown and Y = Z = red brown. Highly coloured pleochroic halos are found around

the numerous very fine-grained zircon inclusions in the biotite crystals. Two planar fabrics are defined by the biotite including a weak schistosity which parallels certain elongate mineral constituents (cordierite and quartz aggregates) and a younger dominant schistosity which parallels the large scale layering in the rock.

The garnets occur as idioblastic to subidioblastic porphyroblasts up to 1 cm in diameter. They are distinctively zoned with an inner core filled with numerous inclusions (predominantly quartz) which form straight and curved inclusion trails. The outer rim is relatively free of inclusions although large inclusions (.2 mm across) of staurolite, biotite and quartz are present in some garnets.

The staurolite occurs as small ( $\approx 5$  mm) xenoblastic crystals distributed throughout the rock and as larger ( $\leq 4$  mm in length) subidioblastic tabular crystals with good straight inclusion trails. The inclusion trails are randomly oriented with respect to the main schistosity defined by the biotite. The subidioblastic shape of the staurolite crystals is due to a secondary later stage of overgrowth, as the larger crystals display inclusion-free outer rims.

The cordierite occurs as coarse, extremely poikiloblastic poorly defined crystals. It is elongate (up to 1.5 cm in length) and generally lies at an angle to the dominant biotite schistosity (i.e. parallel to the weaker biotite schistosity). In places the large cordierite crystals are fragmented and biotite crystals appear to have grown in the fractures. Single crystals are often only

recognized as single crystals because of the optical continuity of the large xenoblastic lensoid patches of cordierite.

The cordierite may be distinguished from the quartz by its biaxial negative character, and from the plagioclase because it is in disequilibrium with staurolite and garnet. A reaction rim of quartz (?) is present wherever cordierite and staurolite are in contact (Figure 2.10). Contacts between cordierite and garnet are always obscured by admixtures of biotite, quartz and sillimanite (Figure 2.11). Under high magnification very pale yellow pleochroic halos surrounding very fine grains of zircon were observed.

The sillimanite is a minor constituent and occurs as slightly radiating clusters of very fine, prismatic fibres (fibrolite). The sillimanite is often found at garnet-cordierite contacts (Figure 2.11) but may also be found associated with cordierite crystals throughout the pelitic schist.

#### 2.2.3.2 Grey Schist

The grey schist is found only in the cores of the megascopic antiforms, where it separates the overlying amphibolite of the Hunt River Belt from the underlying homogeneous gneiss. The upper contact with the amphibolite is generally quite distinct but locally it appears to be completely transitional. The lower contact was not observed in the southern area, while in the northern area it is abrupt.

In the field the grey schist is a fine-grained, dirty white

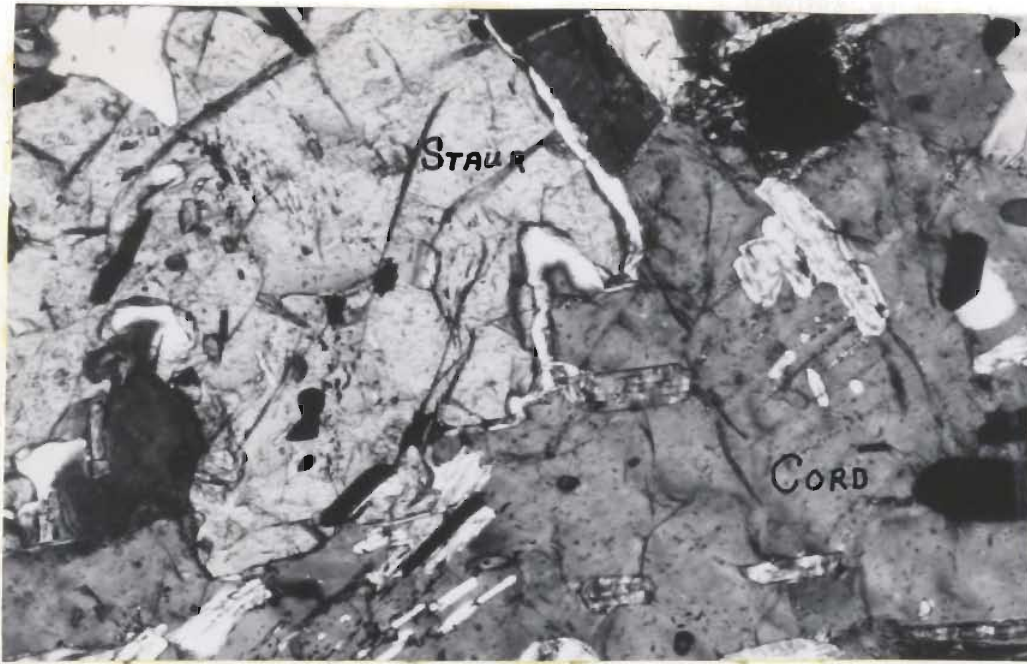


FIGURE 2.10: Photomicrograph of pelitic schist showing the disequilibrium reaction between staurolite and cordierite (scale X 120).



FIGURE 2.11: Photomicrograph of pelitic schist showing sillimanite (fibrolite) needles growing at a garnet-cordierite contact (scale X 120).

to grey rock. In places the biotite is altered, giving the weathered surface a buff colour.

The mineral assemblages observed include:

1. plagioclase + quartz + biotite + hornblende + garnet
2. microcline + quartz + plagioclase + biotite.

Opaques, zircon and sphene are trace accessories while chlorite and epidote are common alteration products of biotite and hornblende. The plagioclase is often quite clouded.

In thin section the grey schist displays a fine-grained lepidoblastic texture defined by elongate, parallel hornblende and biotite crystals in a matrix of granoblastic quartz and feldspar (Figure 2.12). Hornblende, which is abundant near the upper amphibolite contact, is not present in thin sections containing microcline, which is most abundant near the lower contact with the homogeneous gneiss.

The quartz and feldspar occur together as fine-grained, granoblastic equidimensional to slightly elongate crystals. The feldspar is mainly clouded plagioclase where hornblende is present, but is predominantly microcline where hornblende is absent. The appearance of microcline is accompanied by an overall increase in grain size. Individual quartz and feldspar crystals up to 1.5 mm across may be found in the microcline-bearing thin sections.

Fine-grained subidioblastic laths of biotite are evenly distributed throughout the rock and define a strong schistosity. The biotite is pleochroic (X = pale brown, Y = Z = dark brown) and in places it is partially altered to chlorite or epidote.

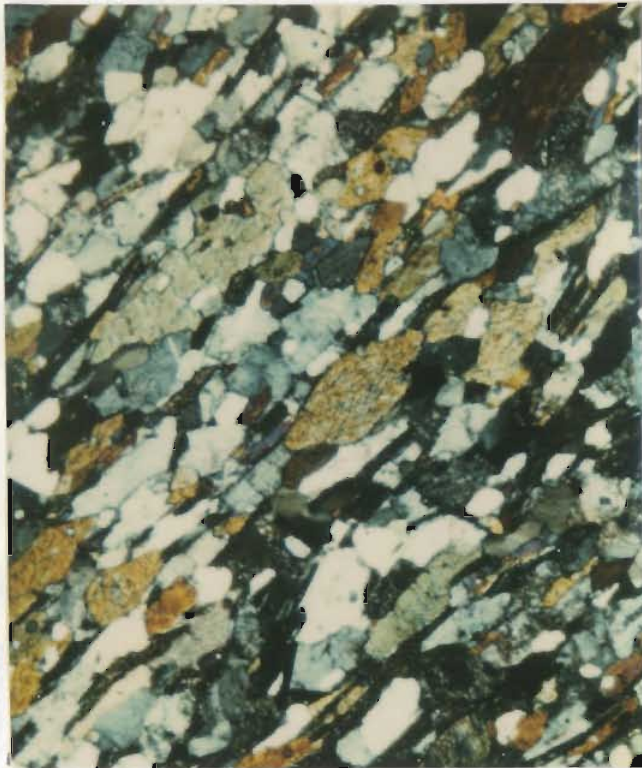


FIGURE 2.12: Photomicrograph of grey schist showing lepidoblastic texture defined by elongate parallel hornblende and biotite in a matrix of granoblastic quartz and feldspar. The biotite is dark brown, the hornblende is dark green, and the light green mineral is chlorite after biotite (scale X 25).

The hornblende occurs as fine-grained ( $\approx 0.5$  mm in length) xenoblastic elongate crystals parallel to the schistosity. Black pleochroic halos are found around very fine zircon inclusions however, the dominant pleochroic scheme is X = blue green, Y = green and Z = light brown. The hornblende content changes drastically across the rock unit. Near the amphibolite contact it forms about 10% of the rock, while near the homogeneous gneiss contact hornblende is entirely absent.

#### 2.2.3.3 Rusty Zones

Rusty zones are ubiquitous throughout the Hunt River Belt. They are readily recognized by their typical rusty brown gossan cover, and range in size, from small lenses several centimetres thick and up to a metre long, to large units comparable in size to other mappable lithologies. The rusty surfaces are a result of oxidation of sulphides and alteration of variable amounts of biotite and garnet. Four distinct associations were observed in the field.

#### Large Mappable Units

There are two occurrences of mappable units. One is found in the northern area and one occurs in the southern area (Figure 2.1). Both are parallel and concordant with the stratigraphy, and possibly represent discrete meta-sedimentary units. The rock is generally fine-grained and appears to be significantly more siliceous than the adjacent normal amphibolite. Although small lenses occur sporadically it appears that the rusty nature of this rock type is predominantly

due to alteration of a relatively high amount of biotite and garnet. However, due to the extent of the alteration, as is the case with most of the rusty zones, the original mineralogy is almost completely obliterated.

#### Small Discontinuous Lenses or Pods

These smaller, seemingly randomly distributed occurrences are variable in size ranging from several centimetres across up to five metres across. The host rock for these rusty zones is highly variable although it generally seems to be relatively enriched in feldspar and quartz. The rusty nature of these occurrences may be in part due to the alteration of biotite, but appears to be primarily the result of oxidation of very fine-grained sulphides.

In a number of lenses that were relatively enriched in fresh sulphide, samples were collected for polished section studies. Only the predominant features of the sulphide-bearing rusty zones are considered here.

The sulphides seen in these rusty zones include chalcopyrite, galena, pyrrhotite and pyrite. The galena was found only in a hand specimen from a single outcrop and was restricted in occurrence to a few small crystals ( $\leq 5$  mm) which exhibited perfect cubic cleavage. The most abundant sulphide throughout the rusty zones is pyrite which occurs generally as very finely disseminated grains throughout the amphibolitic host rock. In the more enriched zones sulphides occur in discontinuous lenses or stringers ( $\leq 5$  mm wide), and pyrrhotite is more abundant than the pyrite (Figure 2.13). The

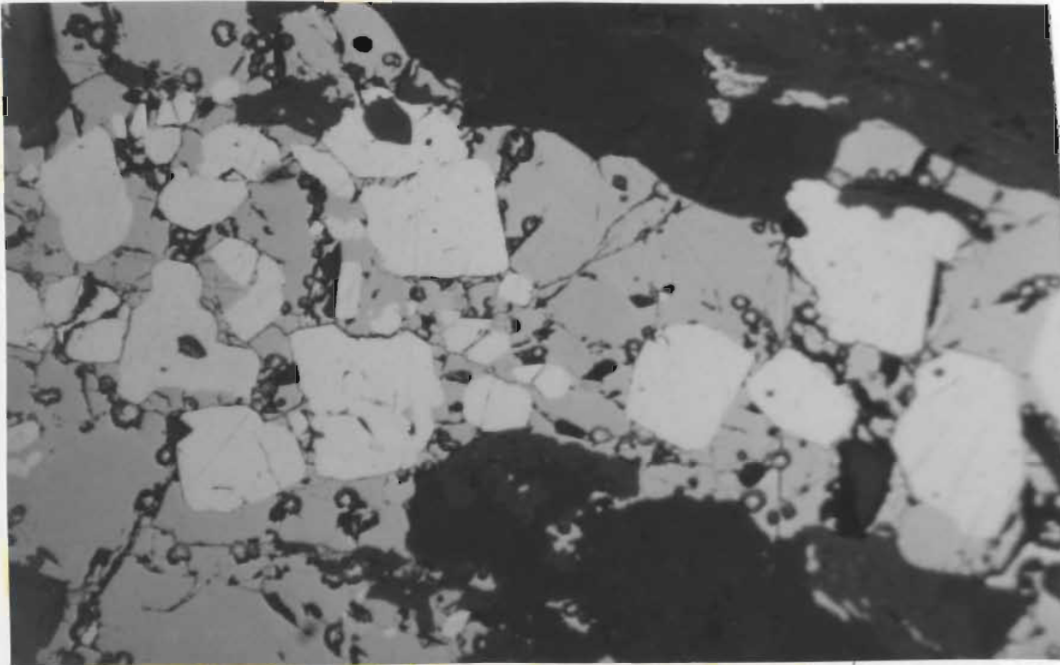


FIGURE 2.13: Rounded euhedral white pyrite crystals growing in a matrix of light grey massive pyrrhotite. In places, the pyrite crystals are fragmented and partially replaced by the pyrrhotite (scale X 25).

pyrrhotite in places can be seen to be replacing pyrite, possibly in response to an early high temperature fluctuation. The pyrite forms small, highly fractured grains as a result of its brittle response to the deformation. This contrasts with the pyrrhotite which behaved in a more ductile manner.

#### Associated With Faults of Shear Zones

This is the most limited occurrence of the rusty zones. A further restriction of this association is that the rusty zones are associated only with faults or shears that have a low angle with the dominant foliation of the country rock. It is difficult to correlate these rusty zones with any particular lithology. No fresh sulphides were observed.

#### Associated With Ultramafic Rock Units

Almost all of the ultramafics exhibit associated rusty zones, either along the contact with the amphibolite or within the ultramafic but near the margins. The majority of these rusty zones are simply local zones which are heavily enriched with garnets. In some ultramafic bodies tremolite-rich zones display visible sulphides including pyrrhotite and chalcopyrite.

### 2.3 QUARTZOFELDSPATHIC GNEISS COMPLEX

Understanding the geological development of the quartzofeldspathic gneiss terrain is one of the most challenging aspects of this thesis. In the field the gneisses are highly variable

structurally and mineralogically. Five major types of gneiss were distinguished according to field relationships, microstructures and dominant mineralogy. These types of gneiss may be broadly outlined on a megascopic scale, however it should be kept in mind that the contacts between the gneiss types in Figure 1.2 are very approximate and in places intercalation of gneiss types occurs over tens of metres. It is interesting to note that the gneisses, as subdivided in the field, exhibited distinctive bulk chemical compositions (Chapter 3, Section 3.4.1).

The majority of gneisses are considered to be orthogneisses derived from a plutonic suite of rocks, although minor meta-sedimentary and meta-volcanic slivers may be found intercalated with the orthogneisses. This intercalation took place during an early stage of tectonic interleaving (Chapter 4, Section 4.1.2) and involved the banded gneiss. The homogeneous gneiss, mixed gneiss and agmatite did not achieve their present aspect until further plutonic and tectonic episodes of deformation took place.

Unfortunately, time allowed for little more than reconnaissance scale mapping of the gneisses, and this was largely confined to the east and northeast of the Hunt River Belt. Excellent exposure continues eastward to the Labrador coast, a distance of 30 km, and lends itself to future detailed studies of the gneisses and their deformation and metamorphism.

### 2.3.1 Banded Gneiss

Well-banded tonalitic gneiss forms the most abundant rock type in the gneissic terrain. It is readily identified by the conspicuous presence of alternate layers enriched in felsic minerals and layers enriched in mafic (predominantly hornblende) minerals (Figure 4.2). The banding is generally on a scale of 2 - 3 cm thick, however the size of the hornblende-enriched layers grades from several millimetres in thickness to fairly large units of amphibolite schist tens of metres thick. Throughout the banded gneiss terrain there is evidence (such as numerous intrafolial folds) of a long and complex deformational evolution.

The dominant gneissic layering of the banded gneiss was inherited during the last intense penetrative deformation which involved both the gneissic terrain and the Hunt River Belt. This deformation resulted in a tectonic interleaving or intercalation of the banded gneiss and the meta-volcanic amphibolites. The large lenses of amphibolite schist outcropping within the banded gneiss terrain are therefore interpreted to be tectonic schlieren derived from the Hunt River Belt. Whereas the larger amphibolite units retain some of their pre-intercalation character, many of the smaller units are completely transposed and incorporated into the gneissic banding.

The polydeformational history of the banded gneiss precludes any interpretation of its original character. The mafic component of the banded gneiss may have been derived, in part, from contamination (tectonic interleaving) with mafic rocks from the Hunt River Belt.

Alternatively, the mafic material may represent deformed diabase dykes, or mafic differentiates of the gneissic protoliths.

In thin section the following mineral assemblages were recognized:

1. hornblende + quartz + plagioclase
2. hornblende + quartz + biotite + microcline.

Trace accessories include zircon, sphene, apatite, metamorphic allanite and opaques. Epidote and chlorite are common alteration products of hornblende and biotite respectively.

The microstructures are generally heteroblastic and fine- to medium-grained. The mafic layers are composed predominantly of mosaics of hornblende and plagioclase, while the felsic layers are relatively enriched in quartz.

The hornblende occurs as medium- to coarse-grained ( $\leq 2$  mm across) hypidioblastic crystals in mafic-enriched layers with plagioclase, and as fine-grained ( $\leq 1$  mm) xenoblastic crystals in plagioclase-quartz-enriched layers. Well-developed amphibole cleavage is present and the pleochroic scheme is X = dark green to blue green, Y = green and Z = pale green to pale brown ( $X > Y > Z$ ).

The plagioclase is fine- to medium-grained, xenoblastic, and displays irregular curved boundaries with quartz and hornblende. It is well-twinned according to Albite, Pericline and Carlsbad twin laws, however extensive alteration to sericite and epidote made an optical determination of its composition difficult. In one relatively fresh thin section the plagioclase was measured at  $An_{35}$  however, a range of An values is to be expected throughout

the banded gneiss.

The quartz commonly displays strong undulatory extinction in rounded xenoblastic crystals and has sutured self-boundaries in quartz-rich aggregates.

Biotite occurs as fine-grained highly chloritized subidioblastic flakes less than .1 mm in length, oriented parallel to the gneissic banding. The occurrence of biotite ( $\approx 1 - 2\%$ ) is restricted to rocks which are relatively enriched in quartz.

Microcline, apart from its occurrence in secondary pegmatite veining that often parallels the gneissic banding, is sometimes present as very fine xenoblastic grains in thin sections which contain biotite that has been completely chloritized.

### 2.3.2 Homogeneous Gneiss

The homogeneous gneiss (granodioritic to trondhjemitic) is predominantly a coarse-grained, strongly foliated quartzofeldspathic gneiss containing 5 - 10% biotite. The gneiss is distinguished from the banded gneiss by the lack of a well-developed leucocratic - melanocratic banding, although in many places a gneissic banding is present as a result of parallel pegmatite veining.

The largest single unit of homogeneous gneiss (2 km X 12 km) lies to the east of the Hunt River Belt (Figure 1.2). The northwestern boundary is extensively agmatized while the southwestern boundary is in fault contact with the banded gneiss. The entire western boundary of the homogeneous gneiss has also been extensively

reworked tectonically to form, in part, the "mixed gneiss". Elsewhere, the homogeneous gneiss crops out in the core of the megascopic antiform in the northern area, and also in the northern part of the thesis area.

The homogeneous gneiss is greatly affected in places by extensive discordant pegmatization related to the development of the agmatite to the northeast.

The homogeneous gneiss is less complexly deformed and is thought to be younger than the banded gneiss. On a regional scale there is a complete lack of mesoscopic to megascopic amphibolite schlieren contained within it, and this would not be the case if the homogeneous gneiss had been present at the time of the early tectonic interleaving.

In thin section the following mineral assemblages were found:

1. quartz + plagioclase + biotite
2. quartz + plagioclase + biotite + microcline
3. quartz + plagioclase + biotite + microcline + hornblende.

Euhedral to subhedral apatite and sphene, rounded zircon and metamict allanite are common accessories. The fine-grained allanite is almost always surrounded by an alteration rim of highly birefringent epidote. An unusual feature of the allanite is that in places the surrounding quartz and feldspar is penetrated by a series of radial cracks up to 2 mm in length, extending outward from the allanite crystals. These cracks resulted from expansion of the allanite due to alteration and hydration (Deer, Howie and Zussman, 1966).

The homogeneous gneiss displays a medium- to coarse-grained inequidimensional heteroblastic microstructure. A strong foliation is defined by the parallel alignment of laths of biotite and, to a lesser extent, by the alignment of irregular elongate crystals of quartz and feldspar. Elongate accessories (apatite prisms and sphenes) also parallel the foliation.

Quartz occurs as very fine rounded grains completely enclosed in feldspar, and as coarse-grained ( $\leq 3$  mm across) xenoblastic elongate to amoeboid-shaped grains, and shows undulose extinction in some thin sections.

The plagioclase ( $An_{30}$ ) is predominantly xenoblastic, medium- to coarse-grained, with curved although irregular grain boundaries. Many of the plagioclase crystals are elongate and are oriented with their long axes parallel to the foliation defined by the biotite. The plagioclase is well-twinned and highly variable in the amount of alteration to very fine-grained sericite.

Biotite occurs as subidioblastic medium-grained flakes (.1 - 1 mm in length) which are aligned to give the homogeneous gneiss a prominent foliation. The pleochroism is X = pale brown, Y = Z = very dark brownish green. The biotite is commonly altered to colourless epidote.

Microcline is present in almost every thin section. However, when hornblende is present the potassium feldspar appears to be an untwinned orthoclase. The microcline occurs as unaltered medium- to coarse-grained xenoblastic crystals exhibiting cross-hatched or tartan twinning. Grain boundaries are curved to lobate.

They are concave when in contact with quartz and convex when in contact with plagioclase.

Hornblende rarely occurs. It is found as coarse-grained (2 - 3 mm across) pale green granoblastic crystals in thin sections that are also characterized by relatively high amounts of sphene. Based on their field relations and microstructures the rocks containing hornblende are included in the homogeneous gneiss unit, indicating that the homogeneous gneiss lithology actually comprises petrographically distinct kinds of rocks.

### 2.3.3 Mixed Gneiss

The mixed gneiss is actually a number of discrete gneiss types which are intercalated on a scale of several metres and cannot be meaningfully separated on a 1:50,000 scale of mapping. It outcrops extensively to the east of the Hunt River Belt, always as linear zones separating the homogeneous gneiss from the banded gneiss (except where in fault contact).

The mixed gneiss comprises a series of well-banded granodioritic and hornblende-biotite-rich units which are intercalated with layers of banded gneiss and homogeneous gneiss.

From the field evidence it appears that the mixed gneiss may have attained a large part of its present character during the magmatic emplacement of the granodioritic protolith to the homogeneous gneiss. During the emplacement, sheets of granodiorite were injected into the country rock (banded gneiss terrain). Post-homogeneous gneiss deformation has obscured many of the original

field relationships. It is possible, for example, that the intercalation of rock units may in part be a result of tectonic processes (interleaving or folding). Also, the occurrence of the banded granodioritic gneiss and other gneiss types peculiar to the mixed gneiss terrain points to a long and complex magmatic as well as tectonic evolution.

Although the mixed gneiss was not examined petrographically, a chemical study was undertaken (Chapter 3, Section 3.4.1) in order to determine the geochemical relationship of the mixed gneiss to the other gneiss types.

The zones of mixed gneiss proved very useful in establishing the structural chronology of the thesis area. For example, in the mixed gneiss terrain, post-homogeneous gneiss deformation can be readily observed because thin layers of homogeneous gneiss are highly folded by the deformation. The effects of the same deformation would be difficult to observe in the homogeneous gneiss terrain.

#### 2.3.4 Agmatite

There are two occurrences of agmatite in the thesis area. Agmatite crops out in a north to northeasterly trending linear zone about 2 km wide X 10 km long in the northeastern part of the thesis area (Figure 1.2). It coincides with the axial trace of the folded megascopic synform. Agmatite also crops out in the core of the megascopic antiform in the north. Agmatite as defined here comprises paleosome fragments which are completely enclosed by a leucosome. The proportion of the leucosome varies from about 10% to as much as 60%.

The agmatite varies structurally and texturally along its extent. Only the major variations are briefly noted here and there is no attempt to classify or subdivide the mesoscopic structures according to existing classifications.

#### Leucosome

The leucosome is predominantly a very coarse-grained quartz-feldspar (plagioclase + potassium feldspar)-biotite rock which in places appears almost pegmatitic. A peculiar characteristic of the quartzofeldspathic leucosome is that it contains a relatively strong anastomosing fabric. In contrast, paleosome fragments are highly angular and lack this fabric (see Figure 4.15). This indicates that the leucosome was emplaced during a tectonically active period. Emplacement during the latter stages of tectonism appears to be the most logical answer to the juxtaposition of a tectonically deformed leucosome and a relatively undeformed paleosome.

#### Paleosome

The agmatite is developed within both amphibolite schists and quartzofeldspathic gneisses. In the amphibolite horizons the leucosome fraction is generally 10% of the outcrop. The paleosome fragments are fairly large, up to 5 - 10 m across, and tend to be tabular or rectangular in shape. Within the gneissic terrain, especially in the highly folded gneisses, the leucosome fraction forms about 50% of the outcrop. The paleosome fragments are

noticeably smaller (5 m across) and are more irregular in shape.

The agmatite zone becomes increasingly deformed as the rock unit is traced from the south to the north towards the nose of the megascopic synform. The paleosome fragments become strongly deformed into large augen shaped structures. The enclosing leucosome in this area exhibits a fairly well-developed gneissic banding. This gneissic banding is probably inherited from tectonic mixing of the leucosome and completely assimilated paleosome fractions. In places where the augen shaped gneissic fragments are preserved, the gneissic banding of the paleosome is clearly discordant to the surrounding tectonic fabrics.

#### 2.3.5 Anorthositic Gabbro

A small body of intensely deformed anorthositic gabbro outcrops in the banded gneiss south of the Hunt River Belt (Figure 1.2). In the field the rock is light grey to white in colour, medium-grained and exhibits a strong foliation. A coarse gneissic banding is not developed, although a strong schistosity is defined by intricately layered discontinuous lenses ( $\approx 5$  mm across) of plagioclase and green hornblende.

The extent of this rock type and its field relationship to the banded gneiss was difficult to establish, however it does appear to be structurally conformable with the country rock gneisses. The anorthositic gabbro compares favourably with Archean anorthosite found elsewhere in Labrador (cf. Weiner, 1975). The Archean anorthositic bodies from Labrador are generally

regarded to be comparable to occurrences from West Greenland described by Windley (1969a) and Bridgwater et al. (1973c) (Collerson et al., 1975).

The mineral assemblage is:

1. plagioclase + hornblende.

Accessories include trace amounts of zircon and opaques. A small amount of quartz may be present also but it is restricted to thin veinlets parallel to the foliation and it is considered to be secondary. Red-brown biotite occurs as an alteration product of hornblende and it is further altered to light green chlorite.

The microstructures are granoblastic, medium- to coarse-grained and are composed of alternating thin lense-like aggregates of xenoblastic hornblende which alternate with aggregates of thin layers of xenoblastic to subidioblastic plagioclase.

The plagioclase ( $An_{68}$ ) averages 1 - 2 mm in grain size. The crystals are zoned and exhibit both Albite and Pericline twinning. Extensive alteration to sericite has affected the plagioclase and tends to accentuate the zoned nature. The zoning is also demonstrated by uneven extinction and appears to be concentric in some crystals, parallel in others and irregular in the remaining crystals. It is difficult to say if the zoning represents an igneous fractionation remnant or whether it is a result of metamorphic recrystallization.

The hornblende is generally coarser in grain size (1 - 3 mm across). It occurs both as xenoblastic to subidioblastic crystals in monominerallic aggregates forming thin discontinuous layers or

lenses up to 5 mm in thickness and as fine- to medium-grained xenoblastic crystals distributed throughout the plagioclase-enriched fractions. It displays irregular to concave boundaries with the plagioclase and appears interstitial in places. The hornblende exhibits good amphibole cleavage and its pleochroic scheme is X = green, Y = light green and Z = pale brown (X>Y>Z).

#### 2.4 BORDER ZONE

A large part of the Hunt River Belt including the northwestern part and much of the eastern area is in direct fault contact with the quartzofeldspathic gneisses. The contact relations along the southwestern portion of the Belt are poorly exposed. Throughout much of the remaining contact region the quartzofeldspathic gneisses are separated from the Hunt River Belt by a series of unique lithologic rock units forming a border zone. These lithologic units crop out asymmetrically and bound both sides of the Belt. A pink muscovite gneiss crops out within the megascopic antiformal cores of the Belt, and a variable quartzofeldspathic gneiss crops out along the outer margin of the Belt.

If the adjacent gneisses are older than the Hunt River Belt, then they may have served as basement to the meta-volcanics, and major structural unconformities may have been present. If the gneisses are younger than the Belt, then intrusive contacts, either sharp or gradational may have been present. The gneisses could also have been in part derived from a sedimentary or silicic-volcanic fraction of the supracrustal belt. In this case the original contacts would have

been conformable to begin with. However, during early intense deformation all primary discordant lithologic contacts were either completely obliterated or deformed to such an extent that they now appear conformable and are very difficult to discern.

#### 2.4.1 Pink Muscovite Gneiss

In the field the pink muscovite gneiss is a very distinctive lithology. It is fine- to medium-grained, salmon pink in colour and has a strong planar fabric defined by platy quartz and foliated mica. The mica (muscovite) is not randomly distributed throughout the rock but is concentrated in discrete, very thin, semi-continuous laminae. This imparts a very good widely spaced cleavage to the rock along the micaceous laminae.

The pink muscovite gneiss crops out as a thin conspicuous unit averaging 3 - 5 m in width and mappable over a total length of about 8 km. It is restricted to the cores of the megascopic antiforms. In the northern antiform it separates the overlying grey schist from the underlying homogeneous gneiss (Figure 2.14). In the southern area it occurs completely within the grey schist and does not appear on the solid geology map, Figure 1.2, because the exposure is in a vertical cliff face. On a mesoscopic scale the pink muscovite gneiss is structurally conformable with adjacent rock types, however, on a megascopic scale it appears to exhibit a regional discordant relationship with the grey schist.

The mineral assemblage of the pink muscovite gneiss is:

1. quartz + plagioclase + microcline + muscovite + garnet.



FIGURE 2.14: Contact between the Hunt River Belt and the pink muscovite gneiss in the northern part of the thesis area. The outcrop is on the north-western limb of the megascopic antiform, looking towards the northeast. A small sinstral fault is apparent in the hornblende-bearing grey schist by the offset concordant pegmatite layers.

A fine dusty scattering of accessory opaques also occurs.

The fine- to medium-grained microstructure is inequigranular and granoblastic. The quartz and feldspars form an interlocking xenoblastic matrix in which foliated muscovite and coarse-grained platy quartz define a strong planar fabric. Grain boundaries are curved and are commonly mutually embayed.

The quartz has two habits. It occurs as fine-grained xenoblastic to spherical crystals intimately mixed with the feldspar, and as large (up to 1 mm thick X 1 cm in diameter) platy crystals which lie parallel to the aligned mica. The large platy quartz crystals exhibit irregular undulose extinction, and the fine-grained crystals display relatively even extinction.

The plagioclase ( $An_{10}$ ) occurs as fine- to medium-grained xenoblastic crystals in a quartz-feldspar mosaic. It is also found as subidioblastic crystals in plagioclase monomineralic aggregates. Carlsbad, Pericline and Albite twins are common and there is negligible alteration. The plagioclase crystals are generally slightly elongate parallel to the foliation.

Microcline occurs as fine- to medium-grained xenoblastic crystals with well-developed cross-hatched twinning. Grain boundaries are curved and generally embayed to quartz and plagioclase, which gives the crystals an interstitial appearance.

The muscovite, which is pale green in hand specimen, is colourless in thin section. Thin micaceous laminae are comprised of single thin subidioblastic laths ( $\approx 1$  mm in length) aligned end on end.

The garnets are fine-grained (<1 mm across), xenoblastic elongate to oval shaped and are oriented with their long axes parallel to the foliation.

#### 2.4.2 Variable Quartzofeldspathic Gneiss

Along its eastern boundary the Hunt River Belt is separated from the quartzofeldspathic gneiss complex by a variable but distinct lithology of quartzofeldspathic gneiss. The gneiss varies from 5 - 40 m in thickness and has quite a sharp and concordant contact with the amphibolites (Figure 2.18). It exhibits a similar contact with the banded gneiss to the east. In the north, this border zone unit is fine-grained, white and quartzitic-looking in the field. Further south, through the middle of the map area, the unit remains fine-grained but appears to be relatively enriched in potassium feldspar and takes on a pink colour. In the south the unit contains significant amounts of hornblende and a regular alternation of pink to reddish felsic bands and black mafic bands is prominent.

Mineral assemblages include:

1. quartz + plagioclase
2. quartz + plagioclase + hornblende + microcline
3. quartz + plagioclase + microcline + muscovite
4. plagioclase + hornblende + quartz.

The mineral assemblages above show the variation in lithology from the north to south. Microstructures are also highly varied from north to south, reflecting the changing lithology. Epidote is a common secondary mineral and is commonly found coating joint surfaces.



FIGURE 2.15: Contact between the variable quartzofeldspathic gneiss and the meta-volcanic amphibolite of the Hunt River Belt. Photograph is taken near the southern extension of the eastern limb of the megascopic antiform in the north, looking towards the northeast. Note the leucocratic layering in the amphibolite and the thin dark zone of hornblende-enrichment right at the contact.

In the north (mineral assemblages 1. and 2.) the microstructures are granoblastic equidimensional mosaics of fine-grained quartz and feldspar with minor ( $\approx 1\%$ ) green hornblende and microcline. In contrast to microstructures in the pink muscovite gneiss, the grain boundaries are highly irregular and appear to be cataclastic.

Further south near the middle of the Hunt River Belt (mineral assemblage 3.) hornblende disappears, tartan-twinned microcline increases and fine-grained subidioblastic ribbons of colourless muscovite appear. The change in mineralogy is accompanied by a general increase in grain size giving the rock a heteroblastic texture. Grain boundaries are much more regular however the rock is penetrated by numerous fine fractures which are filled with a very fine-grained mixture of quartz, feldspar and epidote.

In the south, east of the megascopic antiform, the variable quartzofeldspathic gneiss crops out as a medium- to coarse-grained pink banded gneiss (mineral assemblage 4.). The microstructure is heteroblastic as individual crystals range from less than .1 mm up to 2 mm in length. There is an unusually large amount of zircon and sphene ( $\approx 5\%$ ) occurring with trace rectangular opaques. No potassium feldspar was observed in thin section. The plagioclase is thoroughly clouded, although relic polysynthetic twinning is still recognizable in most crystals. The hornblende is pleochroic in shades of green and brown. The quartz exhibits strong irregular undulose extinction patterns. The rock is penetrated by a large

number of very fine fractures, and the mineral constituents display cataclastic textures.

## 2.5 INTRUSIVES

The selection of rock types included in this discussion is somewhat arbitrary, since most of the various gneisses are interpreted to have been derived originally from plutonic rocks. Only those intrusives which have discordant contact relationships with the country rock, or which retain recognizable igneous textures are included in this section.

### 2.5.1 Meta-quartz-monzodiorite

The meta-quartz-monzodiorite occurs as two distinct bodies. One is found in the northern area and one is found in the southern area. It is largely fault bounded with the adjacent amphibolite. In the field the rock is homogeneous, well-foliated and has a pronounced linear fabric. It is fine- to medium-grained and composed of about 40 - 60% hornblende and porphyritic feldspar crystals up to 1 cm in diameter. Tabular feldspars are occasionally found and are aligned, while the majority of feldspar crystals have been deformed into an augen structure which gives the rock a coarse, anastomosing planar fabric (Figure 2.16). The linear fabric, defined by elongate mineral constituents, overprints the planar augen foliation, and in both bodies it parallels the fold axes of the megascopic synforms.

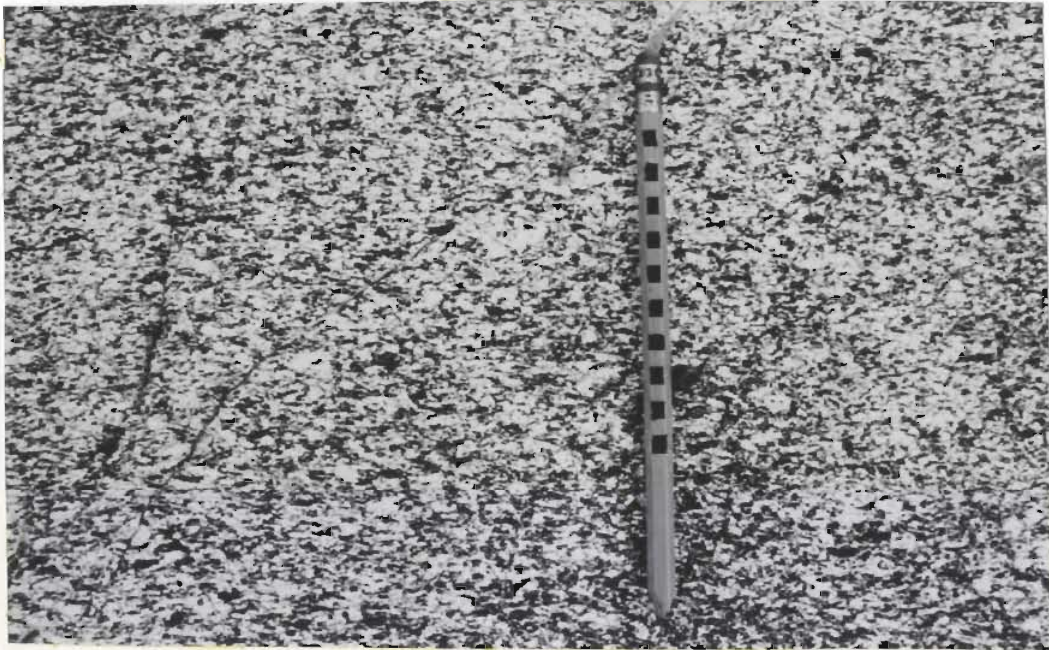


FIGURE 2.16: Glacial polished surface of quartz-monzodiorite showing the anastomosing planar fabric on a surface nearly perpendicular to the lineation. Pencil is marked off in cm.

In thin section the following mineral assemblages were observed:

1. hornblende + plagioclase + quartz + biotite
2. hornblende + plagioclase + quartz + biotite + microcline.

Accessories include sphene, apatite, chlorite, epidote and trace carbonate.

The rock is dark in appearance due to the high hornblende content. In places the feldspars take on a pinkish colour but this seems to be a reflection of the amount of alteration of the plagioclase. While the igneous textures are locally well-preserved, exhibiting euhedral porphyritic feldspars, more commonly the feldspars have been deformed and augened.

The hornblende, pleochroic from green to blue green to brown, is highly variable in size. The larger crystals (approximately 5 mm in diameter) are generally very poikilitic and commonly display a zoned nature.

The quartz and feldspar in the less deformed rocks displays a fresh interlocking mosaic igneous texture, although a planar fabric is defined by an alignment of the mica flakes.

The biotite is generally completely altered to chlorite but some brown biotite is preserved in some of the fresher rocks.

#### 2.5.2 Granodiorite

One small body of granodiorite cropping out in the southwest probably represents the youngest igneous plutonic intrusion in the map area. The outcrop is circular, approximately 500 m in diameter, and

is fault bounded along the southwestern margin. The rock is medium- to coarse-grained and in the field it appears to be composed essentially of pink feldspar and quartz, with minor mafics. In certain places near the margins, a penetrative schistose fabric is seen defined mainly by a parallel orientation of the mafic minerals, and to a lesser extent, by elongation of the quartz and feldspar. The nature of this fabric (igneous or metamorphic) is uncertain, as the actual contacts with the surrounding gneisses are either not exposed or are obscured by pegmatites. However, the fabric does appear to be roughly parallel to the contacts with the country rock.

In thin section the granodiorite was seen to be composed mainly of plagioclase with about 30% quartz and trace biotite. The texture is allotriomorphic-granular and consists of an irregular mosaic of interlocking medium- to coarse-grained crystals. Minor areas of cataclastic texture are noticeable along some of the quartz boundaries.

The feldspar is predominantly a thoroughly clouded plagioclase up to 2 mm in width. Relic polysynthetic and Carlsbad twins are often present, however it was not possible to make any accurate composition determinations optically. There is no primary potassium feldspar present, although some microcline was found forming small rims along quartz-plagioclase contacts.

The quartz occurs as smaller crystals ( $\approx 1.5$  mm) and displays marked undulose extinction.

The mafic mineral component is fine-grained biotite. It

occurs as thin to stumpy flakes approximately .5 mm in length. The biotite is altered to a mixture of chlorite and epidote.

### 2.5.3 Mafic Dykes

Mafic dykes have intruded at various stages throughout much of the tectonic history of the thesis area. Unfortunately, the early deformations were of a very intense and penetrative nature. Thus, mafic dykes which intruded prior to the formation of the main gneissic banding ( $S_1$ ) are rarely preserved. Relatively undeformed 'post-tectonic' diabase dykes are more widespread.

#### 2.5.3.1 Deformed Dykes

The intensity of penetrative deformation during the early tectonic interleaving ( $D_1$ ) was such that pre- $D_1$  structural or igneous elements are rarely preserved. To the north of the Hunt River Belt an important small zone of pre- $D_1$  quartzofeldspathic gneiss was found preserved within the banded gneiss terrain. The gneiss in the preserved zone is a weakly banded hornblende-bearing quartzofeldspathic gneiss which is mineralogically identical to the banded gneiss. The weakly-developed layering is subparallel to the dominant layering in the banded gneiss, however actual contact relations are obscured by overburden.

The important feature of the preserved gneiss is that contained within it are a number of irregular amphibolite pods and lenses which are interpreted to be deformed intrusive dykes. These amphibolite pods are discontinuous irregular units up to 1 metre in

thickness and several metres in length. They are highly discordant to the weak layering, and numerous apophysis-like branches extend out into the gneiss (Figure 2.17). The significance of these deformed dykes and their contribution to the structural chronology is discussed in detail in Chapter 4, Section 4.2.

#### 2.5.3.2 Post-tectonic Dykes

At least two ages of relatively undeformed post-tectonic diabase dykes are present in the thesis area including an older NW - SE trending set and a younger NE - SW trending set. The dykes are generally fresh, fine- to medium-grained, non-porphyrific and have very fine-grained chilled margins. Their orientations appear to be controlled by the two major fault or joint systems also trending NW - SE and NE - SW. Although dykes  $\leq 2$  m are common throughout the thesis area, only the largest dykes are shown on the solid geology map (Figure 1.2).

Petrographically the dykes exhibit very fresh ophitic to sub-ophitic diabasic textures defined by euhedral laths of partially altered plagioclase ( $An_{35-58}$ ) and interstitial pyroxene and olivine (Figure 2.18). Both pale green diopsidic pyroxene and light brown augite were identified, although not in the same dyke.

The older NW - SE set of dykes shows evidence of having been emplaced under somewhat tectonically active conditions. In places where the dykes cut quartzofeldspathic gneisses, the gneisses appear to have partially melted and remobilized along zones parallel and adjacent to the dyke contact. These remobilized zones are seldom



FIGURE 2.17: Exposed outcrop of light coloured, weakly-banded hornblende-bearing gneiss in the banded gneiss terrain. The weak fabric runs approximately from left to right in the photo. The irregular black amphibolite pod lying at a high angle to the gneissic fabric is one of several similar pods which are interpreted to be deformed intrusive mafic dyke.

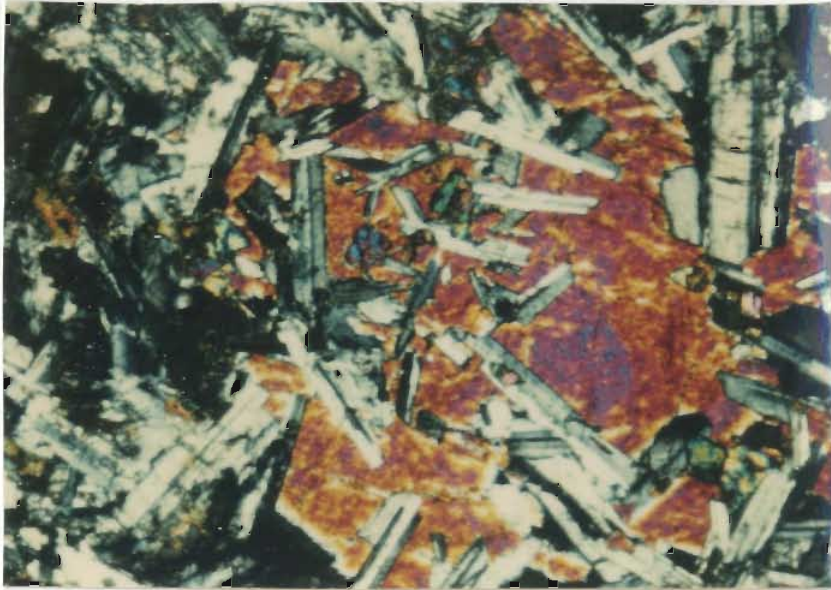


FIGURE 2.18: Photomicrograph showing fresh ophitic textures. Grey laths of plagioclase are embedded in interstitial yellow augite. Some euhedral olivine is also present. (scale X 120). Photo of post tectonic diabase dyke.

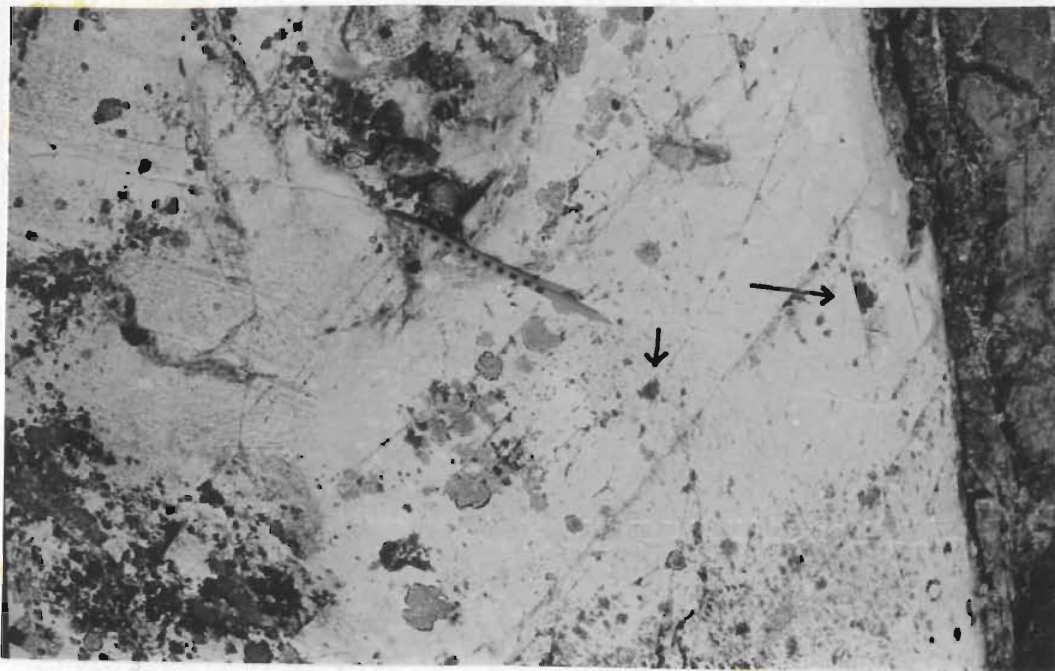


FIGURE 2.19: Diabase dyke (far right) - quartzofeldspathic gneiss contact showing remobilized zone. A small rounded xenolith of the dyke is visible (arrow) below and to the right of the pencil (marked in cm). The gneissic layering is visible on the left side of the photograph.

more than 2 m in thickness. A portion of this remobilized zone is shown adjacent to a chilled margin of a dyke in Figure 2.19. The gneissic layering at the far left of the photograph becomes diffuse and disappears 30 cm from the dyke. In other areas the remobilized gneiss clearly intrudes the diabase dyke, and angular fragments of the dyke are found in several stages of being broken off to be included as xenoliths in the remobilized rock. Where the older NW - SE trending dykes cut through amphibolite schists, a large amount of shearing appears to be associated with the dyke emplacement. More commonly the effects of the shearing are found along the dyke margins. In Figure 2.20 for example, a sinistral movement is evident along the western contact of a NW trending dyke. At this outcrop a chilled margin is still recognizable, however in places the shearing has obliterated the actual contact. Rarely, in the centre of the dykes, thin layers of highly schistose fine-grained amphibolite occur and probably formed in response to the same stresses which deformed the dyke margins. Thermal effects were not recognized in the meta-volcanic amphibolites.

The younger NE - SW trending set of post-tectonic dykes are characterized by unusual jointing features. The joints are generally normal to the dyke-country rock contact. The resultant joint systems are commonly rectangular, and vertically exposed dyke sections sometimes show a spectacular 'building-block' structure. Elsewhere the jointing is of the columnar variety (Figure 2.21). The individual columns often approach perfect hexagonal symmetry.



FIGURE 2.20: Diabase dyke (left side) showing a sheared contact with a foliated amphibolite.



FIGURE 2.21: Post tectonic (post- $D_4$ ) diabase dyke, exhibiting large hexagonal columnar jointing pattern.

#### 2.5.4 Pegmatites

Pegmatites and quartz veins are common throughout the thesis area and range in size from thin bands 1 - 3 mm in thickness to megascopic bodies up to 500 m in thickness.

The earliest recognizable pegmatites occur as small layers (commonly boudinaged) which are co-planar with the dominant gneissic banding ( $S_1$ ). These pegmatites, up to 10 cm in width, rarely show discordant relations with the gneissic banding ( $S_1$ ) except where intrafolial folds are preserved.

It appears from the field evidence (Chapter 4, Section 4.6.4) that much of the pegmatite associated with the younger phases of folding ( $F_2$ ,  $F_3$ , and  $F_4$ ) was emplaced syntectonically and axial planar to the different periods of folding. These pegmatites are in places very large (500 m thick) and show evidence of having been folded and deformed (development of tectonic fabrics) to varying intensities.

The youngest pegmatites in the thesis area have intruded along late stage fault planes. They are generally very coarse-grained (individual feldspar crystals range up to 10 cm across) and are undeformed.

All the early pegmatites observed display a relatively simple mineralogical assemblage and are composed of quartz + K-feldspar + plagioclase + biotite. The late stage pegmatites associated with the faulting however are distinctive in that they contain large books of muscovite ( $\leq 6$  cm thick) and are biotite free.

Pegmatites are often extremely useful in unravelling the tectonic history of a polydeformed gneissic terrain. A discordant

pegmatite or quartz vein may often provide the critical evidence necessary for identifying two separate yet co-axial and/or co-planar phases of deformation. The use of pegmatite and quartz veins in developing the chronological structural history of the Hunt River Belt is discussed in Chapter 4.

CHAPTER 3  
GEOCHEMISTRY

### 3.1 INTRODUCTION

The full value of a geochemical study of a particular geological environment can be realized only when the data is interpreted in conjunction with a sound knowledge of the field relations of the rocks involved. This is most important in geochemical studies of high grade gneiss terrains. The main difficulties encountered in such studies are:

1. mobility of elements during metamorphism,
2. contamination of rocks through pegmatite veining, and
3. structurally controlled interlayering of completely unrelated rock units on a scale as small as tens of centimetres.

Interpretations in the following geochemical discussion are based on a thorough knowledge of the structural and metamorphic development of the Hunt River Belt.

#### 3.1.1 Analytical Methods

Major and trace elements were analyzed in 92 specimens from the thesis area. Representative samples were selected from all the rock types described in Chapter 2. The rock specimens showed very little alteration in thin section and were free of secondary quartz and epidote veins. Some difficulty was encountered in collecting representative samples from the quartzofeldspathic gneisses because of their coarse pegmatite veining and mesoscopic heterogeneity.

The major oxides  $\text{SiO}_2$ ,  $\text{TiO}_2$ ,  $\text{Al}_2\text{O}_3$ , total Fe, MgO, CaO,  $\text{K}_2\text{O}$ , and trace elements were analyzed using x-ray fluorescence methods with a Phillips PW 1220c computerized spectrometer. MnO and  $\text{Na}_2\text{O}$

were determined by standard atomic absorption procedures using a Perkin Elmer 303 Atomic Absorption Spectrometer. FeO was determined by visual titration following the method of Maxwell (1968).  $Fe_2O_3$  was then calculated using the FeO (total iron) value derived from the XRF. Loss on ignition was determined by heating .5 gm of -200 mesh powdered sample in a Thermolyne furnace. Precision and accuracy of the analytical methods are given in Table 3.4.

### 3.2 HUNT RIVER BELT

The Hunt River Belt offers an excellent opportunity to study in detail critical problems related to the geological evolution of early Archean supracrustal sequences within high grade gneiss terrains. Such problems include: (1) assessing the relationship of the ultramafic lenses to the amphibolites (meta-volcanics) and determining if the ultramafic lenses originated as contemporaneous extrusives within the volcanic pile, or as sills intrusive into the volcanic succession, (2) determining the primary nature of the amphibolites, and (3) assessing the nature and environment of deposition of the minor, although significant meta-sediments in the supracrustal sequence.

The chemical characteristics of the mineralogical variations in the amphibolites are described and the limitations of applying the data to a geochemical evaluation are discussed. The Hunt River meta-volcanics are also compared to other volcanic terrains in order to evaluate the chemistry in terms of the tectonic environment of deposition.

TABLE 3.1: Precision and accuracy of analytical data.

Oxide (wt. %)	N	R	X	S
SiO <sub>2</sub>	16	53.21 - 54.86	53.97	.2097
TiO <sub>2</sub>	16	2.20 - 2.24	2.22	.0014
Al <sub>2</sub> O <sub>3</sub>	16	13.51 - 13.85	13.70	.0119
Fe <sub>2</sub> O <sub>3</sub>	16	12.44 - 13.45	13.18	.1023
MgO	16	2.95 - 3.83	3.36	.0566
CaO	16	6.92 - 7.08	7.03	.0004
K <sub>2</sub> O	16	1.66 - 1.77	1.72	.0006
P <sub>2</sub> O <sub>5</sub>	16	0.32 - 0.47	0.37	.0008

Element (ppm)	N	R	X	S
Zr	7	117 - 135	125.4	6.43
Sr	7	91 - 100	94.6	3.21
Rb	7	49 - 53	50.3	1.60
Zn	7	25 - 26	25.7	0.49
Cu	7	13 - 18	15.7	1.70
Ba	7	964 - 1073	1018.1	44.12
Nb	7	12 - 16	14.0	1.53
Ni	7	11 - 12	11.6	0.53
Cr	7	10 - 19	11.4	3.33

N     Number of determinations  
R     Range = maximum-minimum concentration obtained  
X     Mean concentration  
S     Standard deviation from the mean  
Fe<sub>2</sub>O<sub>3</sub> = total iron as Fe<sub>2</sub>O<sub>3</sub>

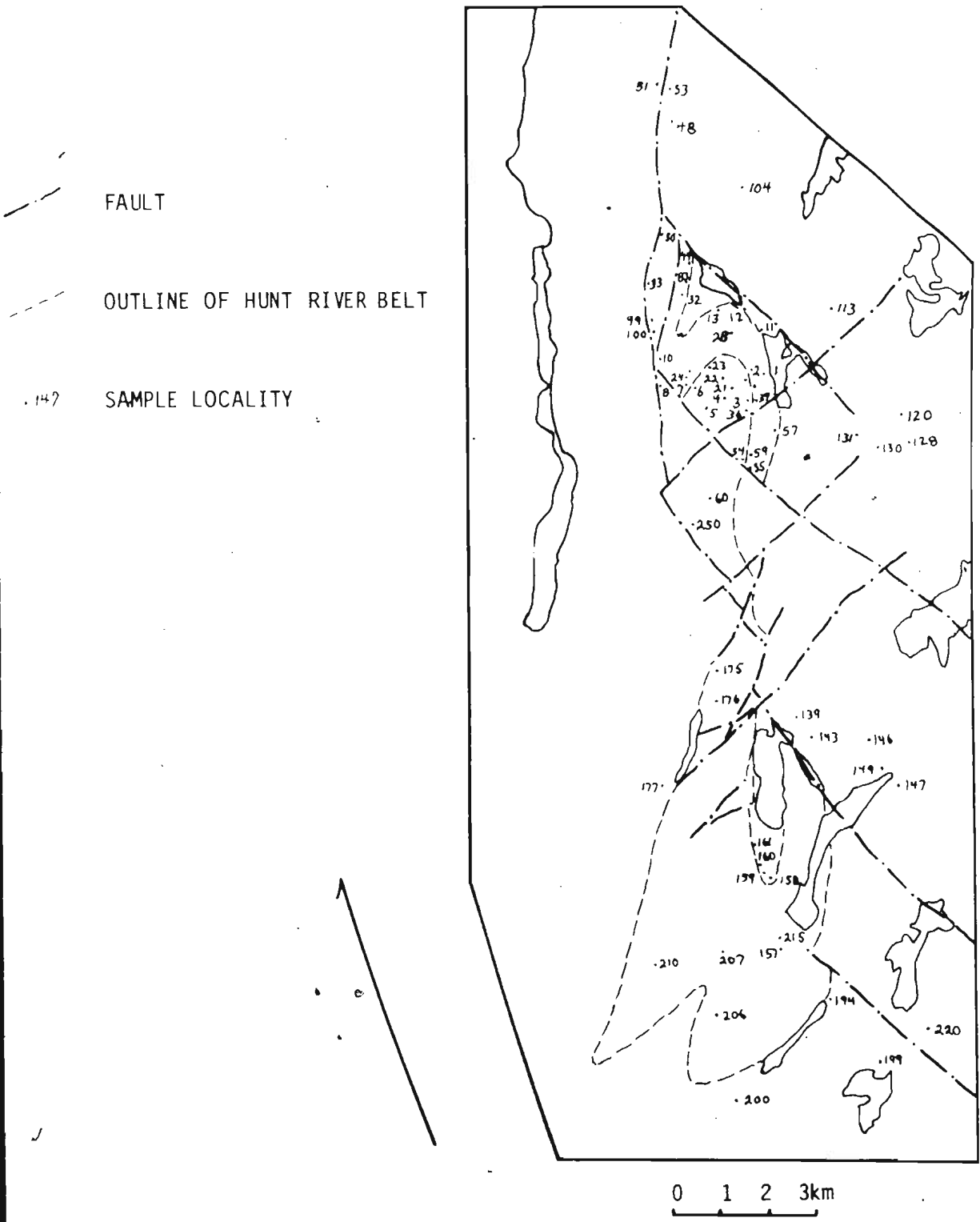


FIGURE 3.0: Localities of geochemical samples.

### 3.2.1 Ultramafics

The chemical analyses of the ultramafic rocks are presented in Table 3.2. When the major elements are plotted on silica variation diagrams (Figure 3.1) the ultramafics lie in fields distinct from those occupied by the amphibolites. The ultramafics are strongly depleted in all trace elements except Ni and Cr, which are anomalously high (averaging 2000 ppm and 3000 ppm respectively). This contrasts with the trace element distribution in the mafic volcanics (cf. Tables 3.2, 3.5 and 3.6). The three ultramafic schists show clear geochemical and mineralogical differences, however, the hornblende and tremolite schists lack meaningful field relations and therefore they do not warrant further chemical study.

Considering the ultramafics as a whole, the chemical data suggests that the ultramafics and amphibolites are not syn-volcanic. Thayer (1967), in a study of an 'alpine-type' ultrabasic-basic association, demonstrated a completely transitional chemical relationship between peridotites, gabbros and basalts. Likewise, Glikson (1970) showed that the volcanics of the Archean Kalgoorlie System, Western Australia, included a series of rock types chemically transitional from ultrabasic and basic rocks into intermediate and acid rocks. If the ultramafics were genetically related to the amphibolites in the Hunt River Belt, a transitional trend between the two should be apparent. The ultramafics show chemical characteristics quite different from the amphibolites and thus are interpreted to have intruded as sills or sheets after the deposition of the main bulk of the supracrustal sequence.

#### 3.2.1.1 Serpentinite Schist

A geochemical study of the serpentinite schist was undertaken

TABLE 3.2: Chemical analyses and C.I.P.W. Norms of the ultramafic rocks from the Hunt River Belt.

WJ-73-	SERPENTINITE SCHIST										HORNBLende SCHIST		TREMOLITE SCHIST
	10	10C	10Q	10E	10F	10W	44A	44B	83	83A	1C	7C	250
SiO <sub>2</sub>	38.60	43.90	38.20	39.10	43.40	37.80	38.20	36.20	37.10	35.80	43.66	46.63	46.78
TiO <sub>2</sub>	0.05	0.05	0.08	0.02	0.02	0.10	0.20	0.10	0.05	0.06	0.41	0.46	0.43
Al <sub>2</sub> O <sub>3</sub>	1.00	0.64	0.34	0.64	1.20	1.43	1.66	1.35	0.80	0.44	3.64	4.52	7.93
Fe <sub>2</sub> O <sub>3</sub>	6.58	6.63	8.32	3.98	4.15	5.27	5.88	8.98	7.63	7.63	2.47	1.08	1.19
FeO	3.92	2.14	4.18	1.44	4.20	2.32	6.42	5.87	2.08	2.26	9.79	3.09	8.66
MnO	0.08	0.13	0.06	0.05	0.13	0.06	0.19	0.23	0.05	0.65	0.21	0.21	1.70
MgO	38.52	36.44	39.70	40.44	36.74	39.41	35.36	34.52	39.41	39.41	17.74	21.58	21.91
CaO	0.08	0.35	---	0.22	1.51	0.30	0.63	1.76	0.59	0.67	11.59	15.42	4.78
Na <sub>2</sub> O	0.10	0.11	0.10	0.08	0.13	0.08	0.08	0.08	0.08	0.07	0.23	0.48	0.10
K <sub>2</sub> O	0.01	0.01	0.01	0.01	0.01	0.01	0.01	0.01	0.01	0.01	0.05	0.08	0.02
P <sub>2</sub> O <sub>5</sub>	n.m.	n.m.	n.m.	n.m.	n.m.	n.m.	n.m.	n.m.	n.m.	n.m.	0.16	0.20	0.09
L.O.I.	11.96	9.12	13.42	13.50	8.73	12.76	11.38	11.18	13.14	13.58	7.86	4.90	5.70
TOTAL	100.89	99.59	100.08	100.05	100.20	99.53	100.20	100.27	100.93	99.96	97.81	98.61	99.18
Zr (ppm)	16	14	12	18	18	16	22	21	14	14	27	26	25
Sr	25	23	21	24	31	25	22	23	23	22	50	52	25
Rb	15	15	12	15	16	15	14	11	11	16	13	13	13
Zn	38	43	29	30	52	37	90	84	25	30	39	65	126
Cu	30	39	9	9	31	13	10	7	7	8	694	185	26
Ba	--	--	2	--	9	--	24	17	20	--	36	28	23
Mb	8	9	6	10	9	8	8	9	8	7	9	8	9
Ni	2512	1724	2921	2125	1731	1858	1667	1283	2543	2279	647	372	424
Cr	3236	3618	3059	3251	4022	3708	2736	3086	2263	2339	2362	3068	2285
K	83	83	83	83	83	83	83	83	83	83	415	664	166
Tl	300	300	480	120	120	599	1199	599	300	360	2458	2758	2578
K/Rb	6	6	7	6	5	6	6	8	8	5	32	51	13
C.I.P.W. Norms													
Q													
Or	0.07	0.06	0.06	0.07	0.06	0.07	0.07	0.07	0.07	0.07	0.33	0.50	0.13
Ab	0.95	1.02	0.92	0.78	1.19	0.78	0.76	0.76	0.77	0.68	2.16	4.31	0.90
An	0.46	1.35	0.07	1.28	2.89	1.72	3.53	3.68	2.04	0.98	9.69	10.55	22.49
Me													
Co	0.75		0.16	0.11		0.84	0.41						
Ol		0.45			4.12			4.76	1.01	2.21	42.41	54.38	1.72
Hy	32.92	56.49	29.10	30.87	42.53	27.87	32.39	22.77	23.06	18.42	24.32	3.92	60.82
Ol	53.30	30.20	55.63	60.00	41.69	59.23	52.18	52.48	61.54	65.11	15.29	22.56	10.49
Mt	10.67	7.01	13.18	4.65	6.53	7.51	9.58	14.54	7.05	9.97	3.97	1.66	1.84
Il	0.11	0.10	0.17	0.04	0.04	0.22	0.43	0.21	0.11	0.13	0.86	0.93	0.87
He		2.46		1.39		0.86			3.79	1.86	--	--	--
Cr	0.78	0.86	0.72	0.81	0.94	0.91	0.66	0.74	0.55	0.58	0.56	0.70	0.52

n.m. not measured

--- not detected

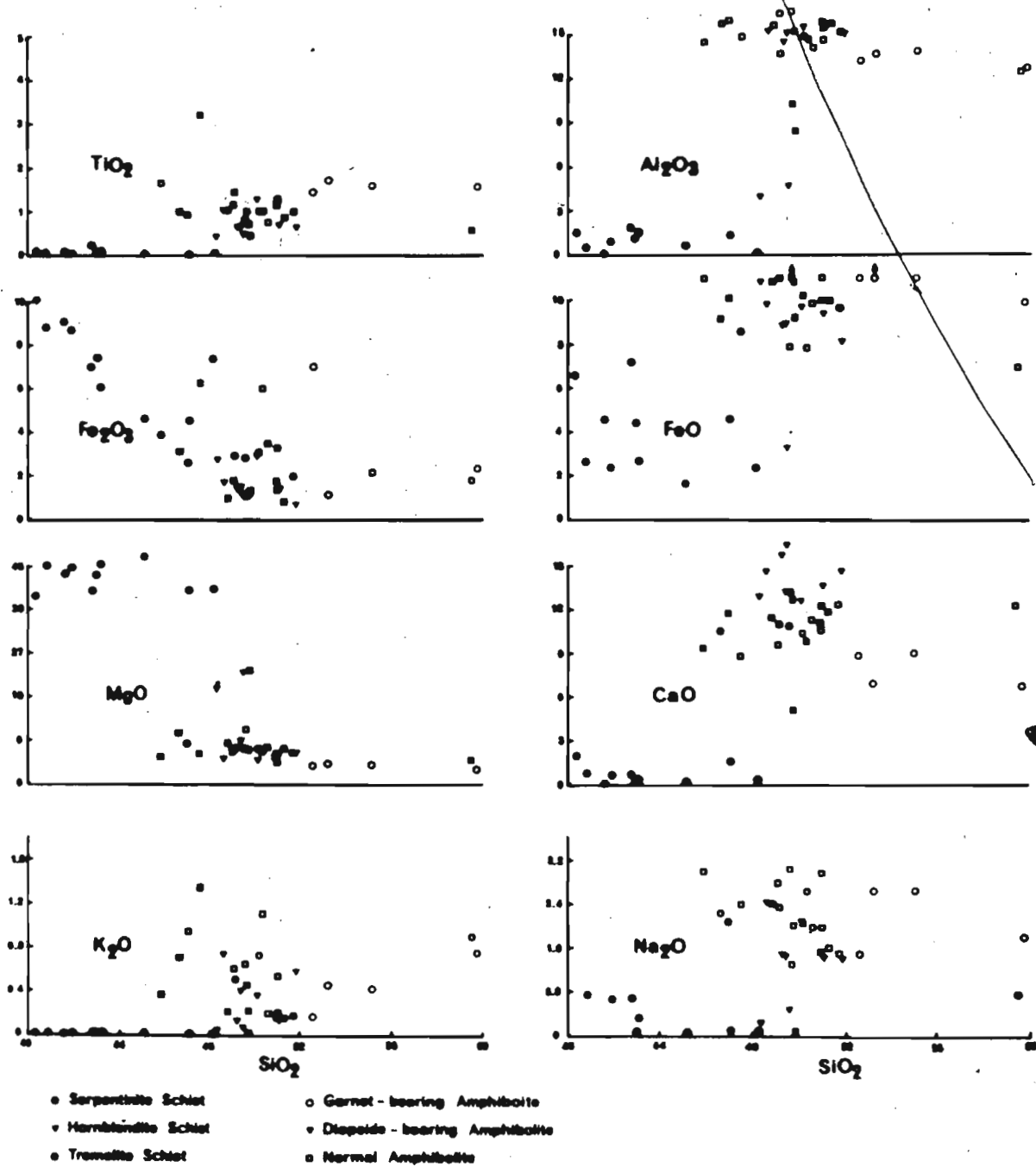
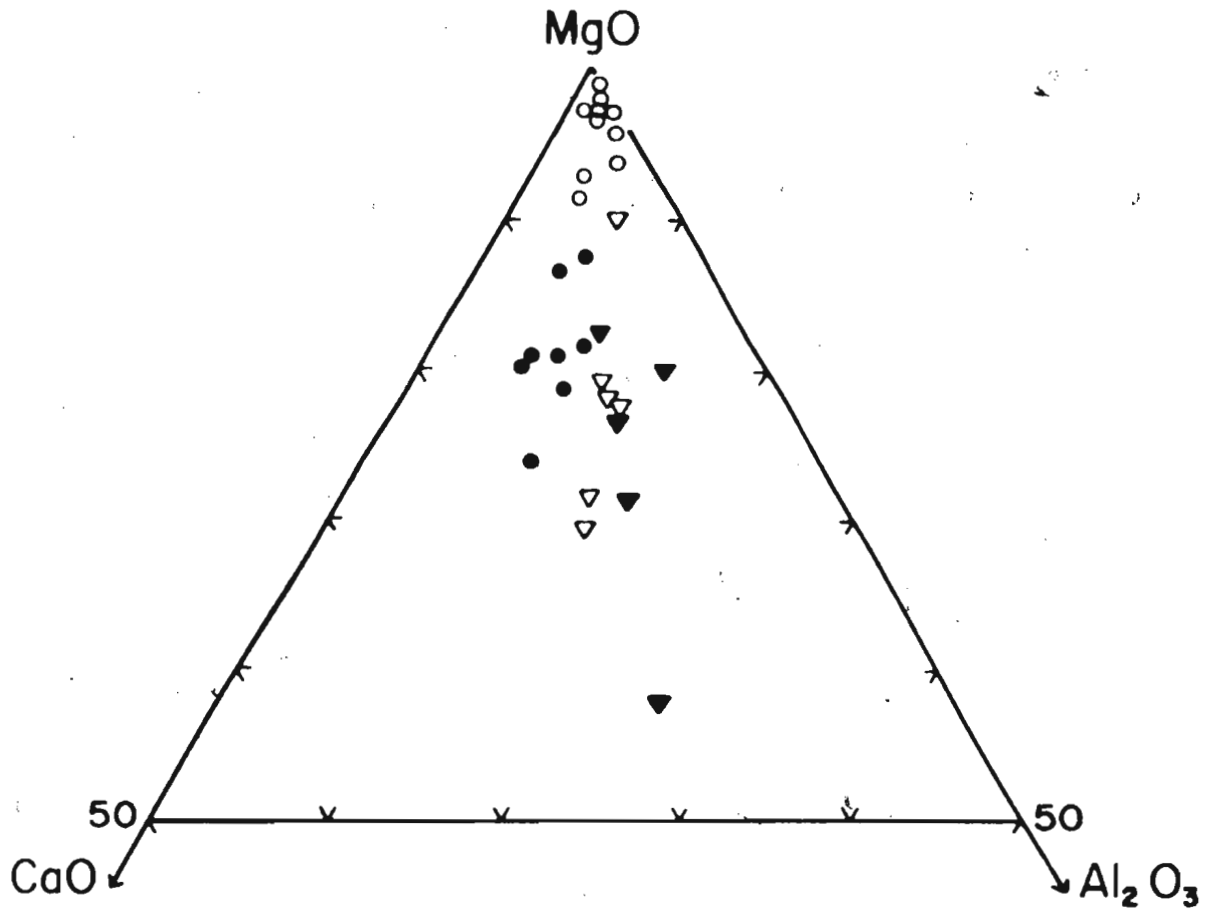


FIGURE 3.1: Major element variations vs. SiO<sub>2</sub> in wt.% for the mafic and ultramafic rocks from the Hunt River Belt.

because in outcrop it commonly exhibits strikingly fresh-looking blocky patches of euhedral, elongate olivine crystals as shown in Figures 2.7, 2.8 and 2.9. Textures in ultramafic rocks characterized by extremely coarse skeletal, platy or blade-like crystals in olivine and pyroxene have received much attention in the recent past. The major occurrence of these textures, known as 'spinifex', is found associated with Archean ultramafic lava flows (Viljoen and Viljoen, 1969a; Nesbitt, 1971; Pyke et al., 1973). Harrisitic textures, comparable in many respects to the spinifex, are less commonly known but are nonetheless well documented (Robins, 1973; Donaldson, 1974). Similar textures are also postulated to have been produced by metamorphic processes (Matthes, 1971; Oliver et al., 1972; Evans and Trommsdorff, 1974).

Chemical analyses of rocks from three of the lenses which exhibit these textures are presented in Table 3.2. Four of the analyzed specimens (WJ-73-10D, -10C, -10E, and -10F) retain varying amounts (up to 30%) of the original mineralogy (olivine and orthopyroxene) and exhibit undeformed, large, elongate crystals. Specimens WJ-73-83 and -83A are completely serpentized but still display recognizable coarse bladed crystal textures, in a highly deformed state. The remaining rocks are completely serpentized, highly schistose, with no preserved coarse crystal texture. No major differences in bulk chemistry between the variably altered and the deformed rocks are revealed in Table 3.2.

When analyses from Table 3.2 are plotted on a  $MgO-CaO-Al_2O_3$  ternary diagram (Figure 3.2) together with analyses of ultramafic rocks



○ HUNT RIVER BELT

BARBERTON MOUNTAIN LAND, SOUTH AFRICA

● (Viljoen and Viljoen, 1969, Table 1, analyses 1-8)

SCOTIA AND MT. IDA, AUSTRALIA

▽ (Nesbitt, 1971, Table 11, analyses 1-4, 5 and 6)

MUNRO AND DUNDONALD TOWNSHIPS, CANADA

▽ (Pyke *et al.*, 1973, Table 1, analyses 1-3, 6 and 7)

FIGURE 3.2: MgO - CaO - Al<sub>2</sub>O<sub>3</sub> ternary diagram comparing the Hunt River Belt serpentinite schist to spinifex-bearing ultramafic rocks from Canada, Australia and South Africa.

from South Africa (Viljoen and Viljoen, 1969a; Table 1), Canada (Pyke et al., 1973; Table 1) and Australia (Nesbitt, 1971; Table 2) it is apparent that the Hunt River analyses differ markedly from occurrences elsewhere. They lie close to the MgO apex and show a spread towards the CaO-Al<sub>2</sub>O<sub>3</sub> base which may be indicative of a fractionation trend towards the other less MgO-rich, but still ultramafic, compositions represented in the analyses from the other terrains.

The CaO content of olivine from the Hunt River Belt (Table 3.3) is significantly lower than values quoted for igneous olivine from Barberton Mountain Land, South Africa (Nesbitt, 1971) and Munro Township, Canada (Pyke et al., 1973) and is similar to values quoted for olivines of unequivocal metamorphic origin (Oliver et al., 1972; Trommsdorff and Evans, 1972). This could be accounted for by the fact that the absolute CaO contents of olivine in ultramafic rocks is largely controlled by the availability of CaO in the host rock and by the composition of other phases in the system.

Comparison of  $\text{CaO}_{(\text{host rock})} / \text{CaO}_{(\text{olivine})}$  ratios shows that the Hunt River values fall within the range of values obtained from olivine which crystallized from ultrabasic igneous melts (Table 3.4). These values are lower than those obtained from the available data for olivines which were formed in metamorphic systems (Table 3.4)

In considering the nature of the elongate olivine textures from the Hunt River Belt two important points should be kept in mind.

1. Any original igneous intrusive relations or morphological structures such as flow tops formed during the emplacement of the ultrabasics have been largely destroyed during metamorphism and tectonism and

TABLE 3.3: Microprobe analysis of olivine  
from ultramafic rock WJ-73-10E (Table 3.2).

---

---

SiO <sub>2</sub>	39.01
TiO <sub>2</sub>	0.00
Al <sub>2</sub> O <sub>3</sub>	0.00
FeO	10.25
MgO	50.23
MnO	0.16
CaO	0.02
TOTAL	99.67

---

Structural formula based on 4 oxygen atoms:

Si	0.965
Ti	0.000
Al	0.000
Cr	0.000
Fe <sup>2+</sup>	0.212
Mn	0.003
Mg	1.853
Ca	0.001

Fo (Molecular percent) = 89.6

---

*Analyst : Dr. C. Klein, Jr.*

*Analysis : average of two spot analyses*

TABLE 3.4: Comparison of  $\text{CaO}_{(\text{host rock})} / \text{CaO}_{(\text{olivine})}$  ratios .

Locality	Source	Ratio
IGNEOUS ROCKS		
Hunt River Belt	this thesis	11.00
Munro Township	Pyke <u>et al.</u> , (1973)	10.32
Munro Township	Pyke <u>et al.</u> , (1973)	15.59
Barberton Mountain Land	Nesbitt (1971)	61.39
METAMORPHIC ROCKS		
Malenco (Italy)	Trommsdorff and Evans (1972)	60.00
Malenco (Italy)	Trommsdorff and Evans (1972)	115.00
Malenco (Italy)	Trommsdorff and Evans (1972)	195.00

therefore the Labrador field relations of the ultramafic rocks are of little value in determining their original environment of formation (cf. Pyke et al., 1973; Donaldson, 1974).

2. Since the rise in popularity of Archean ultramafic lava flows with 'quench textures' and spinifex textures (Viljoen and Viljoen, 1969; Williams, 1972; Pyke et al., 1973) there has been a tendency for workers studying the North Atlantic Craton to ascribe ultrabasic lenses associated with amphibolitic rocks as having originated as co-magmatic lava flows (Bridgwater et al., 1973a; Bridgwater, 1970; Dawes, 1970). If any of the elongate olivines in the serpentinite schist formed during the initial deposition of the volcanic protoliths, then the preservation of the textures through such a prolonged and intense history of deformation is remarkable indeed.

There has been considerable discussion about the origin of the ultramafic and ultrabasic lenses from southwestern Greenland. Rivalenti and Rossi (1972) suggest as 'alpine-type' origin while Misar (1973) considers the lenses to be part of an ophiolite series. These interpretations are based mainly on indirect field evidence, as primary igneous relations and textures have been completely destroyed by the intense nature of deformation and metamorphic recrystallization.

In the Hunt River Belt the ultramafics are thought to have been emplaced at a period in time after the main volcanic sequence was deposited. This interpretation is based on several lines of evidence. The presence of discordant contacts between certain of the ultramafics and the amphibolites (Figure 2.5) suggests an intrusive relation between the two rock types. The bulk major and trace element patterns of the

ultramafics are completely different from the chemistry of the amphibolites (Section 3.2.1). Certain of the textures involving euhedral olivines with interstitial enstatite bear a strong resemblance to an igneous cumulate texture, which could explain some of the chemical peculiarities of the rocks found, for example, in Figure 3.1. A comparison of olivine CaO content of rocks from the thesis area with igneous olivines and metamorphic olivines (Tables 3.3 and 3.4) shows that a strong correlation exists between igneous olivines and the elongate olivines from the Hunt River Belt.

### 3.2.2 Meta-volcanics (amphibolites)

Geochemical variations in the Hunt River meta-volcanics may reflect primary lithological variations in the original protoliths, or may be the result of metamorphic segregation of elements during the deformation and metamorphism of the Belt.

In geochemical studies carried out on other Archean volcanic terrains metamorphosed to greenschist or amphibolite facies (Clifford and McNutt, 1971; Smith and Longstaffe, 1974) it is generally assumed that metamorphism is largely isochemical (Glikson, 1970, p.398). Chemical trends apparent in certain of the linear and triangular variation diagrams therefore are interpreted to reflect original volcanic differentiation trends.

The metamorphic grade of the thesis area is predominantly within the amphibolite facies, although retrogression to greenschist facies occurs locally. There is no evidence to indicate that the rocks have been influenced by crustal migration of certain elements (U, Th,

K, Rb, Ba) either in response to a previous granulite facies metamorphic event or by an unexposed underlying granulite facies terrain.

### 3.2.2.1 Chemical Control on Mineralogy

Chemical analyses of the three major groups of amphibolites are presented in Tables 3.5 and 3.6. The three groups are characterized by their distinctive bulk chemistry. The diopside-bearing amphibolite is readily distinguished by a relatively high CaO content (averaging 13.75%) compared to an average CaO of 10.90% for the normal amphibolite. The diopside-bearing amphibolite exhibits relatively low TiO<sub>2</sub> (0.63%) and FeO (8.90%) compared to normal amphibolite with TiO<sub>2</sub> and FeO averaging 1.05% and 10.60% respectively. The garnet-bearing amphibolite is also characterized by a relatively low CaO content of 7.99%. Other chemical characteristics of the garnet-bearing amphibolite include high SiO<sub>2</sub> (averaging 52.22% compared to 48.30% SiO<sub>2</sub> for normal amphibolite) and slightly lower Al<sub>2</sub>O<sub>3</sub> and MgO contents than the other two varieties of amphibolite.

These chemical-mineralogical relations are very similar to those observed in southwestern Greenland. Kalsbeek and Leake (1970), in a study of basement gneisses and amphibolites in an area between Ivigtut and Frederikshab, concluded that the mineralogy was strongly dependent upon a suitable lithological composition. Metamorphism in the area is interpreted to have been isochemical (Rivalenti, 1975a) and thus the distinctive chemical groupings may well represent lithologic variations in the original volcanic pile. The garnet-bearing

TABLE 3.5: Chemical analyses and C.I.P.W. Norms of the normal amphibolite from the Hunt River Belt.

NORMAL AMPHIBOLITE												
WJ-73-	11B	13	24	32B	39C	54D	54E	57	59	60	206B	207
SiO <sub>2</sub>	48.12	46.36	49.65	47.11	48.12	50.54	44.40	49.46	47.98	49.78	47.93	50.10
TiO <sub>2</sub>	1.00	0.89	1.20	1.09	0.69	0.97	1.59	0.72	1.05	1.22	1.40	0.83
Al <sub>2</sub> O <sub>3</sub>	15.36	15.73	14.16	15.72	14.66	14.72	13.95	13.70	14.85	15.00	13.34	15.29
Fe <sub>2</sub> O <sub>3</sub>	0.93	2.54	1.28	1.71	1.11	1.89	3.74	3.32	1.61	3.16	2.81	0.76
FeO	10.65	9.92	10.78	10.60	10.43	9.41	14.97	9.58	10.55	9.72	11.11	9.72
MnO	0.23	0.22	0.20	0.24	0.21	0.20	0.31	0.22	0.20	0.34	0.22	0.18
MgO	8.13	8.05	5.77	6.71	6.82	6.00	5.29	7.41	5.22	4.28	6.96	7.17
CaO	11.20	11.58	11.90	9.16	12.18	11.98	9.00	11.00	10.37	10.27	10.69	11.51
Na <sub>2</sub> O	2.38	2.05	1.92	2.68	1.95	1.48	2.91	1.94	1.45	2.90	2.29	1.57
K <sub>2</sub> O	0.21	0.93	0.19	0.58	0.21	0.17	0.35	0.19	0.15	0.52	0.49	0.15
P <sub>2</sub> O <sub>5</sub>	0.26	0.31	0.21	0.27	0.26	0.26	0.27	0.20	0.60	0.22	0.22	0.26
L.O.I.	2.32	2.46	1.79	2.87	3.02	2.17	2.59	1.98	1.89	2.13	1.79	1.81
TOTAL	100.79	101.04	99.05	98.74	99.66	99.79	99.06	99.64	95.92	99.63	99.22	99.35
Zr (ppm)	50	50	51	60	39	47	54	43	55	62	96	43
Sr	94	116	147	151	84	108	224	86	111	115	309	88
Rb	27	36	17	30	18	15	20	15	15	25	15	21
Zn	100	104	64	83	84	93	123	71	83	127	114	78
Cu	61	30	226	81	60	73	119	92	125	52	97	94
Ba	120	146	74	156	81	134	114	55	79	135	169	108
Nb	9	8	10	10	9	10	10	10	9	10	11	12
Mf	104	126	87	108	117	110	72	85	117	80	105	107
Cr	394	464	144	589	583	294	14	97	311	349	261	424
K	1743	7720	1577	4815	1743	1411	2906	1557	1245	4317	4068	1245
Tl	5996	5336	7194	6535	4137	5815	9532	4316	6295	7314	8393	4976
K/Rb	65	214	93	161	97	94	145	104	83	173	271	59
C.I.P.W. Norms												
O			2.59					2.47	6.45	1.88		3.06
Or	1.26	5.75	1.15	3.57	1.28	1.03	2.14	1.15	0.94	3.15	2.97	0.91
Ab	20.44	17.58	16.70	23.63	17.06	12.82	25.43	16.79	13.04	25.17	19.87	13.61
An	31.06	31.39	30.27	30.37	31.60	33.80	24.76	28.75	35.67	27.06	25.30	35.07
Me												
Co												
Di	19.50	20.40	24.21	12.63	24.12	20.99	16.59	21.15	21.47	19.92	22.95	17.95
Hy	10.07	0.48	20.28	12.56	17.95	19.70	2.32	22.87	25.27	15.14	17.14	25.95
Ol	13.67	18.31		11.72	4.16		19.39				4.29	
Mt	1.37	3.73	1.91	2.58	1.66	2.81	5.60	4.92	2.48	4.70	4.18	1.13
Il	1.93	1.71	2.34	2.16	1.35	1.89	3.12	1.40	2.12	2.36	2.73	1.61
Cr	0.09	0.10	0.03	0.13	0.13	0.06		0.02	0.07	0.08	0.06	0.09
Ap	0.61	0.73	0.50	0.65	0.62	0.62	0.65	0.48	1.48	0.52	0.52	0.62

TABLE 3.6: Chemical analyses and C.I.P.W. Norms of garnet-bearing amphibolite and diopside-bearing amphibolite from the Hunt River Belt.

WJ-72-	GARNET-BEARING AMPHIBOLITE			DIOPSIDE-BEARING AMPHIBOLITE					
	1R	54C	215	1	2	7A	8	28	157
S <sub>10</sub> O <sub>2</sub>	53.62	51.44	51.61	49.21	49.65	48.80	49.11	50.49	47.18
TiO <sub>2</sub>	0.54	1.40	1.64	0.66	0.70	0.64	0.12	0.62	1.01
Al <sub>2</sub> O <sub>3</sub>	13.37	12.82	13.16	15.07	14.78	14.35	15.12	14.60	14.83
Fe <sub>2</sub> O <sub>3</sub>	2.07	6.83	1.10	1.48	1.35	1.44	2.86	0.68	1.68
FeO	10.76	11.21	14.94	8.89	9.14	8.78	9.46	7.92	9.51
MnO	0.20	0.21	0.26	0.23	0.22	0.21	0.20	0.23	0.20
MgO	3.96	3.84	4.24	8.91	6.16	7.56	4.95	6.27	4.98
CaO	8.69	8.59	6.70	13.11	13.24	15.51	12.30	14.18	14.12
Na <sub>2</sub> O	2.59	1.48	2.58	1.44	1.40	1.49	2.05	1.37	2.38
K <sub>2</sub> O	0.41	0.27	0.44	0.40	0.14	0.13	0.35	0.56	0.72
P <sub>2</sub> O <sub>5</sub>	0.12	0.17	0.20	0.07	0.25	0.09	0.38	0.32	0.32
L.O.I.	2.41	1.29	2.10	1.13	2.78	1.65	2.56	2.12	3.10
TOTAL	99.74	99.55	98.97	100.60	99.81	100.65	100.58	99.27	100.03
Zr (ppm)	67	52	62	39	41	39	n.m.	39	61
Sr	72	46	87	99	80	101	164	110	172
Rb	17	15	20	22	14	16	15	29	39
Zn	110	157	114	74	86	72	104	67	97
Cu	136	40	11	130	27	97	61	123	160
Ba	158	70	144	184	182	30	29	125	164
Nb	9	9	8	9	10	9	n.m.	9	9
W	48	41	52	116	110	115	90	115	97
Cr	46	18	34	625	751	547	181	578	345
K	3404	1411	3653	3321	1162	1079	2906	4649	5977
Tl	9232	8393	9832	3957	4196	3838	4734	3717	6055
K/Rb	200	94	182	151	83	67	194	160	153
C.I.P.W. Norms									
Q	9.88	5.83			4.04		3.25	3.38	
Or	2.48	2.68		2.37	0.85	0.78	2.11	3.40	4.39
Ab	22.52	22.53		12.24	12.19	12.72	17.71	11.91	17.31
An	24.30	23.77		33.62	34.62	32.38	31.66	32.91	28.51
Ne									1.87
Co									
Dl	16.20	7.89		25.54	25.94	36.68	23.41	30.71	34.69
Hy	18.23	31.96		17.90	18.22	9.57	14.28	14.58	
Ol				4.62		4.21			7.90
Mt	3.08	1.65		2.15	2.01	2.11	4.23	1.01	2.51
Il	3.00	3.21		1.62	1.37	1.23	2.40	1.21	1.98
Cr	0.01	0.01		0.14	0.17	0.12	0.04	0.13	
Ap	0.29	0.48		0.16	0.60	0.21	0.90	0.76	0.77

n.m. not measured

amphibolites, however, may have acquired some of their distinctive chemistry through contamination by mixing with sediments (Kalsbeek and Leake, 1970). This may also account for the formation of the garnet-bearing amphibolite in the Hunt River Belt.

Although trace elements may not have a significant control on the mineralogy, it is interesting to note that the three amphibolite types in the Hunt River Belt display no systematic variation in trace element contents. The only exception is that the garnet-bearing amphibolite is quite depleted in Ni and Cr, which may also be a result of mixing with sediments (Heier, 1962).

#### 3.2.2.2 Major Element Chemistry

Chemical analyses of representative amphibolites from the Hunt River Belt are given in Tables 3.4 and 3.5. They display a restricted range of  $\text{SiO}_2$  values (49%-52%) which is similar to other Archean volcanic terrains (cf. Rivalenti, 1975a). The  $\text{SiO}_2$  frequency curve for the Yellowknife Group in the Slave Province (Baragar, 1966, p.21) shows a maximum at about 52% and falls off very sharply with increasing silica. Volcanic belts in the Kalgoorlie-Norseman district of the Eastern Goldfields region, Western Australia, are made up of basalts ( $\text{SiO}_2 \approx 51\%$ ) almost to the exclusion of "intermediate rocks" (Hallberg, 1972). In contrast, major oxide frequency curves for the Noranda Volcanic Belt in the Superior Province (Baragar, 1968) display a relatively large proportion of intermediate and felsic volcanics.

Plots of major oxides against  $\text{SiO}_2$  are shown in Figure 3.1.  $\text{Al}_2\text{O}_3$  and  $\text{MgO}$  appear to decrease with increasing  $\text{SiO}_2$ , however the

relatively strong linear pattern shown by  $\text{Al}_2\text{O}_3$  may be in part due to the restricted range of  $\text{Al}_2\text{O}_3$  values, as well as reflecting a true chemical trend. The plots shown by  $\text{FeO} + \text{Fe}_2\text{O}_3$ ,  $\text{CaO}$ ,  $\text{Na}_2\text{O}$  and  $\text{K}_2\text{O}$  show no distinctive variation with  $\text{SiO}_2$  which suggests that these elements reacted to metamorphism with a relatively higher degree of mobility than  $\text{Al}_2\text{O}_3$  and  $\text{MgO}$ .

Variation diagrams in Figure 3.1 are not, by themselves, very useful in interpreting the primary chemical character of the meta-volcanics. They do indicate that metamorphism has affected the chemistry to such an extent that any linear or curvilinear differentiation patterns which may have been present are virtually obliterated. They also indicate that some of the more fundamental chemical differences may have been preserved (Gunn, 1975). Therefore chemical plots in which certain broad 'fields' or 'areas' are significant may be more useful in understanding the geochemistry of the meta-volcanics. In this way a certain amount of metamorphic homogenization of the chemistry would not significantly alter the overall position of the plots of the analyses in the diagrams. For example, by plotting the total alkalis ( $\text{Na}_2 + \text{K}_2\text{O}$ ) against  $\text{SiO}_2$  (as in Figure 3.3) the analyses may lie either in an alkaline field or a sub-alkaline field. The two fields are so broad that small scale migration of elements would not move the plots unless they were right on or very close to the MacDonald and Katsura (1964) dividing line from one field to the other. Indeed, metamorphism and metasomatism would have to be very intense to move the majority of sub-alkaline plots into the alkaline field. In Figure 3.3 the Hunt River amphibolites plot well into the sub-alkaline field. Therefore, even though subjected

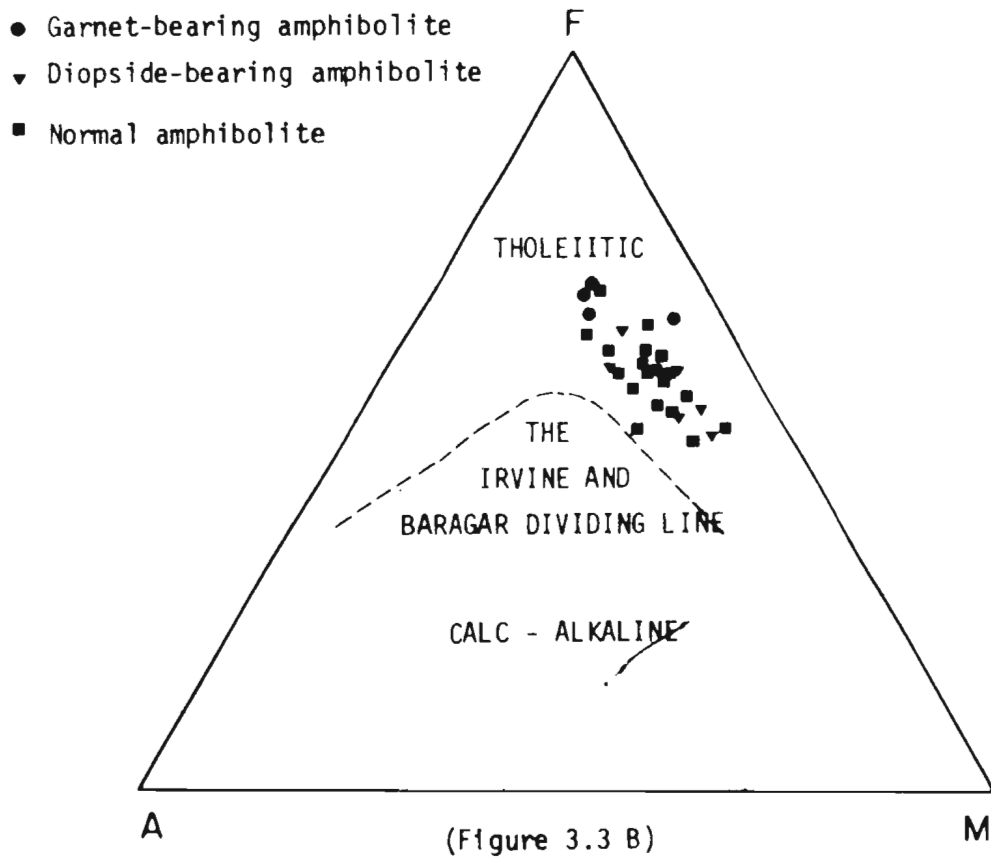
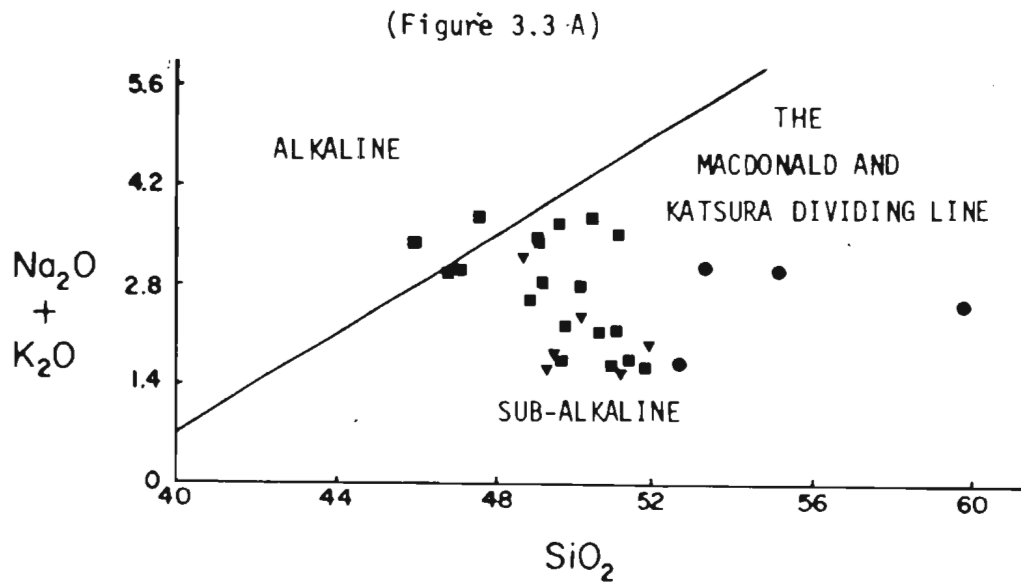


FIGURE 3.3 A: Na<sub>2</sub>O + K<sub>2</sub>O - SiO<sub>2</sub> variation diagram for the three varieties of amphibolite in the Hunt River Belt.

FIGURE 3.3 B: A(Na<sub>2</sub>O + K<sub>2</sub>O) : F(total iron as FeO) : M(MgO) ternary diagram of the three varieties of amphibolite in the Hunt River Belt.

to amphibolite facies metamorphism the rocks may have retained some aspect of their original bulk chemical identity.

Irvine and Baragar (1971) have shown that volcanic suites with tholeiitic and calc-alkalic affinities both plot in the sub-alkaline field of the alkali versus silica diagram. When plotted on a ternary AFM diagram in Figure 3.3, the Hunt River amphibolites show a diffuse yet distinctively Fe-enriched trend, lying in the field of tholeiitic rather than calc-alkaline rocks.

Major elements then appear to be useful in determining the broad chemical affinities of the meta-volcanics from the Hunt River Belt.

#### 3.2.2.3 Trace Element Chemistry

The trace element data is presented in  $\text{SiO}_2$  variation diagrams (Figure 3.4) to enable direct comparison with chemical trends of the major elements. Nb has such a restricted range in values (Tables 3.2 and 3.5) that it was not included.

In comparison to the major element variation diagrams (Figure 3.1) the ultramafics appear to plot in separate fields from the amphibolites. Sr and Ba are somewhat similar geochemically, although in Figure 3.4 the Ba is seen to plot in a rather diffuse pattern, whereas the Sr exhibits a marked decrease with increasing  $\text{SiO}_2$ . Rb is unusual in that it also shows a negative correlation with increasing  $\text{SiO}_2$ . Zr shows only a slight increase with increasing  $\text{SiO}_2$ . The absolute values for Zr are considerably less than the average value of 150 ppm for basalt given by Taylor (1965). Cu and Zn exhibit relatively random plots

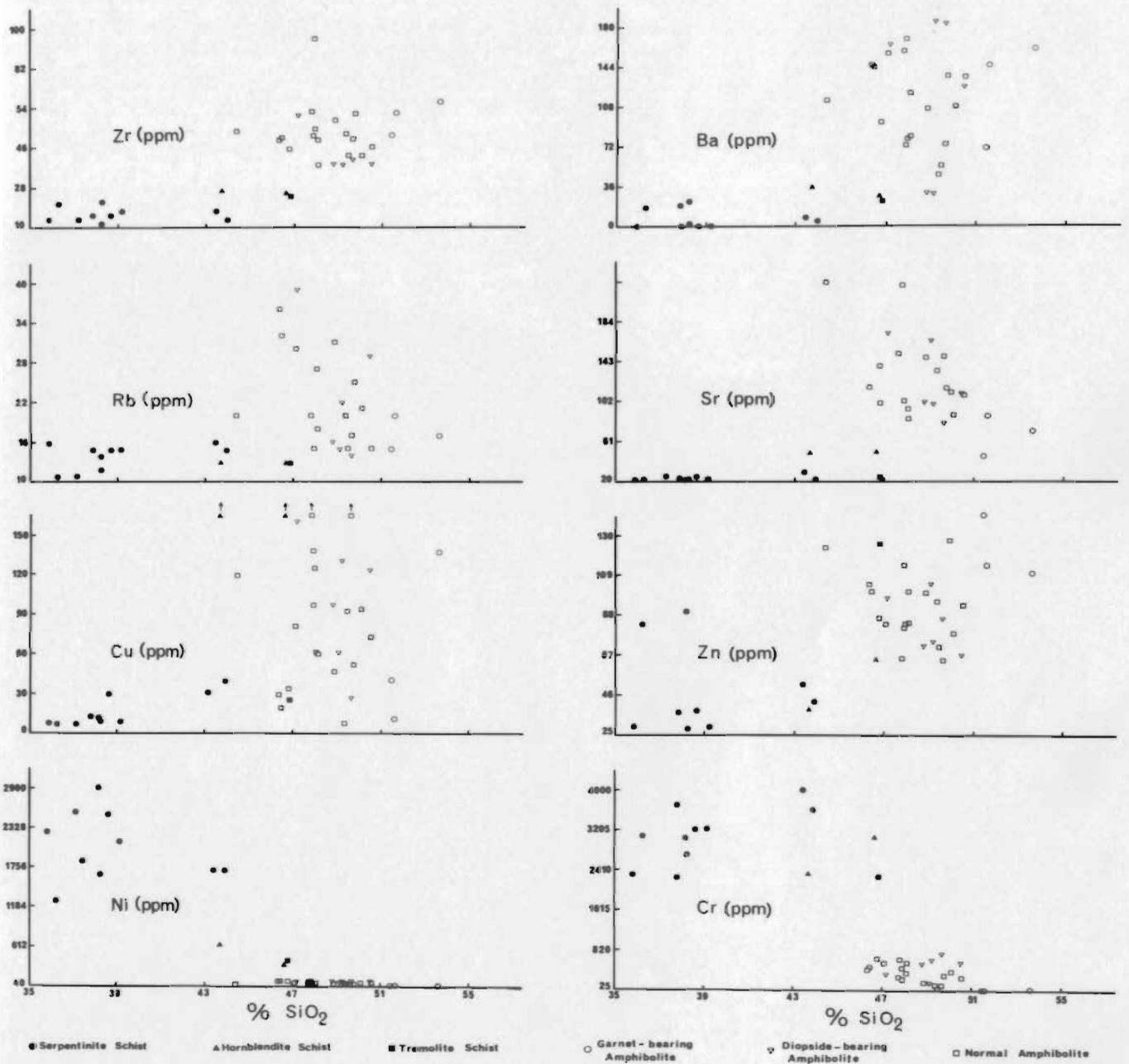


FIGURE 3.4: Trace element variations vs. SiO<sub>2</sub> in wt.% for the mafic and ultramafic rocks from the Hunt River Belt.

for both the ultramafics and the amphibolites. These elemental abundances may in part be affected by the distribution of the sulphide-bearing rusty zones, some of which have formed by secondary enrichment. Ni and Cr show anomalously high values in the ultramafics in comparison to the amphibolites. The Ni shows a gradual decrease while the Cr plots into two distinctly separate fields for the two major rock types.

In Table 3.7 trace elements of meta-volcanics from the Hunt River Belt are compared to values from other volcanic environments. Island arc tholeiites are characterized by very low Ni-Cr contents whereas oceanic tholeiites display very high Ti contents. Apart from a marked discrepancy in the zirconium contents, the Hunt River meta-volcanics compare most favourably with basic rocks (the non high-magnesium series) associated with ultramafics in the lower parts of volcanic cycles from Archean greenstone belts.

The K/Rb ratios for the amphibolites (averaging 250) are anomalously low when compared to values of  $<1000$  reported as typical of oceanic tholeiites (Engel et al., 1965). Metamorphism has little or no effect on whole rock K/Rb ratios except at upper amphibolite and higher grades (Heier and Adams, 1964; Lambert and Heier, 1968; Jäkes and White, 1970), although amphibolite facies rocks can be largely influenced by K and Rb migration if regional granulite facies metamorphism occurs in underlying rocks (Heier, 1973). In previous studies, low K/Rb ratios in meta-volcanic amphibolites from the northern Nain Province have been considered to be the result of metamorphism (Collerson et al., 1975). This is a reasonable assumption

TABLE 3.7: Trace element comparison of Labrador meta-volcanics with modern volcanic environments and other Archean terrains.

ROCK TYPE	SOURCE	NO. OF ANALYSES	Ti	Zr	Sr	Ni	Cr
Amphibolite	Saglek Area (Collerson <i>et al.</i> , 1975)	6	6174	55	134	100	337
Amphibolite	Hunt River Area	14	4077	45	79	147	599
Oceanic Tholeiite	Pearce, 1975	92	8033	92	131	--	310
Island Arc Tholeiite	Jakes and White, 1971	--	4796	70	200	30	50
Calc-Alkali Basalt	Hallberg and Williams, 1972	--	6295	330	100	25	40
Meta-Basalt (Ultrabasic - Basic Suite)	Norseman, Western Australia (Glikson, 1971)	83	5755	57	--	116	400
Tholeiitic Basalt	Eastern Goldfields Region, Australia (Hallberg and Williams, 1972)	337	5755	105	61	170	367
Archean Volcanics	Superior Province, Canada (Goodwin, 1972)	835	5635	181	204	105	203

in view of the widespread granulite facies metamorphism throughout the northern Nain Province. However, similar low K/Rb ratios (Tables 3.5 and 3.6) occur in the Hunt River Belt, where there is little evidence for a granulite facies metamorphism event at the present level of erosion in the southern Nain Province. This may indicate that low K/Rb ratios ( $\approx 250$ ) may be typical of Archean basic rocks, as very low K/Rb ratios are also reported from basaltic rocks in the lower parts of Archean greenstone belts (Glikson, 1971).

#### 3.2.2.4 Tectonic Setting

Metamorphosed basic rocks may have been derived from a variety of igneous tectonic environments (Carmichael, Turner and Verhoogen, 1974). Certain trace element plots have been proposed to discriminate between magma types in these environments (Pearce and Cann, 1971, 1973; Pearce, 1975). When the trace elements from the Hunt River amphibolite rocks were plotted on two of these diagrams (the Zr-Ti/100-Sr/2 triangular plot and the Ti-Zr linear plot) the values fell into areas which overlap both the low-K tholeiitic field and the ocean floor tholeiitic field. Thus, further study was necessary in order to arrive at a more precise tectonic setting.

Archean igneous rocks generally display an overall low Ti content relative to modern day (Phanerozoic - recent) igneous rocks (Lambert et al., 1975). Therefore, plotting the actual Ti:Zr ratios, rather than absolute values, appears to be a more significant method for discriminating between the tectonic environments of Archean volcanics. The Ti:Zr trace element values from the Hunt River

meta-volcanics (amphibolites) are plotted in Figure 3.5. They display very high Ti:Zr ratios, a feature which is characteristic of ocean floor basalts rather than island arc tholeiites (Pearce and Cann, 1973). This suggests that the protoliths for the amphibolites in the Hunt River Belt were not deposited onto sialic crust but rather were emplaced in an ocean floor rifting environment.

#### 3.2.2.5 Discussion

Windley and Bridgwater (1971) have suggested that the main difference between Archean greenstone belts and supracrustal remnants found in high grade gneiss terrains is level of exposure; greenstone belts occurring at shallower crustal levels than the high grade gneiss terrains. Apart from structural and metamorphic differences between these two types of Archean association there are also important lithological differences. Amphibolite belts from high grade terrains do not contain readily recognizable sequences of silicic (calc-alkaline) meta-volcanics which are common in Archean greenstone belts and are regarded as an integral part of the stratigraphic sequence (Condie, 1972; Hubregtse, 1975; Baragar and Goodwin, 1971).

Sutton (1973) suggested that the early Archean crust developed in two stages; Stage 1 which involved the formation of an early granitic crust and Stage 2 in which extensive supracrustal sequences were deposited and later deformed along with the granitic basement. Following from this, Collerson et al. (1975) have suggested that early Archean high grade gneiss terrains and their associated amphibolite belts possibly represent a period of sialic crustal development prior to the

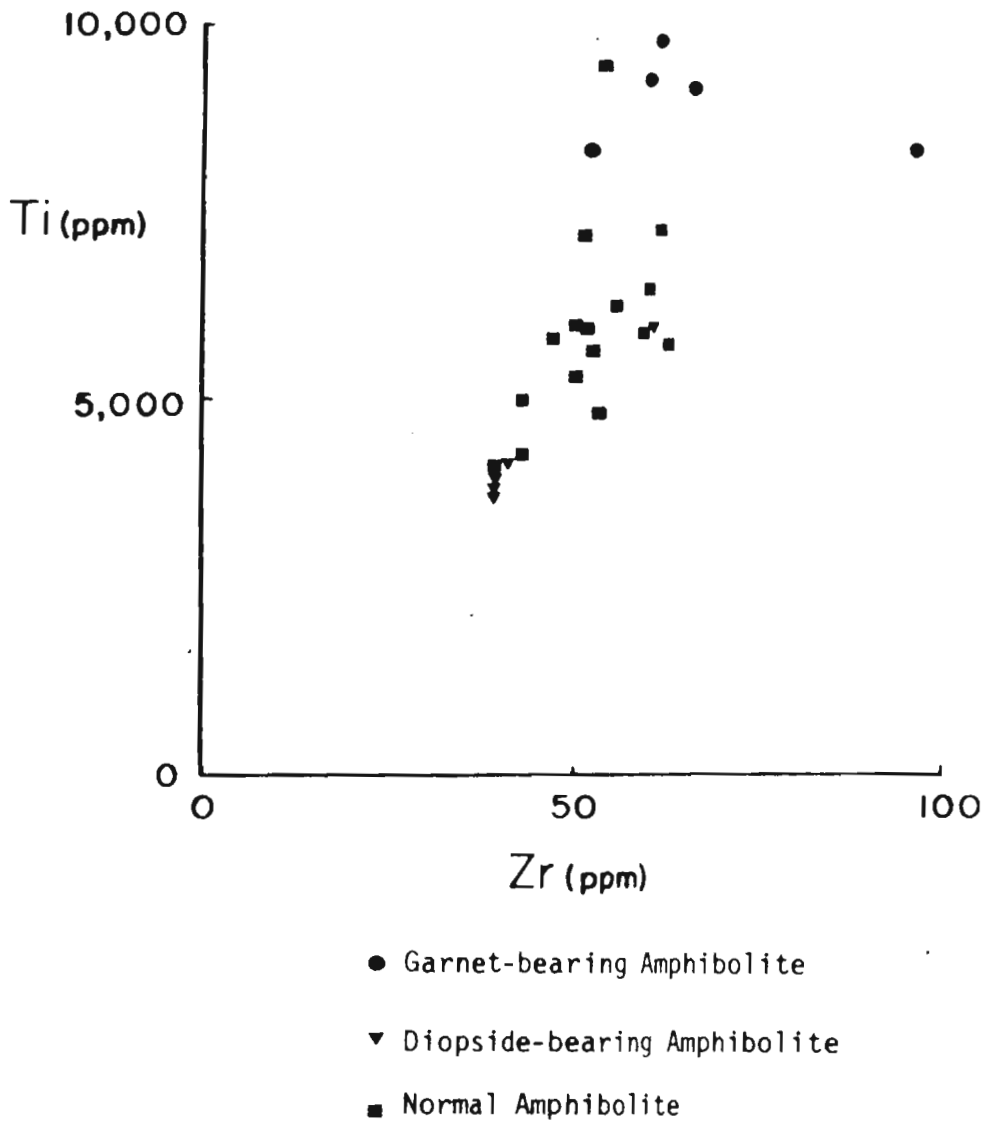


FIGURE 3.5: Ti:Zr variation diagram of the garnet-bearing amphibolite, the diopside-bearing amphibolite and the normal amphibolite in the Hunt River Belt.

formation of greenstone belts. The lack of extensive calc-alkaline volcanics associated with supracrustal belts throughout the North Atlantic Craton may therefore represent a normal condition for that period of crustal development.

Theories for the tectonic evolution of Archean greenstone belts are many and varied. The more traditional views involved the development of volcanic geosynclinal piles on an extensive basaltic crust (Anhaeusser et al., 1969; Anhaeusser, 1973; Glikson, 1970, 1971, 1975). Recently, Condie (1972), Talbot (1973) and Goodwin and West (1974) have applied the plate tectonic theory to account for their formation. Although horizontal tectonic regimes are considered to be important in the structural development of Archean high grade gneiss terrains (Bridgwater et al., 1974), it is not yet possible to accept without reservation the plate tectonic models such as those proposed by Condie (1972) and Talbot (1973).

Studies in the North Atlantic Craton (McGregor, 1973; Bridgwater and Fyfe, 1974; Bridgwater et al., 1974) and in the Kaapvaal Craton (Hunter, 1974) favoured the early development of a sialic rather than basaltic crust. Hunter proposes that greenstone belts developed in rifted linear zones overlying sites of mantle upwelling in response to distention of an earlier sialic crust (high grade gneiss terrain). Hunter (1974, p.259) states further that:

The earlier sialic crust formed as a result of partial and total melting of hydrous basaltic lithosphere under tectonically metastable conditions. Limited sedimentation and volcanism in small basins on this early crust took place during periods of quiescence, following which deformation resulted in the tectonic interslicing of the early sialic crust and the sedimentary-volcanic sequences.

It has been suggested that the Hunt River Belt formed in a rifting environment (Section 3.2.2.4). It is possible that the processes which Hunter proposes for greenstone belt development can be further extended back into Archean time.

### 3.2.3 Meta-sediments

Geochemical studies were carried out on both the pelitic schist and the grey schist from the Hunt River Belt to assess the relation between the meta-sediments and meta-volcanics, and to place constraints on the paleoenvironment of deposition of the Belt.

The pelitic schist is very interesting geochemically, although it is quite limited in occurrence in the Belt. The trace element chemistry in particular is compared to other geochemical studies of meta-sedimentary pelitic schists in order to determine the provenance of the pelites.

Analyses of the meta-sedimentary grey schist is presented in an effort to see if the transitional nature between this unit and the amphibolites, apparent in the field, can be observed chemically.

The meta-sedimentary rocks designated as 'rusty zones' in Chapter 2, Section 2.2.3.3 are not discussed because they are affected by extensive surficial weathering.

#### 3.2.3.1 Pelitic Schist

The pelitic schist is only a small component of the Belt however it is geochemically very distinct, as shown by the analyses presented in Table 3.8. The major element chemistry agrees closely

TABLE 3.8: Chemical analyses and C.I.P.W. Norms of the meta-sedimentary schists from the Hunt River Belt.

WJ-73-	GREY SCHIST										PELITIC SCHIST
	3	6	23C	36B	54A	54B	55B1	158	159	161	210B
SiO <sub>2</sub>	63.15	70.88	52.60	62.43	71.43	62.99	61.36	57.02	68.98	61.99	54.36
TiO <sub>2</sub>	0.57	0.29	1.04	0.73	0.19	0.59	0.63	0.83	0.38	0.73	0.97
Al <sub>2</sub> O <sub>3</sub>	15.79	14.85	14.54	15.77	15.31	15.73	18.56	15.34	14.96	16.11	20.30
Fe <sub>2</sub> O <sub>3</sub>	1.43	0.73	n.m.	1.91	0.39	0.87	1.24	1.41	1.44	1.43	5.83
FeO	3.24	1.84	n.m.	4.46	1.06	4.92	3.97	6.06	2.09	5.21	5.20
MnO	0.09	0.04	0.16	0.09	0.08	0.08	0.05	0.12	0.07	0.11	0.18
MgO	1.65	0.57	6.49	1.64	0.56	2.62	1.75	3.67	0.89	2.03	4.83
CaO	4.84	2.79	8.89	4.89	1.54	4.81	4.81	6.76	3.43	5.09	1.70
Na <sub>2</sub> O	3.40	4.29	2.66	3.31	3.96	2.79	4.24	2.69	3.65	2.99	0.07
K <sub>2</sub> O	0.70	1.89	0.81	1.26	3.90	0.92	0.92	0.99	1.84	1.34	2.23
P <sub>2</sub> O <sub>5</sub>	0.20	0.05	0.13	0.20	0.01	0.14	0.14	0.33	0.10	0.22	0.03
L.O.I.	1.92	0.59	1.71	2.00	0.72	2.46	1.78	2.48	1.12	1.36	2.44
TOTAL	96.98	98.81	89.03	98.69	99.15	98.92	99.45	97.70	98.95	98.61	98.18
Zr (ppm)	145	123	68	146	99	130	110	126	158	149	25
Sr	250	311	134	238	305	238	227	233	236	201	49
Rb	48	86	25	43	125	45	38	38	82	47	4
Zn	89	64	94	107	41	87	75	110	67	85	45
Cu	12	12	22	12	19	31	30	46	11	23	186
Ba	178	545	131	299	876	264	205	224	396	247	22
Nb	13	15	9	14	10	13	14	13	14	15	4
Ni	33	22	120	40	14	57	46	112	20	62	1546
Cr	19	17	420	25	12	64	27	200	8	73	1114
K	5811	15690	6724	10460	32376	7637	7637	8218	15275	11124	15358
Ti	3417	1739	6235	4376	1139	3573	3777	4976	2278	4376	2398
K/Rb	121	182	269	243	259	170	201	216	186	237	3840
C.I.P.W. Norms											
Q	27.90	31.35	4.47	24.16	28.99	26.88	18.59	16.26	31.92	23.36	
Or	4.35	11.37	4.92	7.70	23.40	5.63	5.56	6.14	1.11	8.14	
Ab	30.25	36.94	23.12	28.95	34.02	24.46	36.72	23.89	31.56	26.00	
An	24.06	14.02	26.03	23.92	8.02	23.96	23.65	28.19	16.92	26.40	
Ne											
Co	1.11	0.71		0.50	1.70	1.73	2.17		0.91	0.98	
D1			15.13					4.08			
Hy	8.52	3.86	2.85	9.98	2.90	14.51	9.90	16.80	4.46	12.78	
Ol											
Wt	2.18	1.08	3.07	2.86	0.57	1.31	1.84	2.15	2.13	2.13	
Il	1.14	0.56	2.03	1.43	0.37	1.16	1.22	1.65	0.74	1.42	
Cr			0.09	0.01		0.01	0.01	0.05		0.02	
Ap	0.49	0.12	0.31	0.48	0.02	0.34	0.33	0.80	0.24	0.53	

n.m. not measured

with the average composition of pelitic rocks given by Shaw (1956). Nickel and chromium concentrations are anomalously high and trace element values differ greatly from the average values of Shaw (1954a).

Despite the fact that one sample may not be quantitatively significant, the nickel-chromium contents are similar to high values found in pelitic schists from Saglek, in northern Labrador (Collerson et al., 1975). Figure 3.6 for example, shows a nickel-chromium plot of the pelitic schist and amphibolite from the Hunt River Belt in relation to values obtained from pelitic schists at Saglek. It is significant that the amphibolitic meta-volcanics associated with the pelitic rocks at Saglek display the same chemical distribution of major and trace elements as those occurring in the Hunt River Belt (Collerson et al., 1975).

Nickel and chromium are regarded as weathering resistates, and may even be enriched to ore grade, as in certain New Caledonian deposits (Park and MacDiarmid, 1970). However, weathering would also have produced high concentrations of other trace elements such as Ti, Zr and Sr, which are also considered resistant to weathering (Pearce and Cann, 1973), and these are not found. The anomalous trace element patterns in the Hunt River pelite therefore cannot be attributed to recent weathering.

Shaw (1954a, 1956) concluded that there was little major or trace element change in pelitic rocks metamorphosed to sillimanite grade. Therefore, the concentration of the trace elements probably reflects an original sedimentary geochemical pattern.

The chemistry of the pelitic schist from the Hunt River Belt

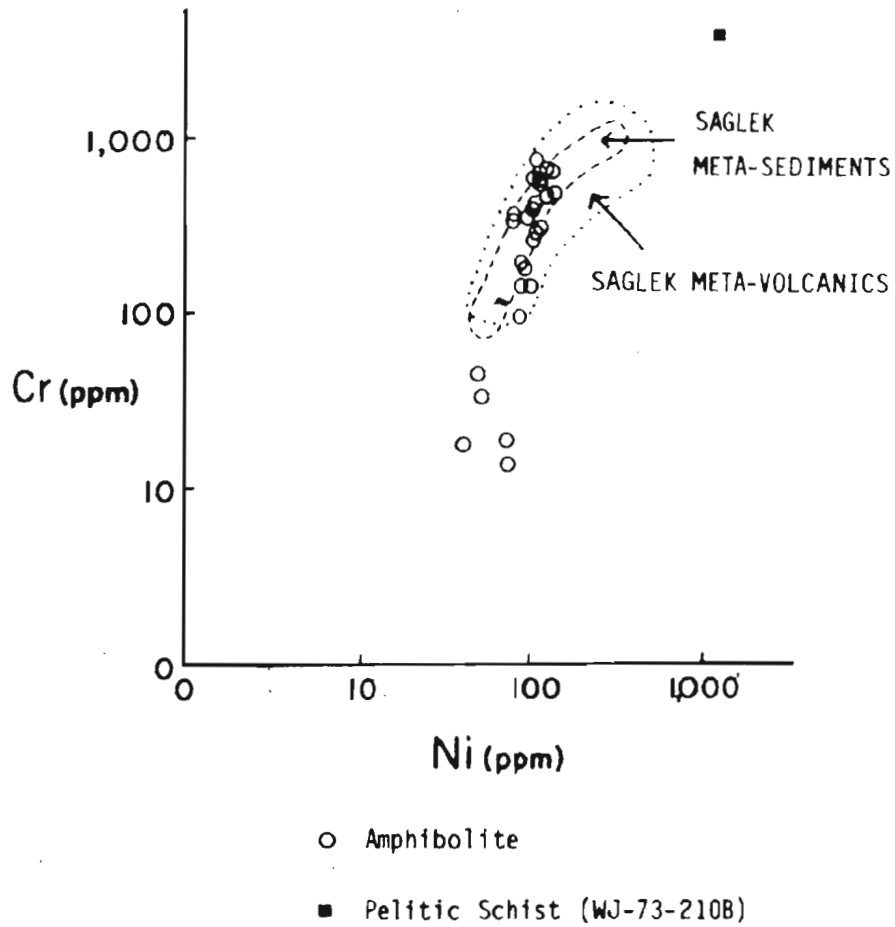


FIGURE 3.6 : Cr:Ni variation diagram comparing meta-volcanic and meta-sedimentary schists from the Hunt River Belt to rocks from the Saglek area, northern Labrador

suggests that the provenance contained a high proportion of ultramafic material which contributed detrital matter rich in nickel and chromium. The contribution of ultramafic rocks as a source material for sedimentation has been inferred in other Archean terrains (Hunter, 1974; Condie, 1975; Lambert et al., 1975). The Hunt River ultramafics discussed in Section 3.2.1 are interpreted as late intrusives into the volcanic pile, and therefore they may have been available as source material for sedimentation late in the depositional history of the Hunt River supracrustals. However, there is no conclusive evidence that the pelites were deposited later than the amphibolites.

#### 3.2.3.2 Grey Schist

Analyses of ten grey schists representative of the compositional variability of the unit are presented in Table 3.8. Compositions range from basic-intermediate ( $\text{SiO}_2 < 55\%$ ) near the overlying amphibolite to acidic ( $\text{SiO}_2 > 70\%$ ) near the underlying homogeneous gneiss. Major elements show considerable variation with  $\text{SiO}_2$ ;  $\text{Na}_2\text{O}$  and  $\text{K}_2\text{O}$  show a positive correlation and  $\text{TiO}_2$ ,  $\text{MnO}$ ,  $\text{MgO}$  and  $\text{CaO}$  a negative one. The trace elements Sr, Rb, Ba, Ni and Cr also exhibit positive correlations with  $\text{SiO}_2$  variation. Nickel and chromium values range up to 120 ppm and 420 ppm respectively, thus overlapping with the range displayed by the amphibolites (Figure 3.6).

The chemical evidence suggests that there is a complete transition between the grey schist unit and the amphibolites, indicating that they are possibly genetically related. The transitional

character of the grey schist is not regarded as a metamorphic effect because of the concomittant variation in the more immobile elements such as Ni, Cr, Ti, Zr and Sr.

Chemically the grey schist displays strong calc-alkaline affinities which are in sharp contrast to the tholeiitic iron-enrichment trend of the amphibolites (Figure 3.7). This could be interpreted as reflecting an original igneous fractionation trend within the volcanics with the grey schist representing metamorphosed intermediate to acid volcanics or tuffs. However, it is also quite possible that the calc-alkaline character of the grey schist unit may simply reflect sedimentary reworking (Robinson and Leake, 1975) of mafic material which could have been derived from the Hunt River Belt.

### 3.3 BORDER ZONE

Two groups of quartzofeldspathic gneisses occur in the border zone of the Hunt River Belt: pink muscovite gneiss and variable quartzofeldspathic gneiss. Analyses of the pink muscovite gneiss presented in Table 3.9 are from widely separate locations yet they are chemically almost identical. The variable quartzofeldspathic gneiss is similar in appearance and major element chemistry to the pink muscovite gneiss (Table 3.9). Both groups of border zone gneisses however display markedly different trace element distribution patterns (compare Zr, Sr, Rb and Ba in Table 3.9). In addition, the K/Rb ratios of two of the variable quartzofeldspathic gneisses (WJ-73-11 and -12) are anomalously high (704 and 611 respectively) when compared with values

TABLE 3.9: Chemical analyses and C.I.P.W. Norms of the pink muscovite gneiss and the variable quartzofeldspathic gneiss from the Border Zone.

	PINK MUSCOVITE GNEISS			VARIABLE QUARTZOFELDSPATHIC GNEISS		
	WJ-78- 238	55B2	160	11	12	55C1
SiO <sub>2</sub>	75.51	75.37	75.04	75.20	70.43	69.79
TiO <sub>2</sub>	0.01	0.02	0.01	0.02	0.21	0.17
Al <sub>2</sub> O <sub>3</sub>	13.01	13.33	14.16	13.53	14.64	15.73
Fe <sub>2</sub> O <sub>3</sub>	0.65	0.35	0.66	0.00	1.04	1.31
FeO	0.28	0.40	0.40	0.75	1.43	0.95
MnO	0.05	0.01	0.09	0.02	0.05	0.05
MgO	---	0.14	---	---	0.44	0.65
CaO	0.54	0.54	0.28	0.50	2.81	4.13
Na <sub>2</sub> O	4.22	4.17	4.69	5.76	4.84	4.80
K <sub>2</sub> O	4.45	4.24	3.91	4.24	2.43	1.60
P <sub>2</sub> O <sub>5</sub>	---	---	---	---	0.03	0.13
L.O.I.	0.27	0.38	0.35	0.69	0.55	0.50
TOTAL	98.99	99.15	99.59	100.71	98.90	99.71
Zr (ppm)	37	42	29	128	112	151
Sr	42	46	28	537	299	742
Rb	142	183	248	50	33	68
Zn	31	23	41	32	44	36
Cu	13	20	16	14	17	12
Ba	7	35	30	495	545	391
Nb	16	21	31	12	13	19
Ni	10	14	16	13	27	24
Cr	14	17	23	14	20	25
K	36942	35198	32459	35198	20173	13282
Ti	60	120	60	120	1259	1019
K/Rb	260	192	131	704	611	195
	C.I.P.W.			Norms		
Q	33.16	33.79	32.27	23.13	26.63	26.64
Or	26.64	25.42	23.28	24.54	14.59	9.52
Ab	36.17	35.71	39.99	47.74	41.61	40.91
An	2.74	2.75	1.42	2.79	11.22	16.77
Na						
Co	0.26	0.92	1.71	0.41		
D1					2.56	3.45
Hy	0.05	0.79	0.34	1.35	1.37	0.46
O1						
Mc	0.95	0.51	0.96		1.53	1.91
Il	0.02	0.04	0.02	0.04	0.41	0.33
Cr						0.01
Ap					0.07	

--- not detected

from other units in the thesis area.

The origin of these two rock types is uncertain. The chemistry of the pink muscovite gneiss is constant throughout its extent. The chemistry of the variable quartzofeldspathic gneiss is consistent throughout its thickness at any particular outcrop, however it varies considerably along strike.

Field relations of the pink muscovite gneiss suggest that it has a regional discordant contact with the overlying grey schist. It is therefore interpreted to be intrusive in origin, possibly representing a granitic sheet which is in accordance with its 'granitic' chemistry. The high K/Rb values of the variable quartzofeldspathic gneiss are not considered to be the result of high-grade regional metamorphism, as the values are decidedly local in extent and the host rocks do not contain orthopyroxene. None of the other quartzofeldspathic gneisses from the area, for example, approach K/Rb ratios of over 600. Therefore these values are thought to be the result of an unusual igneous condition, and the variable quartzofeldspathic gneiss is interpreted to be an intrusive rock unit.

#### 3.4 QUARTZOFELDSPATHIC GNEISS COMPLEX

Polygenetic quartzofeldspathic gneisses make up about 90% of the gneissic terrain. The remaining rocks are distinctive, discontinuous layers and lenses of amphibolite. On the basis of field evidence and degree of structural complexity the gneisses are subdivided into several varieties, each of differing age and mode of formation. Chemical analyses of the different gneiss types are presented in Tables 3.10 and 3.11.

TABLE 3.10: Chemical analyses and C.I.P.W. Norms of the banded and homogeneous gneisses from the Quartzofeldspathic Gneiss Complex.

BANDED GNEISS					HOMOGENEOUS GNEISS							
WJ-73-	177	194	199A	199B	5	21	22	48	53	146	149	200
SiO <sub>2</sub>	69.26	54.96	66.51	55.65	67.54	72.22	72.73	69.67	73.93	71.66	70.97	49.20
TiO <sub>2</sub>	0.40	1.03	0.36	0.47	0.40	0.22	0.23	0.36	0.16	0.19	0.30	0.21
Al <sub>2</sub> O <sub>3</sub>	15.42	16.10	14.47	13.99	16.34	14.62	14.05	16.00	13.89	15.50	15.52	26.60
Fe <sub>2</sub> O <sub>3</sub>	1.67	2.49	1.34	2.21	2.07	0.01	0.41	0.64	0.53	0.16	0.21	0.69
FeO	0.30	7.18	2.61	4.88	0.56	1.75	1.98	2.01	0.79	1.27	1.63	2.45
MnO	0.03	0.06	0.06	0.14	0.01	0.02	0.04	0.02	0.01	0.01	0.01	0.07
MgO	1.54	4.44	1.71	7.13	0.75	0.97	0.61	1.05	0.33	0.25	0.77	1.55
CaO	2.36	8.77	4.44	9.18	2.73	1.63	2.32	3.28	1.16	2.24	3.09	11.03
Na <sub>2</sub> O	4.84	2.69	3.25	2.68	4.36	4.14	4.51	4.96	3.89	3.58	4.87	3.31
K <sub>2</sub> O	1.01	0.61	1.17	0.76	1.85	3.06	1.40	1.35	4.04	3.66	1.00	1.13
P <sub>2</sub> O <sub>5</sub>	0.01	0.40	0.07	0.25	0.12	---	---	0.06	---	0.10	0.03	0.42
L.O.I.	0.72	1.35	1.47	1.64	1.09	0.81	0.73	0.81	0.78	0.55	0.86	2.14
TOTAL	97.56	100.02	96.46	98.98	98.02	99.45	99.01	100.21	99.51	99.17	99.26	98.80
Zr (ppm)	155	132	86	82	152	114	105	130	193	109	135	35
Sr	334	179	307	219	437	267	199	393	225	263	581	214
Rb	36	23	40	28	79	118	89	70	196	109	39	118
Zn	47	115	65	79	65	46	73	45	23	41	44	48
Cu	23	18	22	21	19	15	23	19	13	9	10	28
Ba	555	190	453	120	797	1120	224	186	724	1399	365	129
Nb	10	16	10	8	7	9	12	10	16	5	8	7
Hf	43	93	56	158	19	17	16	20	18	15	15	47
Cr	22	171	116	672	13	15	13	19	12	13	20	66
K	8385	5064	9713	6309	15358	25403	11622	11207	33538	30383	8301	9381
Tl	2398	6175	2158	2818	2398	1319	1379	2158	959	1139	1798	1259
K/Rb	233	220	243	225	194	215	131	160	171	278	213	80
C.I.P.W. Norms												
Q	30.75	10.86	31.01	9.10	28.73	30.41	34.21	26.08	32.80	31.29	30.37	
Or	6.16	3.65	7.20	4.61	11.27	18.32	8.41	8.02	24.17	21.91	6.00	6.91
Ab	42.27	23.06	28.63	23.27	38.03	35.49	38.79	42.20	33.32	30.69	41.85	28.96
An	12.30	30.44	22.32	24.52	14.57	8.55	12.26	16.20	6.09	11.02	15.73	53.91
Ne												
Co	2.06				2.05	1.42	0.71	0.48	0.93	1.68	0.76	0.85
Dl		9.16	0.32	16.61								
Hy	3.96	16.12	7.59	16.94	1.93	5.36	4.58	5.25	1.61	2.56	4.32	4.31
Ol												2.58
Mt		3.66	2.02	3.29	0.70	0.01	0.60	0.93	0.78	0.24	0.31	1.03
Il	0.72	1.98	0.71	0.92	0.78	0.42	0.44	0.69	0.31	0.37	0.58	0.41
Cr		0.04	0.03	0.15								0.01
Ap	0.02	0.94	0.17	0.60	0.29			0.14		0.24	0.07	1.01

--- not detected

TABLE 3.11: Chemical analyses and C.I.P.W. Norms of the amphibolite and mixed gneisses of the Quartzofeldspathic Gneiss Complex.

	AMPHIBOLITE GNEISS							MIXED GNEISS				
	wj-73-	130B	51	104A	104-5	131	139	199C	220	104-7	120	128
SiO <sub>2</sub>	59.33	47.83	46.46	48.87	49.37	47.91	46.80	60.99	66.70	71.71	70.38	68.54
TiO <sub>2</sub>	1.55	0.96	0.98	0.99	0.80	0.94	3.12	0.58	0.22	0.25	0.31	0.22
Al <sub>2</sub> O <sub>3</sub>	12.50	9.88	15.66	14.16	16.61	14.15	14.59	15.89	16.94	15.29	14.79	15.39
Fe <sub>2</sub> O <sub>3</sub>	2.31	1.01	3.08	5.75	2.79	2.89	6.13	1.00	0.52	0.28	0.76	0.09
FeO	9.86	11.03	9.10	7.56	7.83	9.71	8.42	4.45	1.81	1.40	2.09	1.68
MnO	0.10	0.24	0.21	0.05	0.17	0.18	0.19	0.09	0.83	0.02	0.06	0.01
MgO	3.21	10.67	10.34	6.33	7.24	6.79	5.96	2.98	0.05	0.62	1.10	0.13
CaO	6.67	12.65	10.47	9.44	10.78	9.87	8.59	6.00	3.74	2.80	3.73	3.10
Na <sub>2</sub> O	1.80	1.25	2.24	2.56	3.03	1.97	2.36	3.71	5.09	4.26	4.46	4.56
K <sub>2</sub> O	0.75	0.43	0.70	1.07	0.64	0.69	1.32	1.08	1.11	2.18	1.15	0.83
P <sub>2</sub> O <sub>5</sub>	0.07	0.25	0.29	0.22	0.30	0.27	0.85	0.20	0.07	0.02	0.06	0.04
L.O.I.	1.18	2.28	1.96	1.90	1.35	1.58	1.84	1.36	0.55	0.60	0.94	0.92
TOTAL	99.33	98.57	101.49	98.90	100.91	95.95	100.17	98.33	97.63	99.46	99.83	95.42
Zr (ppm)	60	63	51	59	53	52	46	129	122	106	118	118
Sr	80	221	100	146	133	102	138	279	599	395	298	576
Rb	283	20	32	31	20	15	24	53	47	65	56	29
Zn	109	65	100	99	95	81	86	50	60	33	49	47
Cu	16	446	20	47	8	138	34	17	15	25	21	14
Ba	162	158	144	106	47	73	94	177	212	893	204	468
Nb	9	10	9	10	11	9	8	10	10	9	13	9
Ni	70	133	137	88	101	139	124	48	34	15	22	20
Cr	19	861	506	196	144	483	669	41	51	15	17	17
K	6226	3570	5811	8883	5313	5728	10958	8966	9215	18097	9547	6890
Ti	9292	5755	5875	5935	4796	5635	18704	3477	1319	1499	1858	1319
K/Rb	22	179	182	287	266	382	457	169	196	278	170	238
	C.I.P.W.							Norms				
Q	23.13			2.03		1.09	3.17	17.10	13.62	31.02	27.82	32.47
Or	4.51	2.64	4.15	6.52	3.80	4.27	7.92	6.58	6.75	13.02	6.87	5.18
Ab	15.52	10.98	19.03	22.32	25.74	17.46	20.28	32.36	44.33	36.43	38.15	40.76
An	24.26	20.84	30.72	24.72	29.95	29.05	25.71	24.24	18.98	14.29	17.12	16.37
Na												
Co	7.64								0.63	0.75		1.38
Ol	3.78	34.96	15.88	17.93	17.81	16.85	9.70	4.36			1.14	
Hy	18.37	18.43	2.05	15.36	5.32	24.25	16.02	12.25	4.31	3.54	5.04	3.16
Pl		7.99	21.02		11.06							
Mt	3.41	1.52	4.48	8.59	4.06	4.39	9.03	1.49	0.78	0.41	1.11	0.14
Il	3.00	1.89	1.87	1.94	1.53	1.87	6.02	1.14	0.43	0.48	0.60	0.44
Cr		0.15	0.11	0.04	0.03	0.11	0.15	1.01	0.01			
Ap	0.17	0.60	0.68	0.53	0.70	0.66	2.01	0.48	0.17	0.05	0.14	0.10

### 3.4.1 Chemical Character of the Banded, Homogeneous and Mixed Gneisses

In Table 3.10 the gneiss types are grouped as they were identified in the field. The banded gneiss is predominantly tonalitic and ranges in composition from intermediate (55-65% SiO<sub>2</sub>) to sub-acid (65-70% SiO<sub>2</sub>). The homogeneous gneiss ranges in composition from sub-acid (65-70% SiO<sub>2</sub>) to acid (>70% SiO<sub>2</sub>) and when plotted on a normative anorthite-orthoclase-albite diagram (Figure 3.7) it overlaps several compositional fields, ranging from tonalite and trondhjemite to adamellite and granite. Both groups of gneisses differ in their major and trace element chemistry (Table 3.10). The banded gneiss contains relatively higher concentrations of TiO<sub>2</sub>, MgO, CaO, Ni and Cr, and lower amounts of SiO<sub>2</sub>, K<sub>2</sub>O and Rb than the homogeneous gneiss.

The mixed gneiss (Table 3.11), when plotted in Figure 3.7 and in other variation diagrams in this chapter, occupies an area that lacks a definite linear trend, overlapping the compositional fields of both the banded gneiss and homogeneous gneiss. It is interpreted to have formed as a result of tectonic mixing of the banded and homogeneous gneiss types.

Figure 3.7 also shows a normative anorthite-orthoclase-albite ternary compositional diagram of Archean gneisses (Nuk gneisses) from the Godthaab district, West Greenland (McGregor, 1975). The similarity between the Greenland gneiss plots and the thesis area quartzofeldspathic gneiss plots is remarkable indeed, and will be discussed further in Chapter 5.

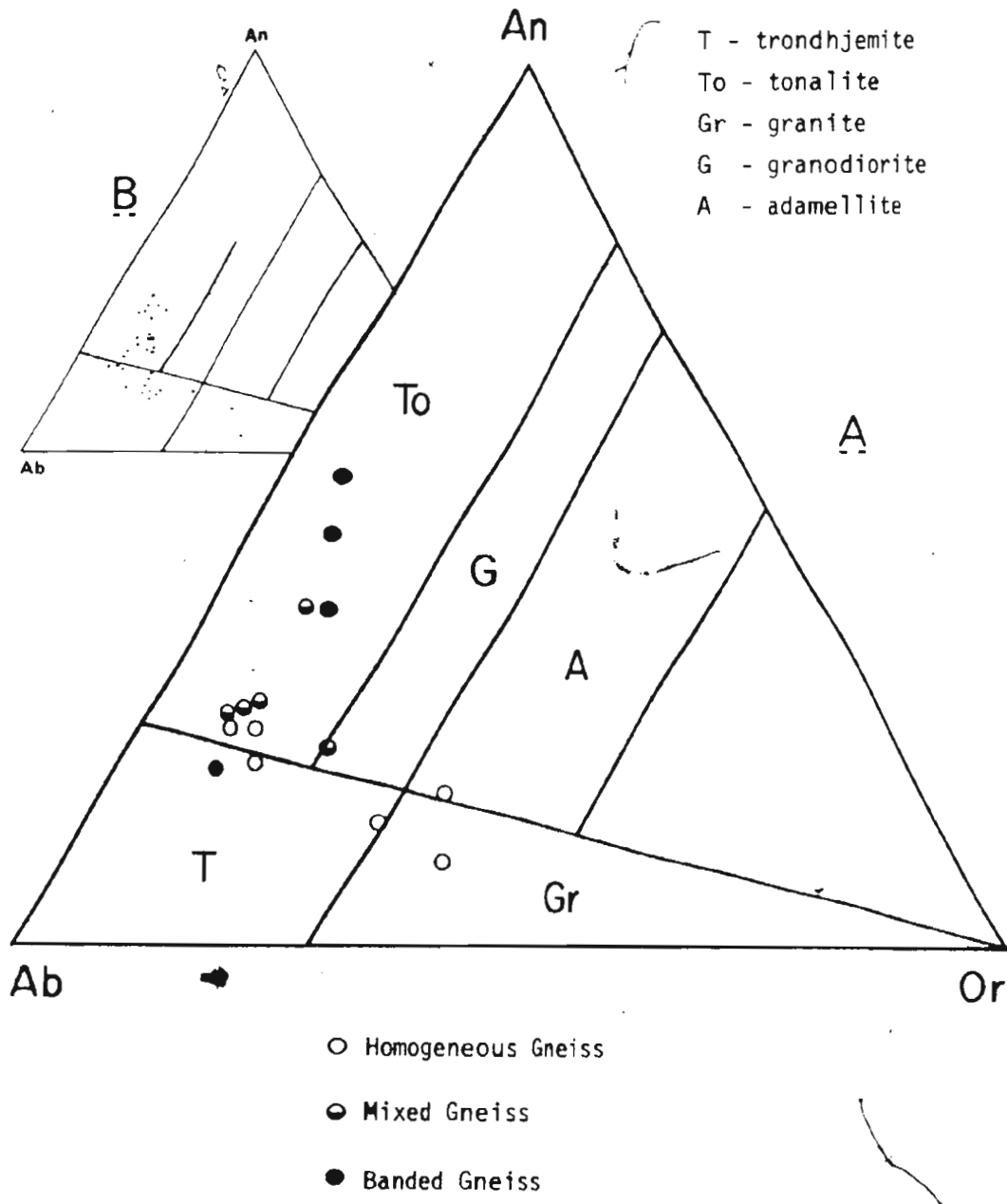


FIGURE 3.7 : (A) Normative anorthite-orthoclase-albite ternary compositional diagram of the quartzofeldspathic gneisses (after McGregor, 1975). (B) Normative anorthite-orthoclase-albite ternary compositional diagram of the Nuk gneisses, Godthab district, West Greenland (McGregor, 1975).

### 3.4.2 Geochemical Interpretation of Polygenetic Gneisses

The banded gneisses are polygenetic in origin. They are composed of a variety of rock types of different ages and chemical affinities. Although their present chemical character cannot be related in any way to their primary chemistry, a chemical study is of use in determining regional lithological correlations. If the intensity of deformation which deformed and transposed an original heterogeneous sequence of rocks was of sufficient strength to produce a gneissic layering, then the banded gneisses so formed would assume a similar chemical character on a megascopic scale which could be distinguished chemically from younger generations of granite (s.l.) emplaced into that terrain.

The banded and homogeneous gneisses display contrasting chemical trends in certain diagrams. Two distinct chemical trends are apparent in Figure 3.8. The banded gneisses plot in a linear field parallel to the quartz-plagioclase join, and display very little enrichment in orthoclase. The homogeneous gneisses on the other hand, exhibit a strong orthoclase-enrichment trend with minor variations in the quartz content. The mixed gneisses do not plot in a random fashion but lie in either of the two well-defined linear trends.

On purely chemical evidence, Figure 3.8 could represent unrelated suites of igneous rocks, each displaying discrete chemical trends. However, the field relations clearly indicate that the gneisses are polygenetic. Therefore, it would be misleading to use a chemical variation diagram of this kind to interpret a genetic igneous evolution for the thesis area.

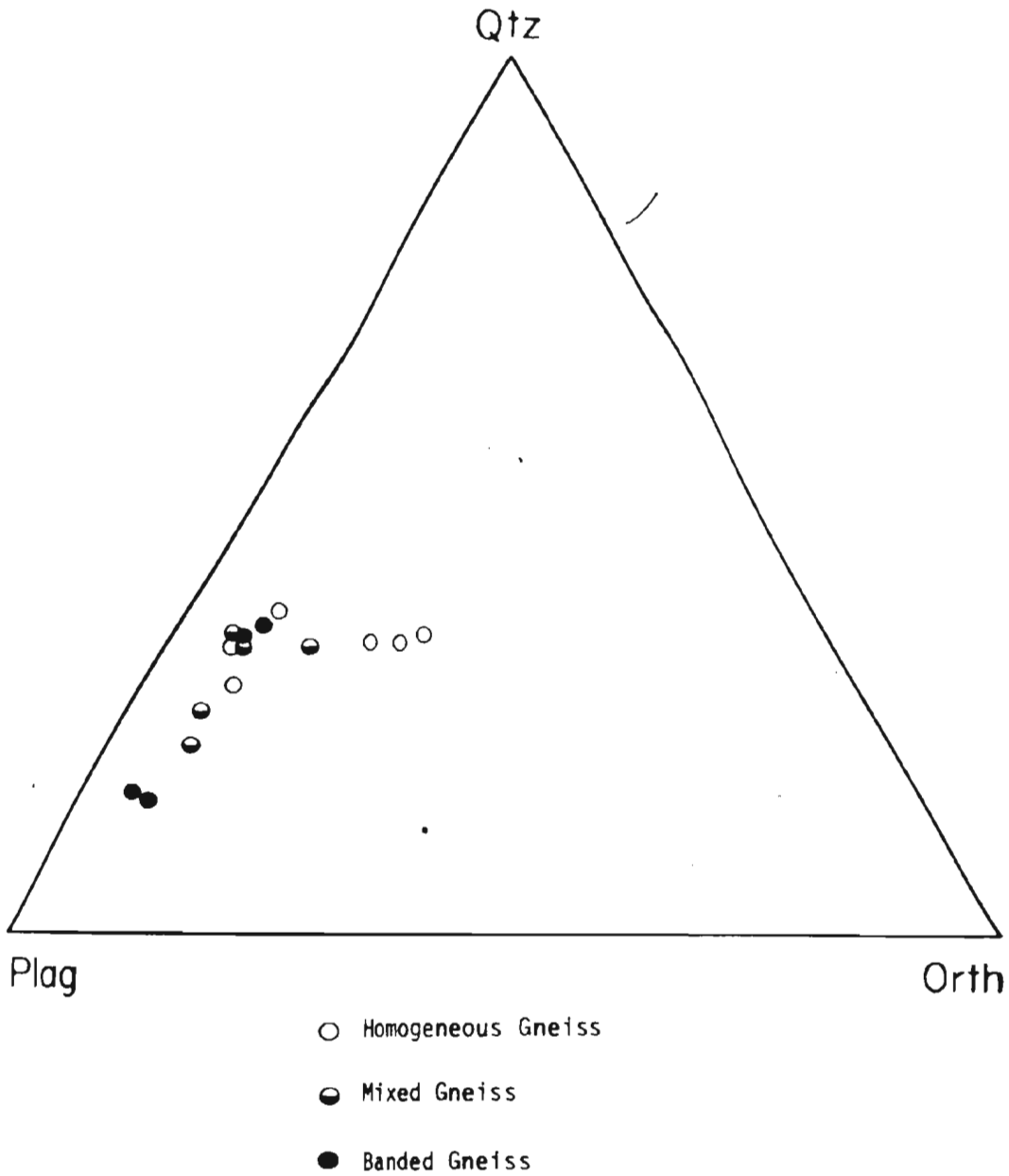
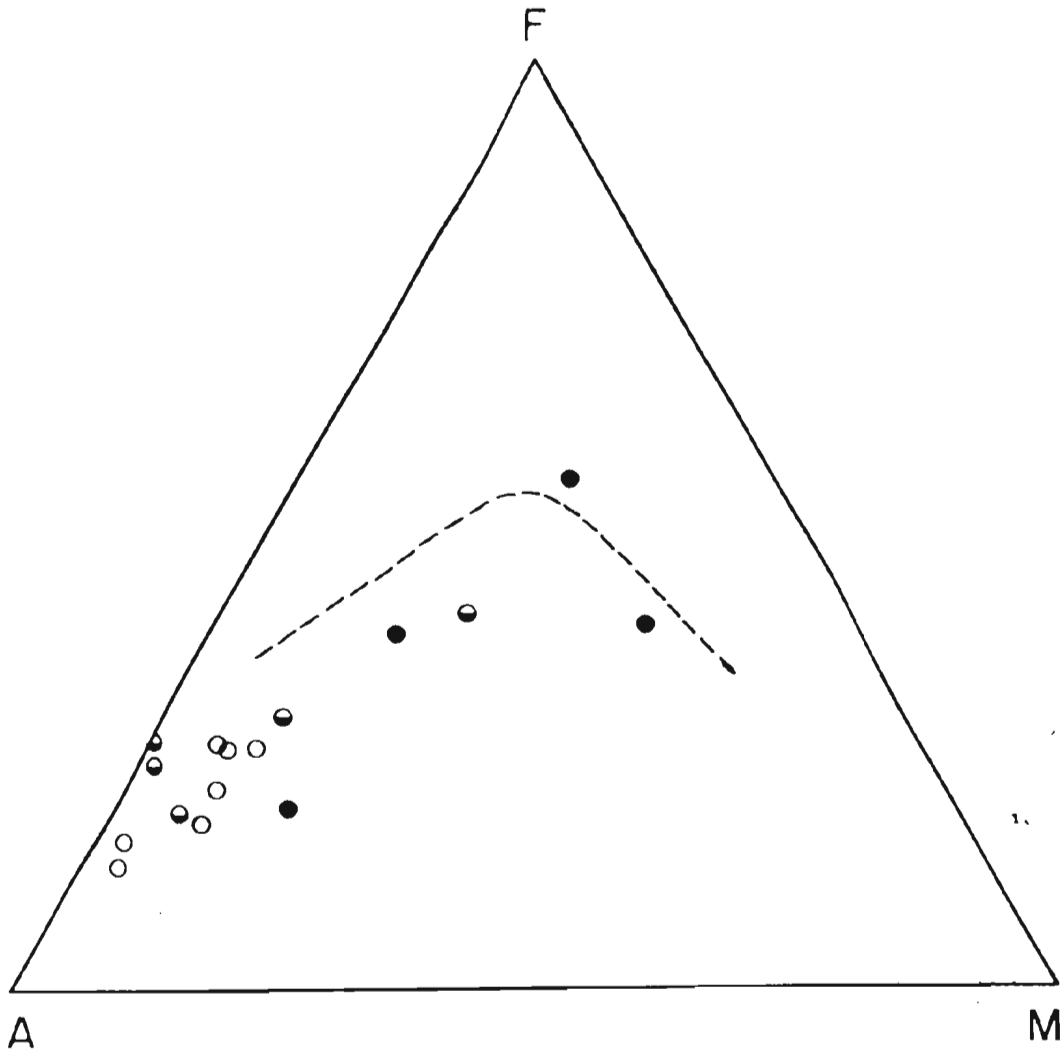


FIGURE 3.8: Normative quartz-orthoclase-plagioclase variation diagram of the quartzofeldspathic gneisses.



- Homogeneous Gneiss
- ◐ Mixed Gneiss
- Banded Gneiss

FIGURE 3.9:  $A(\text{Na}_2\text{O} + \text{K}_2\text{O}) : F(\text{total iron and FeO}) : M(\text{MgO})$  ternary diagram of the quartzofeldspathic gneisses.

In Figure 3.9 the gneisses appear to define a crude calc-alkaline trend. Detailed geochemical relationships however are much more complex. The homogeneous gneisses, the youngest and the least deformed group of gneisses, plot in a fairly restricted field, which may reflect a chemical fractionation trend related to their original period of emplacement. The banded gneisses, in contrast, plot in a very wide field. Although they lie on a crude calc-alkaline trend it must be remembered (Chapter 2, Section 2.3.1) that they are in part derived from mafic rocks (Hunt River meta-volcanics) which in Figure 3.3 are distinctly tholeiitic.

#### 3.4.3 Significance of Crustal Fractionation Processes

Significant research has been conducted on crustal fractionation processes in high grade gneiss terrains (Heier and Adams, 1965; Fahrig and Eade, 1968; Holland and Lambert, 1972; Heier, 1973). Most authors agree that large changes in major element chemistry (Holland and Lambert, 1973) and trace element chemistry (Heier, 1965; Lambert and Heier, 1968; Sighinolfi, 1971) do not occur until medium to high pressure granulite facies conditions are reached. According to Lambert and Heier (1968), rocks subjected to granulite facies metamorphism are relatively enriched in Ca, Mg, Fe, Mn, Ti and show high K/Rb ratios, and are relatively depleted in U, Th, Rb, K and show low Rb/Sr ratios. Rocks which are enriched or depleted during granulite facies metamorphism are believed to retain their diagnostic chemistry although retrogressed to amphibolite facies (Heier and Thoresen, 1971). There is no petrographic evidence to suggest that the amphibolite facies gneisses in the Hunt River area

have been retrograded from granulite facies pressure and temperature conditions.

It is of interest to compare the average chemical composition of the gneisses from the Hunt River area with average values of amphibolite and granulite facies rocks from other areas. Table 3.12 compares the composition of the Hunt River gneisses with the average chemical composition of the crust, the Canadian Shield, average granulite facies rocks and average amphibolite facies rocks. The homogeneous and banded gneisses compare more closely with average values for rocks in the amphibolite facies than those in the granulite facies. Only the K and Rb appear to be relatively depleted. However, this is most likely a primary chemical characteristic, as the K/Rb ratios (Figure 3.10) are in accordance with the average value for amphibolite facies rocks. Therefore, from the chemical evidence it appears that the Hunt River area has not been subjected to granulite facies metamorphism.

### 3.5 INTRUSIVES

#### 3.5.1 Granites (s.l.)

Chemical analyses of intrusive granitic rocks from the Hunt River area are shown in Table 3.13. Two groups of granites (s.l.) have been recognized including:

1. an older foliated quartz-monzodiorite, and
2. a younger granodiorite body.

The quartz-monzodiorite occurs in two widely separate areas but geochemically it maintains a restricted range in composition. It is

TABLE 3.12: A chemical comparison of granulite facies rocks and equivalent amphibolite facies rocks with average chemical values of the crust, the Canadian Shield and average composition of the gneisses from the Hunt River area.

	Crust *	Canadian Shield **	Amphibolite Facies *	Granulite Facies *	Banded Gneiss	Homogeneous Gneiss
SiO <sub>2</sub>	60.3	64.9	65.6	61.2	61.60	71.25
TiO <sub>2</sub>	1.0	0.5	0.5	0.6	0.57	0.27
Al <sub>2</sub> O <sub>3</sub>	15.6	14.6	14.9	16.4	15.00	15.13
Fe <sub>2</sub> O <sub>3</sub>	7.2	1.4	1.1	2.3	1.93	0.58
FeO		2.8	3.4	3.5	3.74	1.43
MnO	0.1	0.07	0.06	0.1	0.07	0.02
MgO	3.9	2.2	2.4	3.0	3.71	0.68
CaO	5.8	4.1	3.4	4.4	6.19	2.35
Na <sub>2</sub> O	3.5	3.5	3.5	4.0	3.37	4.33
K <sub>2</sub> O	2.5	3.1	3.7	3.0	0.89	2.34
P <sub>2</sub> O <sub>5</sub>		0.15	0.1	0.16	0.18	0.04
K	20750.0	25730.0	30710.0	24900.0	7367	19400
Rb	90.0	118.0	155.0	56.0	32	100
Sr	375.0	340.0	338.0	572.0	260	338
Ba	425.0	1070.0	605.0	1162.0	330	689
Zr	165.0	400.0	128.0	144.0	114	134
Pb	12.5		23.7	15.1		
Th	9.6	10.3	13.9	5.1		
U	2.7	2.5	2.2	0.5		
K/Rb	231	218	198	447	230	194

\* after Heier and Thoresen, 1971

\*\* after Shaw et al., 1967

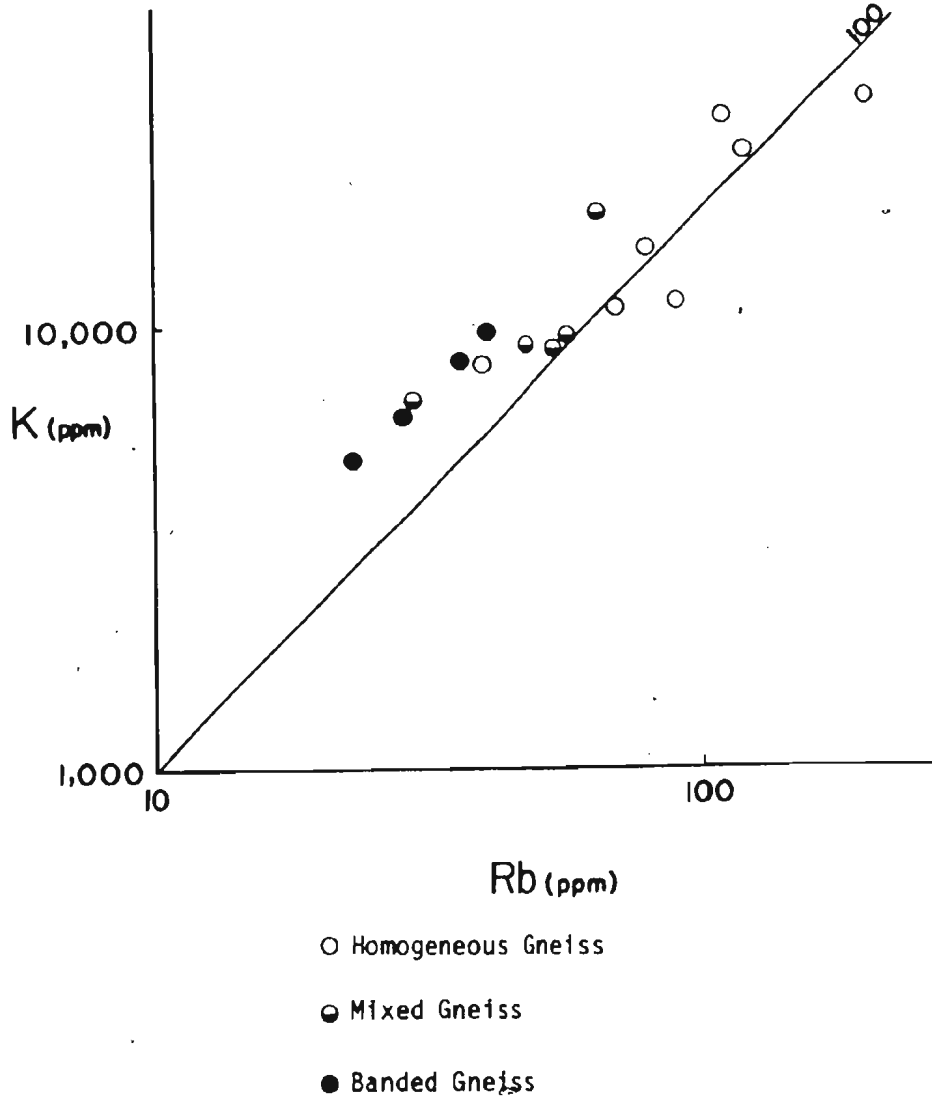


FIGURE 3.10: Log : log plot of K and Rb for quartzofeldspathic gneisses from the Hunt River Belt.

TABLE 3.13: Chemical analyses and C.I.P.W. Norms of the intrusives.

POST TECTONIC DIABASE DYKES						GRANODIORITE	QUARTZ-MONZODIORITE					
WJ-73-	4F	4G	24A	1138	200A	147	33	50	99	100	175	176
SiO <sub>2</sub>	49.53	49.29	50.12	48.13	46.23	70.66	53.26	57.10	59.85	58.73	57.16	57.88
TiO <sub>2</sub>	1.76	1.73	1.51	0.80	1.97	0.15	0.88	0.76	0.76	0.77	0.74	0.75
Al <sub>2</sub> O <sub>3</sub>	13.43	13.43	14.11	14.93	16.61	16.55	16.40	16.82	15.94	15.87	16.12	15.92
Fe <sub>2</sub> O <sub>3</sub>	2.06	2.52	1.03	0.19	1.73	0.27	1.05	1.73	1.07	1.31	0.65	1.10
FeO	12.26	11.68	11.30	11.69	11.54	1.07	6.77	4.91	5.19	5.44	5.41	5.06
MnO	0.22	0.22	0.21	0.21	0.23	0.02	0.14	0.10	0.12	0.10	0.10	0.11
MgO	5.96	6.36	6.35	7.04	7.10	0.42	3.91	0.09	2.90	2.99	3.79	3.05
CaO	9.64	9.91	11.46	11.10	9.15	1.56	7.68	5.06	5.25	5.24	6.11	5.33
Na <sub>2</sub> O	2.22	2.36	2.02	2.36	2.95	5.11	3.32	3.78	4.17	4.29	3.94	4.05
K <sub>2</sub> O	0.70	0.58	0.17	0.78	0.58	2.23	0.99	1.87	1.36	1.68	1.61	1.59
P <sub>2</sub> O <sub>5</sub>	0.23	0.27	0.27	0.24	0.37	0.10	0.58	0.22	0.34	0.36	0.27	0.36
L.O.I.	1.86	1.78	1.88	3.02	3.23	1.27	5.74	2.53	2.20	2.03	2.40	2.44
TOTAL	99.87	100.13	100.43	100.49	99.67	99.41	100.72	98.97	99.15	98.81	98.30	99.64
Zr (ppm)	96	91	70	199	109	118	75	114	116	110	104	135
Sr	161	164	155	251	293	455	347	345	303	262	246	298
Rb	50	52	19	63	22	64	39	70	58	66	56	66
Zn	84	84	76	95	89	31	97	99	89	94	72	86
Cu	322	310	217	28	89	11	50	29	38	33	26	33
Ba	230	204	85	523	356	611	250	450	356	412	511	408
Nb	13	13	10	17	11	6	10	10	12	12	11	12
Ni	69	71	81	89	87	15	88	64	73	76	61	70
Cr	57	61	119	143	57	14	184	109	155	135	101	134
K	5811	4815	1411	6475	4815	18512	8218	15524	11290	13946	13365	13199
Ti	10551	10371	9052	4796	11810	899	5276	4556	4556	4616	4436	4496
K/Rb	116	96	74	182	219	289	211	222	195	211	238	200
						C.I.P.W.	N o r m s					
Q	1.39	0.65	2.01			28.37	6.67	8.98	13.32	10.38	8.08	11.18
Or	4.22	3.48	1.02	4.73	3.48	13.42	6.15	11.45	8.28	10.25	9.91	9.86
Ab	19.16	20.30	17.34	20.46	25.34	44.03	29.55	36.14	36.37	37.48	34.74	35.97
An	25.10	24.74	29.35	28.54	30.82	7.57	28.33	24.25	21.40	19.71	22.45	21.59
Na												
Co						3.06						
Di	18.57	19.55	22.13	22.08	10.77		6.67	0.45	2.82	4.10	6.22	3.28
Hy	24.54	23.58	23.07	4.39	1.63	2.62	3.36	17.07	13.87	13.71	15.47	14.05
Ol				17.35	20.73							
Mc	3.05	3.71	1.51	0.28	2.55	0.40	1.60	2.60	1.60	1.76	0.98	1.67
Il	3.41	3.34	2.91	1.56	3.80	2.29	1.76	1.50	1.49	1.51	1.46	1.50
Cr	0.01	0.01	0.03	0.03	0.01		0.04	0.02	0.03	0.03	0.02	0.02
Ap	0.86	0.64	0.64	0.57	0.87	0.24	1.42	0.53	0.81	0.86	0.65	0.88

characterized by relatively high  $TiO_2$  (0.78%), FeO (5.46%),  $Fe_2O_3$  (1.15%), MnO (0.11%) and high CaO (5.78%). The granodiorite contains higher  $SiO_2$  (70.66%) and lower  $TiO_2$  (0.15%), FeO (0.27%) and  $Fe_2O_3$  (1.07%) than the quartz-monzodiorite. In the C.I.P.W. norms, the quartz-monzodiorite is diopside normative while the granodiorite is corundum normative. The trace element values of the two intrusives do not show significant variations except that the quartz-monzodiorite has relatively high nickel (75 ppm) and chromium (140 ppm) values.

In hand specimen all the feldspar of the granodiorite is pink but in thin section only trace potassium feldspar in the form of microcline was found. The albite, therefore, must contain a substantial amount of potassium in solid solution to account for the chemical abundance of  $K_2O$  (2.23%).

### 3.5.2 Post Tectonic Diabase Dykes

Post tectonic diabase dykes are common throughout the thesis area. Chemical analyses of five dykes are presented in Table 3.13. It is possible to divide the dykes into two chemically distinct groups. One group (WJ-73-4F, WJ-73-4G and WJ-73-24A) is quartz normative. It does not show any diagnostic major element variations, although the samples are slightly lower in  $SiO_2$  and higher in MgO. The other group (WJ-73-223B and WJ-73-200A) is olivine normative. The two groups do, however, show distinctive trace element concentrations. Relatively high Zr, Sr, Ba and to a lesser extent Zn and Ni characterize the olivine normative group. In contrast the quartz normative group

displays higher Cu contents.

Two ages of post tectonic mafic dykes related to a conjugate set of major faults were discussed in Chapter 2, Section 2.5.3.2. Numerous smaller dykes also occur, oriented randomly with respect to the faults. Without further detailed structural observations of the dyke orientations it is not possible to correlate chemical types of dykes with specific structural features.

Chemical research in post tectonic mafic dykes from other parts of Labrador including the Nain-Kiglapait region (Upton, 1974) and the Flowers Bay area (Ryan, 1974) has been carried out. In both studies the dykes were subdivided by composition into chemically distinct groups. There does not appear to be any correlation between the various chemical groupings from the different area. Rivalenti (1975b), in a chemical study of post tectonic dykes near Fiskenaasset, West Greenland, distinguished three ages of dykes, with each suite of dykes more differentiated than the younger suite, and apparently related to a single process of fractionation from a deep crustal magma chamber. Barton (1975a), from work in Labrador in the Kaumajet Mountains, suggested that some of the post tectonic dykes in the region may have served as feeders for the Proterozoic Mugford volcanics. Much detailed work still remains to be carried out on post tectonic dykes from the North Atlantic Craton before any significant regional correlations can be proposed.

CHAPTER 4  
STRUCTURE AND METAMORPHISM

#### 4.1 INTRODUCTION

The tectonic history of the thesis area is extremely complex, involving many stages of folding, faulting and igneous activity. The difficulties encountered in unravelling the structural history of polydeformed high-grade gneiss terrains such as this cannot be over-emphasized. Because a proper understanding of other aspects of geology, especially geochronology, is contingent on a rational interpretation of field relations, a short discussion of some of the difficulties involved in their interpretation is presented below.

##### Lithology

The original mineralogy is usually represented by its high-grade equivalent although original textures and structures are rarely preserved. Migration of the more mobile elements such as Si, K, Rb, Th and U on a regional or local scale may result from temperature and pressure gradients during metamorphism and migmatization. Therefore, the bulk chemistry of different rock types can vary to such an extent that chemical comparisons with possible modern day analyses is misleading.

##### Stratigraphy

Stratigraphic sequences are commonly unrelated to original successions due to modification by tectonic processes. This intercalation of relatively unrelated rock units can result from thrusting and transposition on any scale (Bridgwater et al., 1973c).

Therefore folding of gneissic terrains may not always result in the repetition of rock units in opposite limbs of a fold, especially if compositional layering has been transposed.

#### Fold Style

The dangers of correlating folds on the basis of style have been adequately expressed by Park (1969) and Williams (1970). Folds of different styles may be produced in different rock types even though similar stresses have been imposed (Watson, 1973; Ramsay and Sturt, 1963). Heterogeneous deformation may also cause variable fold styles throughout a terrain of essentially similar lithologies on a regional scale (Coward, 1973) or on an outcrop scale. Other variables such as  $P(H_2O)$  may also affect differential strain patterns in rocks of similar composition.

#### Outcrop Chronology

In terrains which have suffered heterogeneous deformation certain areas commonly escape the effects of one or more deformational episodes. Individual outcrops may therefore show evidence of different events in the regional history. When later deformations are sufficiently intense to completely obliterate evidence of previous tectonic activity, apparently simple structural and microstructural patterns may result and field relations may therefore be misleading in relation to the complete tectonic history of the area.

#### 4.1.1 Nomenclature

The successive phases of deformation and folding are designated  $D_1, D_2, D_3 \dots$  and  $F_1, F_2, F_3 \dots$  respectively, following procedures used by Sturt and Harris (1961). As is commonly the situation in polydeformed gneissic terrains, the earliest recognizable deformation in the area may not be the first deformation affecting the original protoliths. Consequently, numeration of the recognizable discrete deformations is arbitrary. Many geologists term the earliest recognizable deformation  $D_1$  and the associated structural elements  $S_1$  (planar fabric),  $L_1$  (linear fabric) and  $F_1$  (fold). Others attempt to circumvent this absolute labelling of an uncertain event by terming the first recognizable deformation  $D_N$  (Park, 1969). Correlation with adjacent areas is commonly necessary to gain an understanding of the regional structural evolution. It is therefore logical to identify the oldest deformation which can be discerned on a regional scale. The deformation responsible for the formation of the gneissic banding throughout the thesis area is therefore regarded as the datum deformation and is designated  $D_1$ .

##### 4.1.1.1 Deformation

Where applicable, the deformational phases are discussed in terms of homogeneous and heterogeneous deformation. Therefore both a:b:c kinematic axes and X:Y:Z axes of the deformation ellipsoid are used. The types and rates of homogeneous deformation are

defined by k and r.

$$k = \frac{a - 1}{b - 1} \quad (\text{Flinn, 1962}), \text{ where } a = \frac{Z}{Y} \text{ and } b = \frac{Y}{X} \quad (X \leq Y \leq Z)$$

A particular k value describes the relative changes between the various ellipsoid axes but does not give information about the intensity of deformation.

$$r = a + b - 1 \quad (\text{Watterson, 1968})$$

A particular r value defines the amount of deformation. All k values may have suffered the same amount of deformation (r) yet they may display widely varying resultant shapes (k).

#### 4.1.1.2 Fold Geometry

The geometric description of the folds follows the classification outlined by Fleuty (1964).

#### 4.1.2 Outline of the Structural History

The dominant structural features in the thesis area are a well-developed compositional banding of the quartzofeldspathic gneisses and a strong schistosity in the mafic rock units in the Hunt River Belt. The presence of intrafolial folds attests to a history of polydeformation prior to and culminating in the formation of the dominant gneissic banding ( $S_1$ ).  $S_1$  was subjected to three later phases of deformation involving folding and plutonic activity.

The tectonic history of the area is summarized in Table 4.1. In this chapter each phase of deformation is discussed and the

TABLE 4.1: Summary of the geological development of the Hunt River Belt and the surrounding gneiss terrain.

$D_4$	Faulting and Intrusion of Diabase Dykes Megascopic Open Folding ( $F_4$ )
$D_3$	Intrusion of Granodiorite Megascopic Heterogeneous Folding ( $F_3$ )
$D_2$	Intrusion of Quartz-monzodiorite Isoclinal Folding ( $F_2$ )
$D_1$	Intrusion of Granite (parent to the homogeneous gneiss) Interleaving of Supracrustals and Gneisses ( $F_1$ )
	Deposition of Hunt River Supracrustals and Early Deformation
	Presence of Pre-existing Gneiss Terrain

### LEGEND

-  Limit of outcrop
-  Post-tectonic mafic dyke
-  Outline of Hunt River Amphibolite Belt
-  Fault
-  Greasick bending (S.)
-  Axial plane of F<sub>1</sub> fold
-  Plunge of F<sub>1</sub> fold
-  Plunge of F<sub>2</sub> fold
-  Mineral lineation parallel to plunge of F<sub>1</sub> folds
-  Axial trace of megascopic F<sub>1</sub> synform
-  Axial trace of megascopic F<sub>1</sub> antiform
-  Axial plane of F<sub>2</sub> fold
-  Plunge of F<sub>2</sub> fold
-  Axial trace of megascopic F<sub>2</sub> antiform

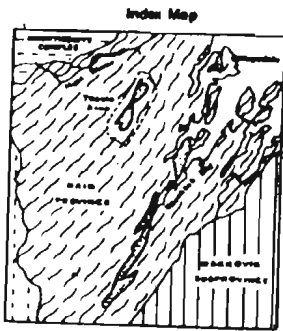
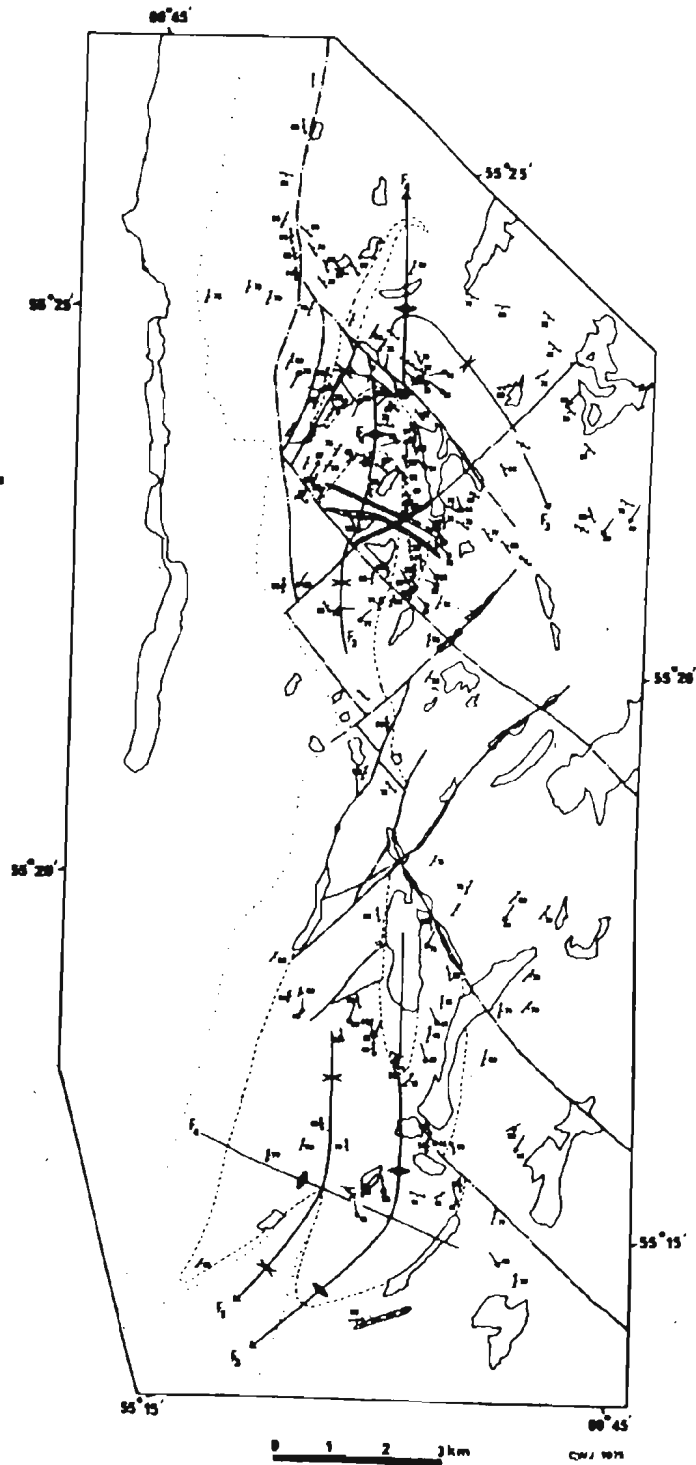


Figure 4.1: Structural Geology of the Hunt River Amphibolite Belt



evidence for each phase is described. Much of the evidence for separating the various phases of deformation was derived from megascopic and mesoscopic fold patterns and from deformed early structural elements (Figure 4.1).

#### 4.1.3 Metamorphism

The determination of metamorphic conditions during a period of deformation is commonly discerned by noting the growth of new minerals. For example, in terrains of progressive regional metamorphism, zones of critical minerals define isograds that delimit areas which have been affected by a particular temperature-pressure regime (eg. Schrijver, 1973). Critical mineral growth may also aid in the determination of temperature and pressure conditions when phases of progressive metamorphism successively overprint a single area (eg. Joubert, 1971).

Microstructural criteria which may be used to determine metamorphic conditions include:

1. new mineral growth,
2. mineral overgrowth,
3. disequilibrium reactions,
4. alteration of minerals (progressive and regressive), and
5. recrystallization.

In the thesis area the dominant mineral assemblage (quartz-plagioclase-hornblende) does not readily lend itself to the growth of new minerals within the restricted range of metamorphic conditions that affected the Hunt River Belt (upper greenschist to high amphibolite

facies). Therefore, alteration of minerals (Binns, 1964; Jakes, 1968) and recrystallization are the two most common criteria utilized to determine the metamorphic changes.

The exception to this generalization is the pelitic schist which displays a variety of different stages of mineral growth. In Chapter 2, Section 2.2.3.1 it was observed that two periods of staurolite + garnet growth were interrupted by a period of cordierite growth. This general relationship was observed in every thin section studied. The pelitic schist shows evidence of two phases of high pressure mineral growth (staurolite + garnet ± sillimanite) separated by a period of relatively low pressure mineral growth (cordierite) (Turner, 1968). It is unfortunate that the pelitic schist occurs as tectonically transposed lenses, localized in very tight synforms of the  $D_3$  deformation. This localized occurrence makes it very difficult to correlate the various stages of mineral growth in these schists to regional poly-deformation, however the pelitic schist is still a potentially valuable lithology for further petrogenetic research.

#### 4.2 PRE - $D_1$ DEFORMATION

Intrafolial folds provide evidence of tectonic and metamorphic events prior to the formation of the dominant gneissic banding ( $S_1$ ) in the quartzofeldspathic gneisses and the dominant schistosity ( $S_1$ ) in the Hunt River Belt amphibolites. The intrafolial folds themselves represent preserved fold closures associated with the  $D_1$  phase of deformation, however they deform pre-existing tectonic fabrics.

In the Quartzofeldspathic Gneiss Complex, intrafolial folds

are commonly preserved in units of banded gneiss. The intrafolial folds are mesoscopic in size and fold a gneissic banding which is similar in fabric and scale to the  $D_1$  gneissic banding (Figure 4.2). In some localities this pre- $D_1$  gneissic banding exhibits an S-fabric defined by a planar orientation of hornblende crystals. This pre- $S_1$  fabric is commonly overprinted by an  $S_1$  mineral growth which is axial planar to  $F_1$  folds.

In the Hunt River Belt, garnetiferous lenses are preserved locally as isolated, rootless, mesoscopic folded structures within otherwise relatively homogeneous amphibolite schists. However, intrafolial folds defined by thin lenses of quartz are more widespread. The quartz lenses occur as isolated, often extremely attenuated, folded structures in units of amphibolite schist. Apparently these units have been subjected to folding and transposition of an early layering and schistosity which was originally parallel to the garnetiferous and quartzitic compositional differences. The folded quartz lenses may, in part, represent pygmatic folds which formed by intense simple shearing of the amphibolite containing discordant quartz veins. This suggests that both the garnetiferous and quartz lenses originally formed part of an earlier layering in the amphibolite schists.

To the north of the Hunt River Belt, poorly exposed outcrops which represent localized zones that escaped much of the intense transposition of the  $D_1$  deformation were found. These zones of a weakly banded quartzofeldspathic-hornblende gneiss (described in Chapter 2, Section 2.5.3.1) contain deformed mafic pods and lenses which are clearly derived from an intrusive suite of dykes. The

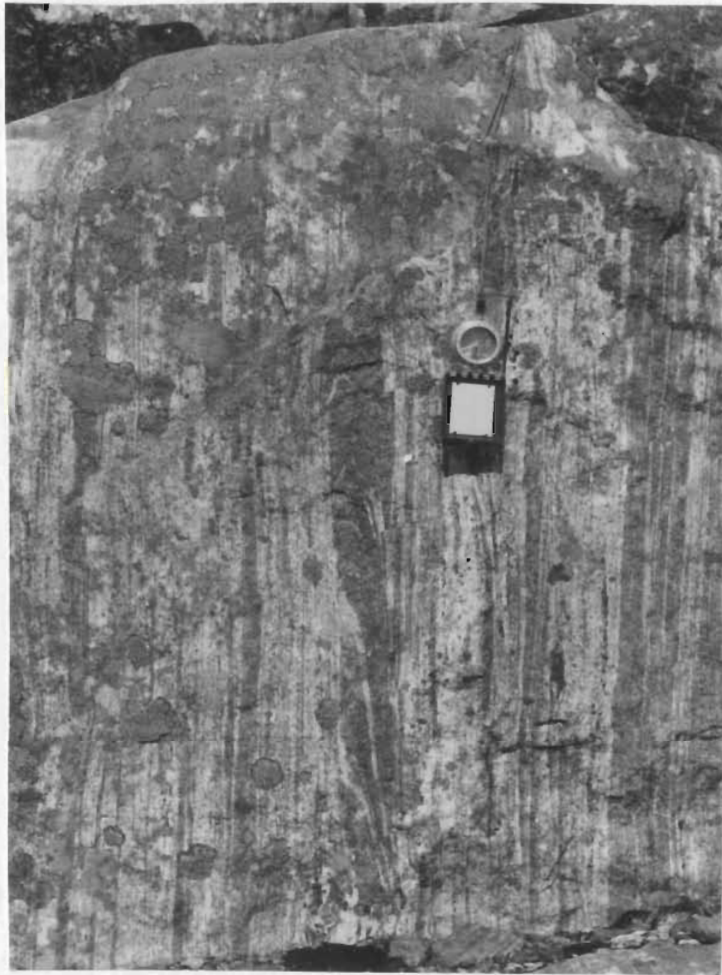


FIGURE 4.2: Typical gneissic banding in banded gneiss terrain. In this outcrop the dominant gneissic banding ( $S_1$ ) is seen to have formed as a result of intense folding and transposition of an earlier gneissic banding which is locally preserved in intrafolial folds.

presence of deformed mafic dykes in gneissic terrains is commonly useful in establishing the tectonic and plutonic chronology of the terrain (Sutton and Watson, 1951). However, the limited occurrence of the deformed dykes in the thesis area places severe restrictions on their usefulness as a means of differentiating the development of the gneissic chronology (cf. McGregor, 1973; Bridgwater et al., 1975).

The nature and regional distribution of the rock types in the map area prior to the  $D_1$  deformation is difficult to ascertain since very few preserved structures and lithological units were found. There is no evidence to prove or disprove that the pre- $D_1$  structures found in the quartzofeldspathic gneisses are spatiotemporally equivalent to the pre- $D_1$  structures in the Hunt River Belt. It is reasonable to assume, however, that an already highly deformed gneiss terrain was in existence prior to the  $D_1$  phase of deformation. Determining the relationship between the banded gneisses and the Hunt River Belt is even more difficult. The gneisses could have acted as a basement to the meta-volcanics, or, alternatively, the meta-volcanics could represent oceanic crust which suffered early tectonic deformation and was later interleaved with the gneisses by tectonic processes.

#### 4.2.1 Pre - $D_1$ Metamorphism

Evidence of the metamorphic conditions prior to  $D_1$  is found in only a few localities, where  $F_1$  intrafolial folds may have preserved pre- $D_1$  mineral assemblages. It should be noted that these isolated occurrences of preserved pre- $D_1$  lithologies can in no way be interpreted to be contemporaneous, and indeed they may reflect several

deformational episodes. At this point, therefore, it is possible only to comment on metamorphic conditions at some time prior to  $D_1$ .

In the amphibolites of the Hunt River Belt only the intrafolial folds defined by garnet and quartz lenses may be considered to be pre- $D_1$  mineralogy. The garnets are red, commonly xenoblastic and poikiloblastic, and contain numerous helicitic inclusions of very fine-grained quartz.

In the banded gneiss of the quartzofeldspathic gneiss complex thin layers (Figure 4.2) or elongate lensoidal portions of pre- $D_1$  lithology are preserved. Field studies of these preserved zones show that the dominant gneissic layering ( $S_1$ ) formed as a result of transposition of an earlier gneissic layering which was very similar in mineralogy and microstructure.

In all the pre- $D_1$  rock studied petrographically, there is no mineralogical evidence to suggest that the thesis area has undergone retrogressive metamorphism from a granulite facies terrain. Sutton (1972) described metamorphic bronzitic hypersthene occurring as polygonal crystals in isolated, zoned, ultramafic boudin-like lenses in the Hopedale Complex in Kaipokok Bay to the south. The presence of this orthopyroxene and the known occurrence of granulite facies gneisses associated with the Nain anorthosite massifs (DeWaard in Morse, 1971) led Sutton to suggest that the Hopedale Complex was derived from reworking of granulites. Recent research, however, (Berg, 1974; Ryan, 1974; Speer, 1975) has shown that granulite facies mineral assemblages discovered in other parts of the southern Nain Province are

entirely a result of contact metamorphism and were formed during intrusion of the anorthosites. The orthopyroxene (enstatite) found in ultrabasic lenses in the Hunt River Belt has been interpreted to be igneous in origin (Chapter 3, Section 3.2.1.1). However, even the occurrence of metamorphic orthopyroxene in the ultrabasic lenses would be insufficient evidence to suggest a granulite facies metamorphic event. There is no sign of orthopyroxene in rocks of basic to intermediate composition (ff. Behr *et al.*, 1971; Collerson and Ethridge, 1972). Also, there is no visible indication that the abundant green pleochroic hornblende has retrogressed from brownish varieties which are characteristic of rocks occurring in the granulite facies (Binns, 1965, 1969; Engel and Engel, 1962).

Therefore, it appears certain that pre-D<sub>1</sub> lithologies in the thesis area were subjected to at least amphibolite facies metamorphism, although details regarding the pre-D<sub>1</sub> event or events cannot be discerned.

#### 4.3 D<sub>1</sub> DEFORMATION

##### 4.3.1 Folds

The D<sub>1</sub> phase of deformation resulted in the formation of the dominant schistose (Figure 2.1) and gneissose (Figure 4.2) tectonic fabrics (S<sub>1</sub>) in the thesis area. S<sub>2</sub> is considered to have formed by metamorphic growth associated with transposition of an earlier layering. No megascopic folds associated with D<sub>1</sub> were recognized. It is apparent from the geometry of the F<sub>1</sub> mesoscopic folds that a large simple shear component was involved in the deformation event. The F<sub>1</sub> folds

commonly have one of their limbs sharply truncated (Figure 4.2). The plane defined by the transposed limb represents a plane of translation, as there is no continuity across this plane. Where both limbs of  $F_1$  folds are preserved, the style of the folds is always S- or Z-shaped and the limbs are extremely attenuated (Figure 4.3).

The  $F_1$  folds are interpreted to have formed in response to a shearing rather than a flattening or buckling mechanism. Fold limbs are extremely attenuated and parallel to  $S_1$ . Away from the preserved  $F_1$  folds, all original pre- $D_1$  planar, curvilinear or linear elements are completely transposed parallel to  $S_2$ . Rare  $L_1$  lineations which could be measured in the field show an orientation perpendicular to the  $F_1$  fold axis (Figure 4.4), indicating that the direction of maximum elongation is parallel to the kinematic  $a$  axis of the fold (Watterson, 1968). In a simple shear environment of great intensity such as that of the thesis area, all linear elements (fold axes) should tend to be rotated towards parallelism with the stretching direction (Escher and Watterson, 1974). Examples in which fold axes retain a high angle with respect to the stretching direction may result from incomplete rotation of folds which developed late in the deformational episode, or development of fold axes at right angles to the stretching direction. Figure 4.2 clearly shows a discontinuity along the left-hand side of the small zone of intrafolial folds. In a simple shear environment no discontinuity will occur at the boundary between undeformed and deformed rocks (Escher and Watterson, 1974). Thus, it appears that in the thesis area a pure shear component was also active during  $D_1$  and therefore there was no rotation of the fold axes.



FIGURE 4.3: Detail of an  $F_1$  intrafolial fold. The fold is S-shaped and both limbs are partially preserved even though they are extremely attenuated.

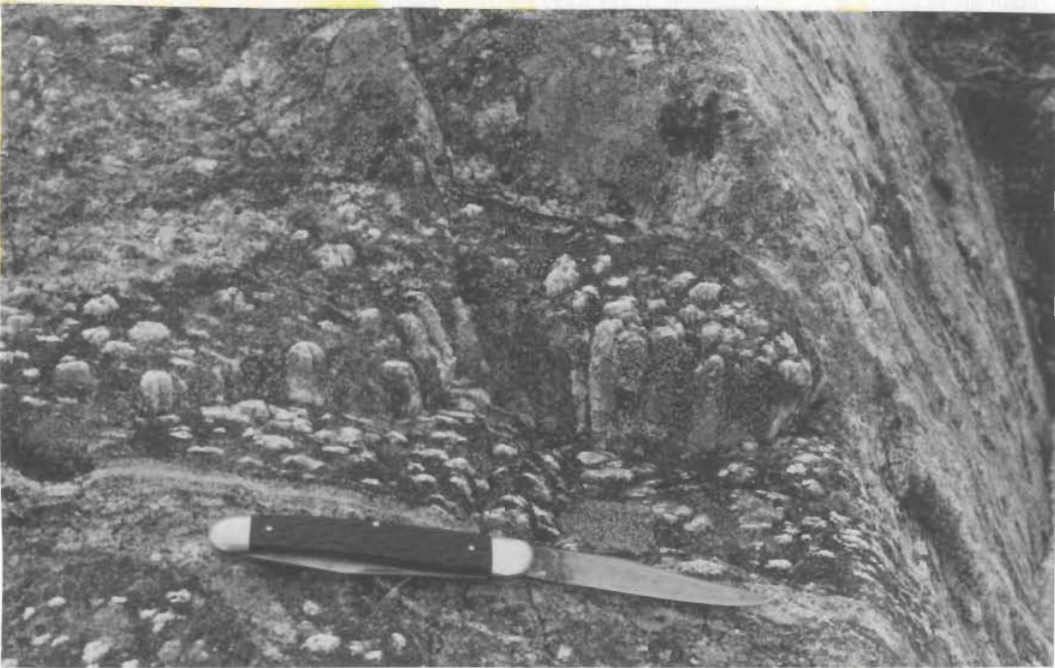


FIGURE 4.4: Steeply plunging  $L_1$  lineations defined by the elongation of feldspars in a banded gneiss.

The large lenses and layers of amphibolite schist described in Chapter 2, Section 2.3.1 are considered to be tectonic schlieren from the main Hunt River Belt, that were emplaced during the  $D_1$  phase of deformation.

A tectonic regime which involved the large scale shearing or 'thrusting' of major lithological units has been suggested as a mechanism for early tectonic development in the North Atlantic Craton (Bridgwater, 1970; Bridgwater et al., 1974). In the thesis area, unfortunately, this deformation was of a more intense and penetrative nature than the possible equivalent deformation at Saglek or Godthaab. Therefore, the early character of the gneisses in the Hunt River area is not preserved.

#### 4.3.2 Homogeneous Gneiss

A weak to strong S-fabric defined by the parallel alignment of biotite is present in the homogeneous gneiss. In places, a gneissic layering composed of alternating layers of grey, medium-grained biotite gneiss and coarse-grained layers of white to pink pegmatitic material is also well-developed. This layering is thought to be the result of igneous injection and subsequent deformation of pegmatitic material rather than metamorphic differentiation.

The homogeneous gneiss is considered to have been emplaced as a series of intrusive sheets into the banded gneiss terrain. It is, however, difficult to determine precisely at what stage it was emplaced. Schlieren of meta-volcanics which are common in the banded gneiss terrain are completely lacking in the homogeneous gneiss.

These schlieren were tectonically formed during  $D_1$ , and it follows that if the homogeneous gneiss was present during the main period of  $D_1$  activity, some interleaving with the mafic volcanics would have occurred. Therefore, the homogeneous gneiss was probably emplaced as a series of discrete sheets along planes of translation or thrust planes during the waning stages of  $D_1$  deformation.

The homogeneous gneiss is interlayered with other distinct gneiss types on a scale of several metres in the mixed gneiss terrain. Refolded isoclinal  $F_2$  folds are present in the mixed gneisses and, in places thin layers of homogeneous gneiss have also been isoclinally folded ( $D_2$ ). The layers of homogeneous gneiss are extremely leucocratic (biotite depleted), however it appears that a weak S-fabric is axial planar to the  $F_2$  isoclinal folds and is possibly contemporaneous with the S-fabric ( $S_2$ ) that is more strongly defined by biotite elsewhere in the homogeneous gneiss. Thus, this places an upper limit (pre- $F_2$ ) for the emplacement of the homogeneous gneiss.

#### 4.3.3 $D_1$ Metamorphism

The Hunt River Belt, the banded gneisses of the Quartzofeldspathic Gneiss Complex and the rock units in the border zone were all subjected to the  $D_1$  phase of deformation and inherited their dominant metamorphic aspect during  $D_1$ . Since the effects of later deformations of  $S_1$  may be readily recognized (eg. folding, boudinage), the predominant mineral assemblages and microstructures present throughout much of the thesis area may be attributed to  $D_1$ .

In the Hunt River Belt amphibolite schists, the mineral

assemblages which are interpreted to have formed during or in response to  $D_1$  are as follows:

1. hornblende + plagioclase
2. hornblende + plagioclase + quartz
3. hornblende + quartz + garnet + plagioclase
4. hornblende + diopside + plagioclase + garnet
5. hornblende + quartz + plagioclase + diopside
6. hornblende + diopside + plagioclase.

The  $D_1$  mineral assemblages identified in the quartzofeldspathic gneisses (including the border zone) are:

7. quartz + plagioclase + hornblende
8. quartz + plagioclase + microcline + hornblende
9. quartz + plagioclase + microcline + muscovite + garnet
10. quartz + plagioclase + microcline + muscovite
11. quartz + plagioclase.

The stable co-existence of muscovite and quartz strongly suggests that the rocks have been subjected to the P-T conditions of the kyanite-almandine-muscovite sub-facies of the amphibolite facies (Kröner, 1971). However, the above mineral assemblages are typical of the sillimanite-almandine-orthoclase sub-facies of the almandine-amphibolite facies of Turner and Verhoogen (1960) and Winkler (1965).

For the purpose of this thesis, the mineral assemblages above are designated as being in the 'amphibolite facies' as originally defined by Eskola (1939) and followed by Turner (1968).

#### 4.4 D<sub>2</sub> DEFORMATION

Although D<sub>2</sub> structural features such as re-oriented discordant veins and boudinaged layers are widely developed in the thesis area, no megascopic F<sub>2</sub> folds were observed. In contrast to the D<sub>1</sub> deformation, the D<sub>2</sub> deformation shows evidence of a different tectonic regime with respect to the relationship between the principal tectonic stress direction and the principal strain direction.

##### 4.4.1 Folds

F<sub>2</sub> folds which fold S<sub>1</sub> are more common in the banded gneiss terrain than in the Hunt River Belt. This is possibly because they are more readily observed in sequences of banded gneiss than in relatively homogeneous units of amphibolite.

Mesoscopic F<sub>2</sub> folds vary from isoclinal to very tight. Both similar and parallel types of folds are recognized. Their style depends upon the tightness of the fold closure and on the rock composition. In rock units of uniform composition, the tighter fold closures display a more similar style of folding (Figure 4.5). In the mafic rock units (amphibolites, Figure 4.6) the folds are more parallel in style than fold closures of comparable interlimb angle in acid rocks such as the banded gneisses (Figure 4.7). Similarly, axial plane fabrics are more strongly developed in folds with tight fold closures (Figure 4.5) and in folded quartzofeldspathic layers (Figure 4.7).

Tectonic fabrics associated with D<sub>2</sub> are predominantly S-fabrics, defined by a preferred mineral alignment in the nose of the folds. L<sub>2</sub> intersection fabrics (the line of intersection between S<sub>1</sub> and



FIGURE 4.5: Isoclinal Z-shaped  $F_2$  fold in banded gneiss. Note the variability of the tightness of the fold closure along the axial trace. A well-developed axial plane schistosity cuts the layering in the lower part of the antiform.



FIGURE 4.6: Isoclinal  $F_2$  fold in amphibolite from the Hunt River Belt. A very weak  $S_2$  axial plane schistosity may be noted and crosses  $S_1$  in the nose of the  $F_2$  fold.



FIGURE 4.7:  $F_2$  parasitic fold in banded gneiss. The fold closure is relatively open yet a strong  $S_2$  axial plane schistosity has developed.

and  $S_2$ ) are weakly developed. The axial planes and fold axes of the  $F_2$  folds and  $L_2$  lineations display variable orientations due to heterogeneous re-orientation by  $F_3$  folding.

#### 4.4.2 Discordant Veins

Discordant quartzofeldspathic and quartz veins show two main structural relationships with the amphibolites in the Hunt River Belt. They are commonly isoclinally folded (Figure 4.8), but in some places they behave in a more passive manner and their deformation approaches ptygmatic folding (Figure 4.9). The presence of these  $D_2$  structures may help solve the question of why few  $F_2$  folds of  $S_1$  have developed. In areas where  $S_1$  was parallel to the kinematic a:b axes, no folds of the layering ( $S_1$ ) will be developed (Watterson, 1968). Therefore, the intensity of deformation is recorded by the re-orientation of discordant veins. As seen in Figure 4.8, although no folding of  $S_1$  is seen, the effect of  $D_2$  has been strong, as shown by the isoclinal folding of the quartz vein. The folded pegmatite vein in Figure 4.9 appears to have passively recorded a more homogeneous style of deformation.

#### 4.4.3 Boudinage

Boudinage structures are common throughout the thesis area, occurring in rock units which are comprised of alternate layers of contrasting ductility. Rock units in the Hunt River Belt which have undergone boudinaging include concordant pegmatites (Figure 4.10), garnetiferous layers (Figure 2.3) and acid rusty layers. In the quartzofeldspathic gneisses the concordant pegmatites, and to a lesser

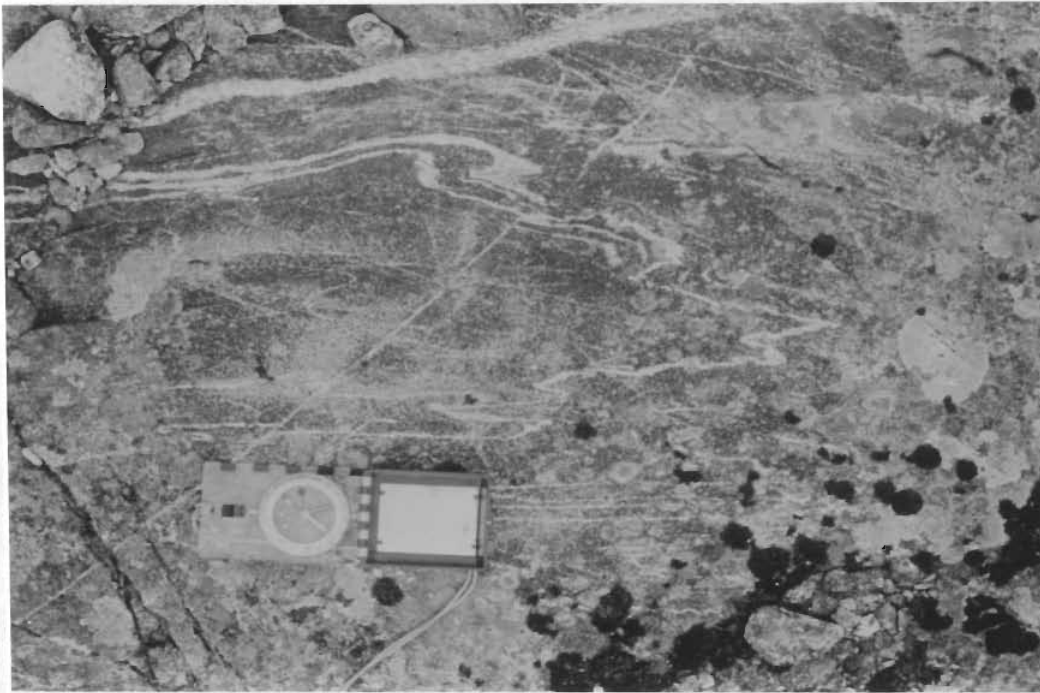


FIGURE 4.8: Thin quartz veins isoclinally folded during  $D_2$ . Note the geometric relationship of S- and Z-shaped parasitic folds on the limbs of the larger fold.



FIGURE 4.9: Discordant pegmatite vein ptygmatically folded during  $D_2$  deformation. The direction of maximum compression (X-axis) is not necessarily perpendicular to the foliation.



FIGURE 4.10: Isolated boudinaged remnant of pegmatite vein forming an augen structure in the amphibolite from the Hunt River Belt.

extent the thin mafic layers, are boudinaged. In a few outcrops where frost action has heaved jointed blocks of rock, the boudinage structures can be viewed in three dimensions. They pinch out in two directions and form disc-shaped augen. Similar augen (disc-shaped) structures are also observed in slabbed hand specimens that contain thinly boudinaged concordant pegmatite veins.

#### 4.4.4 Quartz-monzodiorite

The bodies of quartz-monzodiorite appear to be largely fault bounded. The outcrop patterns are lensoidal to lobate in form and there is no suggestion that  $D_2$  S-fabrics are deformed around the plutons. The bodies contain a single L - S - fabric which is co-planar and co-axial with  $F_3$  fold axes. Primary porphyritic igneous textures, which have surprisingly survived through the intense penetrative nature of the  $D_3$  deformation, are preserved locally on surfaces perpendicular to the  $L_3$  lineation. The emplacement of the quartz-monzodiorite is considered to represent a discrete period of post- $D_2$ , pre- $D_3$  plutonic activity.

#### 4.4.5 Interpretation of the $D_2$ Deformation

Deformational features associated with  $D_2$  indicate that the rocks underwent strong homogeneous flattening. The structures which support this interpretation include:

1. regional development of an S-fabric,

2. isoclinal toptygmatic folding of discordant veins, and
3. boudinaging of concordant veins and competent rock units in two directions forming isolated augen structures.

In relation to the Flinn (1962) deformational ellipsoid, the  $k$  value would approach 0. The intensity and nature of the  $D_2$  deformation may have resulted in the obliteration of much of the  $L_1$ -fabric formed during  $D_1$ .

#### 4.4.6 $D_2$ Metamorphism

Throughout the thesis area there is extensive evidence that considerable reorientation and recrystallization of  $D_1$  mineral constituents took place. However, in the amphibolite schists and the quartzofeldspathic gneisses no new minerals developed.

Recrystallization of the mineral components is most readily observed in the noses of mesoscopic  $F_2$  fold closures (Figures 4.5, 4.6 and 4.7). At these outcrops a weak to moderate  $S_2$  fabric transects the folded  $S_1$  in the amphibolites and a moderate to strong  $S_2$  fabric transects the folded  $S_1$  in the banded quartzofeldspathic gneisses. In places (Chapter 4, Section 4.3.2) the homogeneous gneiss also displays an  $S_2$  fabric defined by the parallel alignment of biotite flakes and elongate quartz and feldspar.

Other effects of the  $D_2$  deformation produced widespread boudinage structures in layered rocks of varying competence (Figures 2.3 and 4.10). Where these boudinaged layers could be

examined in three dimensions and in thin section, they were shown to form circular, disc-shaped boudins.

All the mineral assemblages which formed during  $D_1$  appear to have remained stable during  $D_2$ . The one exception is the predominance of biotite as the mafic mineral in the homogeneous gneiss. Therefore, the single new mineral assemblage developing during  $D_2$  is:

quartz + plagioclase + biotite + microcline + hornblende.

In general then, it could be stated that the metamorphic conditions remained in the amphibolite facies regime. However, it must be remembered that the tectonic environment invoked to produce the structural elements peculiar to  $D_2$  is completely different than that which existed either earlier during  $D_1$  or later during subsequent deformations.

#### 4.5 DISTINCTION BETWEEN $D_3$ AND $D_4$ MEGASCOPIIC FOLDS

Megascopic folds associated with  $D_3$  and  $D_4$  deformations are similar in both style and scale, and it is useful to briefly outline the method that is used for distinguishing between  $F_3$  and  $F_4$ .

The first order structural features in the thesis area are two megascopic antiform-synform couples. One is found in the northern part of the area, and the other occurs in the south (Figure 4.1). Figure 4.11 illustrates the relationship of the megascopic folds to the mesoscopic linear elements (lineations and fold axes). In the southern area (Figure 4.11B) the mesoscopic structural elements display

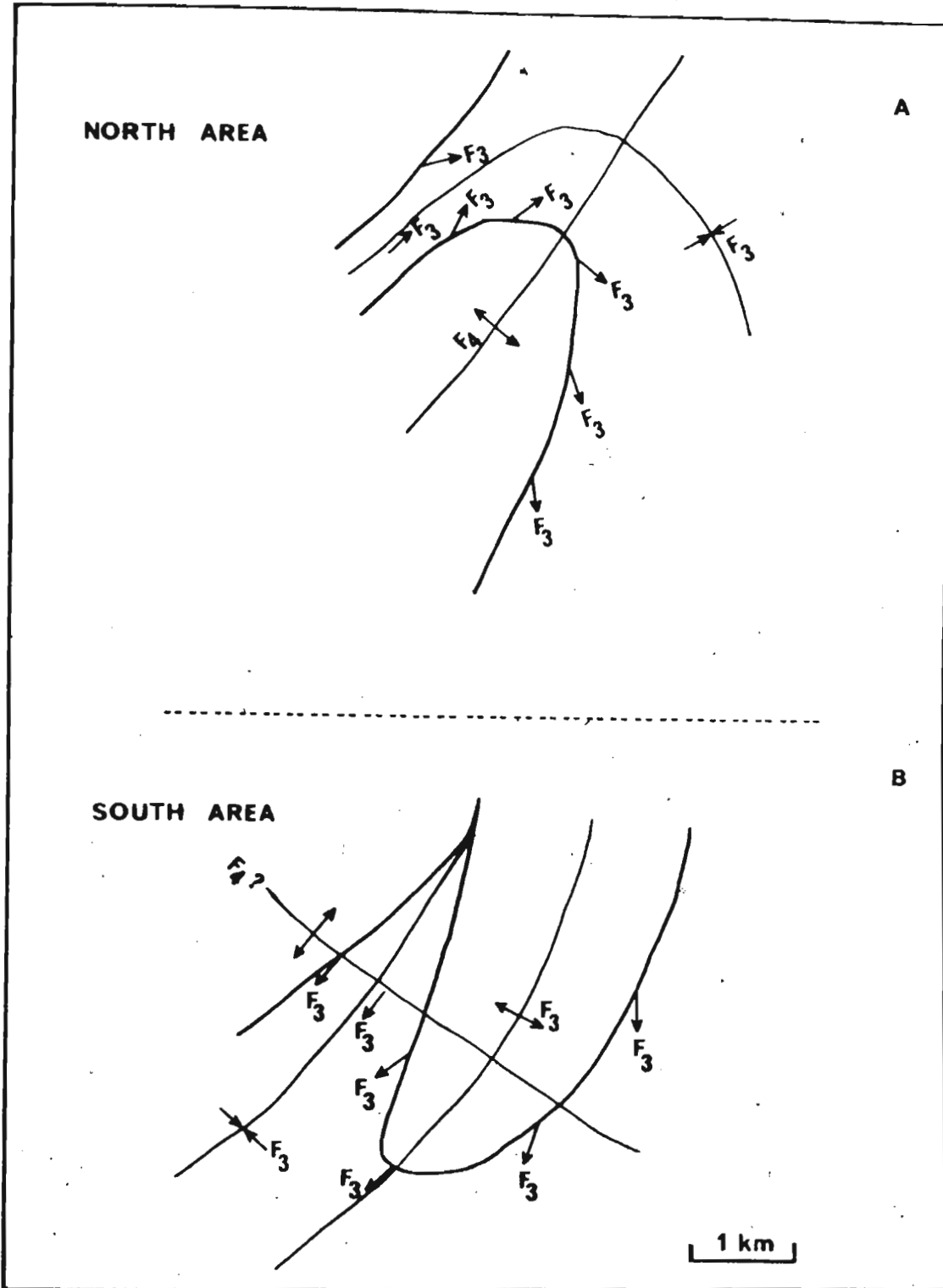


FIGURE 4.11 : Schematic drawing of megascopic synform-antiform couples in the Hunt River area, illustrating geometrical relationship of small scale folds and lineations.

a symmetrical geometrical orientation in relation to the axial planes of the megascopic folds. The lineations and mesoscopic fold axes are approximately co-axial although a definite fanning is present. The synform and the antiform in the south are therefore interpreted to be contemporaneous  $F_3$  folds.

In the northern area (Figure 4.11A) the mesoscopic structural elements display a symmetrical geometrical orientation with the megascopic synform, but they are clearly asymmetrical in relation to the megascopic antiform. The antiform in the north is interpreted to be the result of a later stage of folding ( $F_4$ ) which re-oriented pre-existing structural elements associated with the formation of the tight megascopic  $F_3$  synform.

#### 4.6 $D_3$ DEFORMATION

##### 4.6.1 Megascopic Folds

The  $D_3$  deformation is the earliest deformation for which megascopic folds can be mapped out in the field. The  $F_3$  megascopic folds refolded the Hunt River Belt and are clearly defined by the outcrop pattern of the Belt (Figure 4.1). The  $F_3$  megascopic folds comprise both antiforms and synforms of variable style.  $F_3$  antiforms display relatively open, parallel fold closures, whereas the  $F_3$  synforms have very tight, similar fold closures, and an interlimb angle of less than  $30^\circ$ . The antiform in the south approaches the shape of an isoclinal fold with almost parallel fold limbs. The folds range in size up to 6 km in amplitude and 3 km in wavelength. Due to extensive block faulting and modification from variable amounts of later refolding,

the overall pattern of the  $F_3$  megascopic folds cannot be determined.

The  $F_3$  megascopic folds are upright, symmetrical folds with moderate to shallow plunges. The  $F_3$  antiform-synform couple in the south, least affected by later refolding, plunges at approximately  $20^\circ$  to  $210$  (Figure 4.12A). This is approximately parallel to regional structural trends in the southern part of the Nain Province. The  $F_3$  folds certainly have had a significant effect on the outcrop pattern in the Hunt River Belt, and they may well be the dominant phase of deformation controlling regional structural trends in the southern Nain Province.

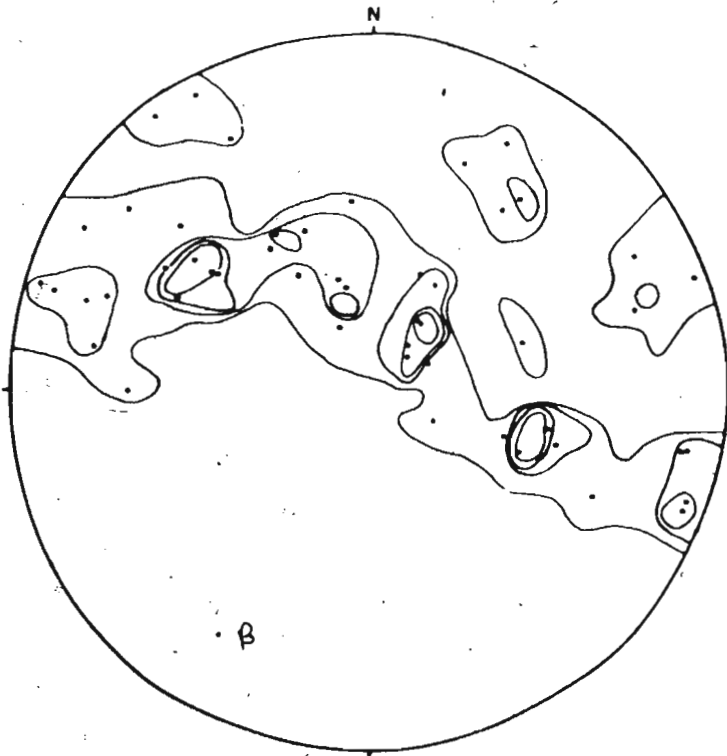
#### 4.6.2 Mesoscopic $F_3$ Folds •

Mesoscopic  $F_3$  folds are abundant throughout the thesis area. Their style varies greatly, depending upon their structural position within megascopic folds. Mesoscopic folds found in the megascopic synforms are generally similar folds with very tight to parallel interlimb angles (Figure 4.13). Mesoscopic folds associated with the megascopic antiforms vary from broad, open folds (Figure 4.14) to folds which may have relatively tight fold closures, but interlimb angles that remain fairly open.

Axes of  $F_3$  mesoscopic folds do not exactly parallel the axes of  $F_3$  megascopic folds. Only in the cores of the synforms are the mesoscopic folds co-axial and co-planar with megascopic folds. Figure 4.12B shows a stereographic plot of linear structures associated with the  $F_3$  antiform in the southern area. The orientation of the data clearly shows an angular relationship between the axial plane of the

- poles to main schistosity
- ↘ plunge of  $F_3$  mesoscopic fold axes
- ↙ plunge of lineation parallel to  $F_3$  fold axes

( A )



( B )

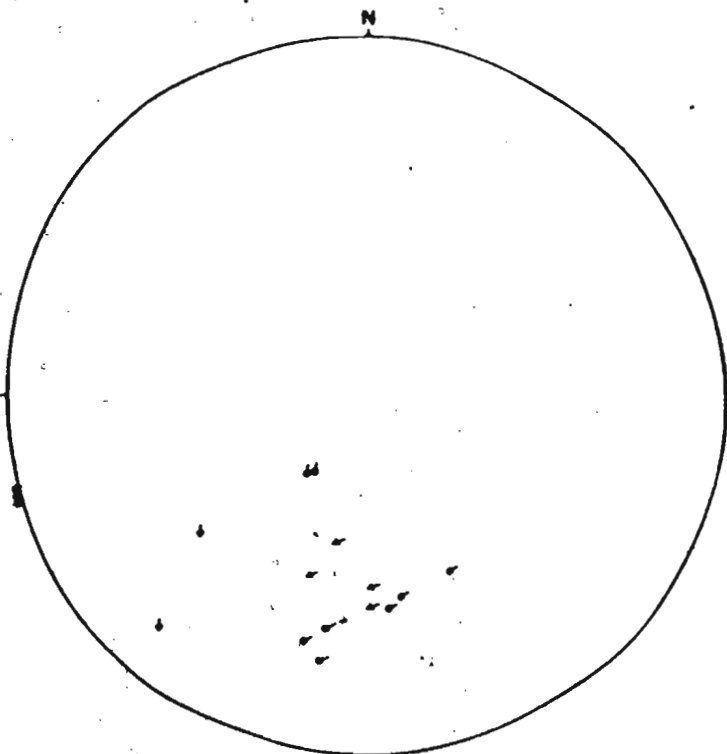


FIGURE 4.12: Stereographic plot of structural elements associated with the megascopic synform-antiform couple in the southern part of the Hunt River Belt.



FIGURE 4.13: Tight mesoscopic folds occurring in an ultramafic lense in the  $F_3$  megascopic synform. The folds are defined by thin magnetite layers which stand out in relief against a schistose serpentinite matrix.



FIGURE 4.14: Broad open mesoscopic fold occurring in an ultramafic lense in the  $F_3$  megascopic antiform. Smaller crenulation folds are also present.

megascopic antiform and the mesoscopic linear elements. This is a result of fanning of the minor fold axes and associated lineations as diagrammatically illustrated in Figure 4.11. The large variation in the angle of plunge is possibly the result of later refolding about a NW-SE fold axis (Figure 4.1).

#### 4.6.3 Granodiorite

Field evidence suggests that the granodiorite intruded after the  $F_3$  phase of folding. It lacks a penetrative tectonic fabric and it is not cut by  $F_3$  pegmatites which are widespread in the immediate vicinity of the pluton. A minimum age of the granodiorite is more difficult to ascertain.  $F_4$  folding was immediately succeeded by faulting and diabase dyke emplacement. It is unlikely that a granitic pluton would have been intruded contemporaneously with mafic dyking. Therefore, the granodiorite is interpreted to have been intruded either syntectonically with the  $F_4$  folding or during the period of quiescence between the  $F_3$  and  $F_4$  periods of folding.

#### 4.6.4 Heterogeneous Nature of $D_3$ Deformation

Heterogeneous deformation is the most characteristic feature of the  $D_3$  phase of deformation. The first order expression of the heterogeneous deformation is the presence of megascopic, relatively broad, open antiforms and tight synforms. This megascopic fold geometry may be achieved by processes other than heterogeneous deformation. Ramsay (1960), for example, has shown geometrically that flexure (parallel) folds die out both upwards and downwards.

Therefore, a cross-section through a folded sequence would expose broad antiformal structures and relatively tight synformal structures. However, structural analysis would show that the mesoscopic deformation is much the same across the length of the cross-section. Watterson (1968), in Vesterland, south-west Greenland, mapped open asymmetric folds along side bands of plutonic mylonites located along attenuated steep limbs of the folds. Detailed structural analysis showed that both structures suffered similar deformation and the discrepancy in the geometry of the structures was caused by the relative orientations of the layering with the a:b:c kinematic axes.

The forms of the mesoscopic  $F_3$  folding in the thesis area are related to heterogeneous development of mesoscopic structures. These structures are described in two groups: those which vary perpendicular to the megascopic axial planes, and those which vary parallel to these planes.

Perpendicular to Axial Planes

Folds: Within the megascopic antiforms the mesoscopic  $F_3$  folds are open parallel structures (Figure 4.14), whereas in the synformal domains the mesoscopic  $F_3$  folds are very tight to isoclinal (Figure 4.13).

Lithologic Relationships: The best examples of rock units are found in the ultramafic bodies. In the antiformal domains the ultramafic bodies form continuous, mappable units and are folded around the antiforms. In the synformal domains the ultramafic rock units are transposed into a series of discontinuous lenses parallel to the axial plane of the synform.

Parallel to Axial Planes

Heterogeneous deformation parallel to axial planes is seen best along the axial traces of the megascopic synforms.

- Folds: In the core of the megascopic  $F_3$  synform,  $F_3$  mesoscopic folds are very tight. Away from the nose region of the megascopic fold,  $F_3$  mesoscopic folds are more open (Figure 4.15).

Lithologic Relationships: A regional development of agmatite occurred syntectonically with  $F_3$  folding. Away from the nose of the megascopic synforms, the agmatite is composed of highly angular blocks of banded gneiss (the paleosome). As the agmatite is traced towards the nose of the synforms, the paleosome blocks are progressively more deformed into augen-like structures, and finally the agmatite is completely transposed into a concordant unit of banded gneiss (Figure 4.16).

Heterogeneous deformation forming megascopic open antiformal domains and tight synformal high intensity deformation domains have been reported from the Laxfordian of South Uist, Outer Hebrides, by Coward (1973). Coward summarized the main theories for the evolution of this style of structure. Ramberg (1966) and Eskola (1949) considered that such structures could be produced by the gravitational updoming of certain basement areas. Ramsay (1967) however showed that buckling of an interface comprising two contrasting viscosities produced a series of antiforms of broad rounded aspect separated by synforms which had smaller interlimb angles. Coward concluded that the structures of South Uist resulted from buckling under compressive stress because dense pyroxene-bearing rocks were located in the lower structural levels of the gneisses.



FIGURE 4.15: Outcrop of agmatite in banded gneiss terrain. The irregular fragment of banded gneiss contains an open  $F_3$  fold closure.



FIGURE 4.16: Outcrop of agmatite in amphibolite unit of the Hunt River Belt. In this outcrop near the nose of the  $F_3$  synform the fragments of amphibolite have been intensely deformed, forming a heterogeneous discontinuous gneissic layering.

In the thesis area density differences were not observed in rocks in the lower structural levels of the  $F_3$  folds which would indicate either an upwelling of lighter material or the presence of a buttress for buckling. There appears to be no physical or geometric condition which could have caused the heterogeneous deformation. Therefore the heterogeneous deformation is regarded as being related to variations in the tectonic stress regime.

Relevant to discussion of the origin of the  $F_3$  structures in the Hunt River area are the style of deformation immediately preceeding and postdating the  $D_3$  deformation, and the extensive development of syntectonic agmatization. The  $D_2$  deformation phase is characterized by a strong penetrative flattening which is interpreted to have occurred through homogeneous deformation at deep crustal levels. The  $D_4$  deformation, on the other hand, is characterized by open parallel folds indicative of deformation at shallow crustal levels (Bowes, 1975). Therefore, the period of  $D_3$  deformation may have occurred during crustal uplift. This would explain why  $D_3$  shows effects of both high and low intensity deformation.

#### 4.6.5 $D_3$ Metamorphism

The  $D_3$  deformational event is characterized by heterogeneous folding resulting in synforms which are very tight, and antiforms which have relatively open fold closures. In the Hunt River Belt, where the amphibolite schists were subjected to intense stress in the  $F_3$  synforms, mineral assemblages have simply undergone recrystallization and reorientation in response to  $D_3$  stress. This is particularly

evident when microscopic and small mesoscopic  $F_3$  folds are examined in thin section. Along the limbs of these  $F_3$  tight folds quartz, plagioclase and hornblende, in thin section cut perpendicular to the fold axes, were viewed as platy sub-idioblastic crystals which parallel the fold limbs. In the nose of these microscopic folds, however, the mineral components appear as equidimensional granoblastic mosaic. Here the minerals were viewed end-on, as they define an elongate mineral lineation paralleling the fold axes.

In the northern area both hornblende (in garnet-bearing amphibolite schist), and pyroxene (in diopside-bearing amphibolite schist), as well as undergoing recrystallization, also occur as coarse ( $\leq 10$  mm across), sub-idioblastic crystals which appear to overgrow the main  $S_3$  fabric. This is indicative of a period of static mineral growth after the main tectonic episode of  $D_3$  deformation.

In the southern area similar petrographic characteristics were observed. Locally however, in a garnet-bearing amphibolite schist, cummingtonite, rather than hornblende, appears to have formed as a post- $D_3$  mineral component. The cummingtonite formed as an alteration product of hornblende and where cummingtonite is present, hornblende is in disequilibrium with garnet (Figure 2.4). In the Abukuma Metamorphic Belt, Japan, Kanisawa (1968) describes cummingtonite-hornblende-bearing amphibolites interlayered with garnet-bearing amphibolites. Kanisawa suggests that the cummingtonite may have formed as a result of decomposition of garnet in response to andalusite-sillimanite type metamorphism of a garnet-bearing amphibolite. This may also be the case in the Hunt River Belt. However, the restricted

range in occurrence of the cummingtonite (to the southern part of the Hunt River Belt) cannot at this time be interpreted as reflecting a metamorphic isograd. A study of the bulk chemical compositions shows that the ~~cummingtonite-garnet-bearing~~ amphibolite schist is lower in CaO and higher in MgO (cf. Hietanen, 1973) than the other garnet-bearing amphibolite schists in the Hunt River Belt. Thus, the appearance of cummingtonite may simply be controlled by local variances in bulk rock chemical compositions.

In the quartzofeldspathic gneiss complex the effects of the  $D_3$  deformation are very heterogeneous. The salient feature however, is the early syntectonic emplacement of abundant, coarse-grained pegmatitic material along megascopic  $F_3$  synforms, to form the agmatite unit. Near the noses of the  $F_3$  megascopic folds this agmatite is highly deformed so that evidence regarding the origin of the leucosome is obliterated. Over much of the remaining agmatite the paleosome fragments are highly angular and in many places could theoretically be pieced back together. This is particularly evident in the more mafic rock units which may contain as little as 10% leucosome fraction. Therefore, the leucosome fraction is not a result of in situ anatexis of the quartzofeldspathic gneiss. It seems more likely that it was derived from quartzofeldspathic gneisses at lower structural levels in the crust, at the time of  $D_3$  deformation.

The change in deformation style from pervasive flattening ( $D_2$ ), to heterogeneous strong to moderate deformation ( $D_3$ ) to open upright folds ( $D_4$ ) and finally to megascopic faulting and dyking suggests that the episodes of deformation may be associated with an overall uplifting of the rocks to shallow crustal levels. The presence of both the leucosome

infusion in the quartzofeldspathic gneiss and the pegmatite intrusion in the southern part of the Belt is interpreted to reflect a magma upwelling associated with the processes that invoke crustal uplift (cf. Bowes, 1975).

#### 4.7 D<sub>4</sub> DEFORMATION

The D<sub>4</sub> deformation is characterized by megascopic open folding. F<sub>4</sub> folds re-fold F<sub>3</sub> folds and form regional interference patterns. Extensive penetrative (axial planar) fabrics are not found associated with the F<sub>4</sub> folds.

The open style of F<sub>4</sub> and lack of associated penetrative deformation indicates that the D<sub>4</sub> phase is probably a relatively shallow level deformation. It is of interest to note that the axial traces of the F<sub>4</sub> folds lie parallel to a late stage set of regional conjugate faults. It is possible that F<sub>4</sub> folding gave way to brittle deformation in response to a further uplift of the rocks.

##### 4.7.1 Megascopic Folds

Megascopic F<sub>4</sub> folds are developed best in the north where an F<sub>4</sub> antiform folds and F<sub>3</sub> synform (Figure 4.1 and 4.11). The antiform is an open, upright, parallel fold which plunges at approximately 60° to the northeast (Figure 4.17A). In the south the F<sub>3</sub> folds are folded about a NW-SE axis by later broad, open warps (Figure 4.1). The axial trace of the open warping in the south is at a high angle to the F<sub>4</sub> axial trace in the north and is only tentatively assigned an F<sub>4</sub> age. The overall style of the F<sub>4</sub> folding is obscured by late stage block faulting.

- poles to main schistosity
- ↙ plunge of lineation parallel to  $F_3$  fold axes
- ↘ plunge of  $F_3$  mesoscopic fold axes
- ↙<sub>N</sub> plunge of  $F_4$  mesoscopic fold axes

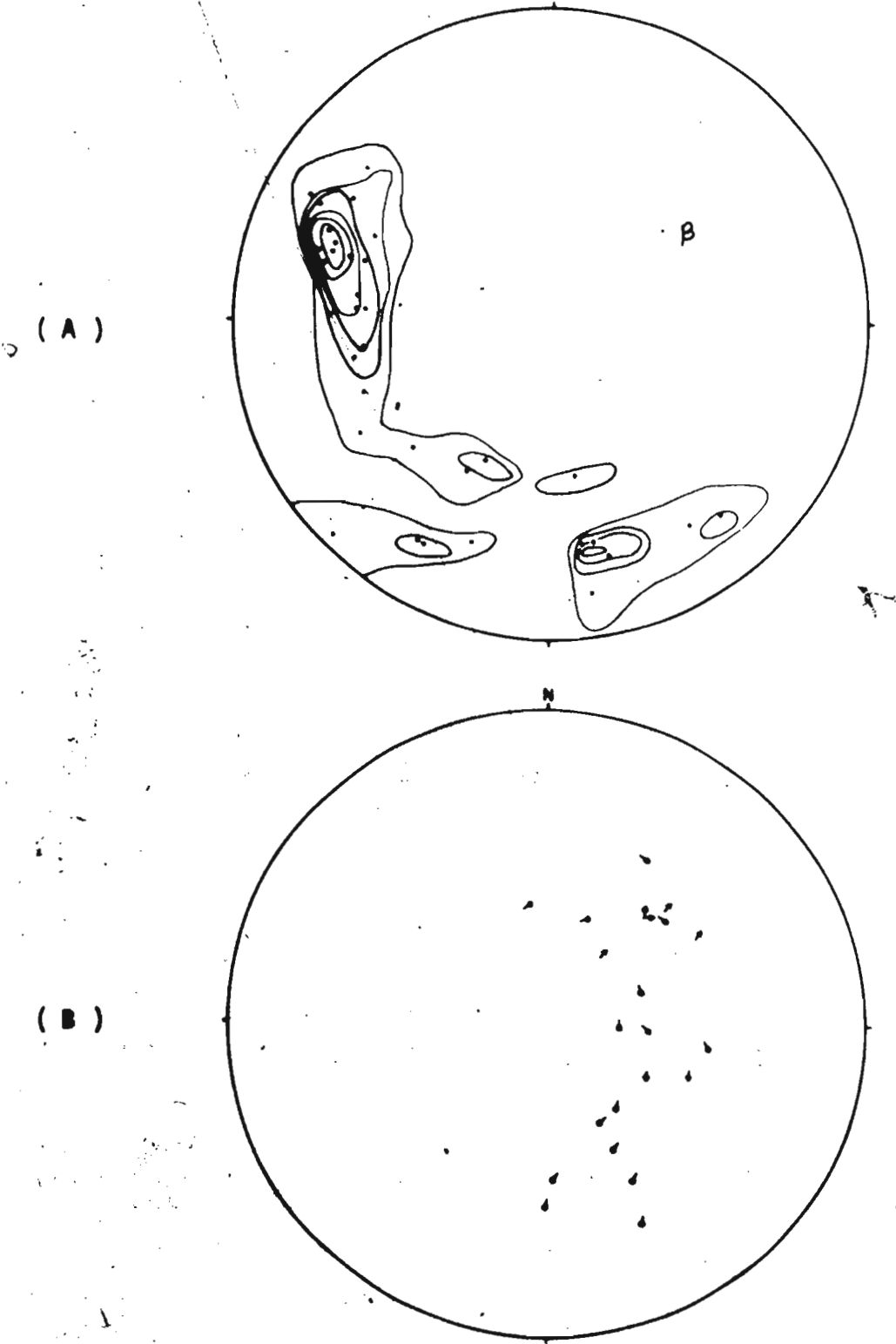


FIGURE 4.17: Stereographic plot of structural elements associated with the mesoscopic synform-antiform in the northern part of the Hunt River Belt.

#### 4.7.2 Mesosopic Structures

In the northern  $F_4$  megascopic antiform, mesoscopic  $F_4$  folds are easily distinguished from earlier  $F_3$  structures on the southeast limb only. On the northwest limb,  $F_3$  and  $F_4$  folds are roughly co-axial and co-planar because of the parallelism of the  $F_3$  and  $F_4$  megascopic axial plunges.  $F_3$  folds on the eastern limb have been re-oriented so that they have a general plunge to the southwest (Figure 4.17B), whereas the  $F_4$  parasitic folds maintain a northeasterly plunge.  $F_4$  mesoscopic folds on the eastern limb are S-shaped (Figure 4.18), parallel, and plunge to the northeast. They are fairly open (interlimb angle of  $45^\circ$ ), however they display tight fold closures. The small amount of apparent thickening in the nose of the fold in Figure 4.18 is due to the attitude of the photographed surface with respect to the fold axis.

Other parasitic  $F_4$  folds occur as crenulations in some micaceous amphibolites in the nose of the antiform. Locally, in the nose of the  $F_4$  antiform, small dome and basin (Type I, Ramsay, 1967) interference patterns are formed by folding of  $F_3$  folds (Figure 4.19). In the south no mesoscopic folds of definite  $F_4$  age were recognized.

#### 4.8 FAULTING AND MAFIC DYKE EMPLACEMENT

Two major fault systems transect the megascopic fold patterns into a series of rhombohedral to rectangular blocks several kilometres across (Figure 4.1). Although the two fault systems (a NW-SE trending set and a NE-SW trending set) appear to be a conjugate set, there is ample evidence supporting the theory that the NW-SE faults represent a period of faulting prior to the development of the NE-SW trending faults.

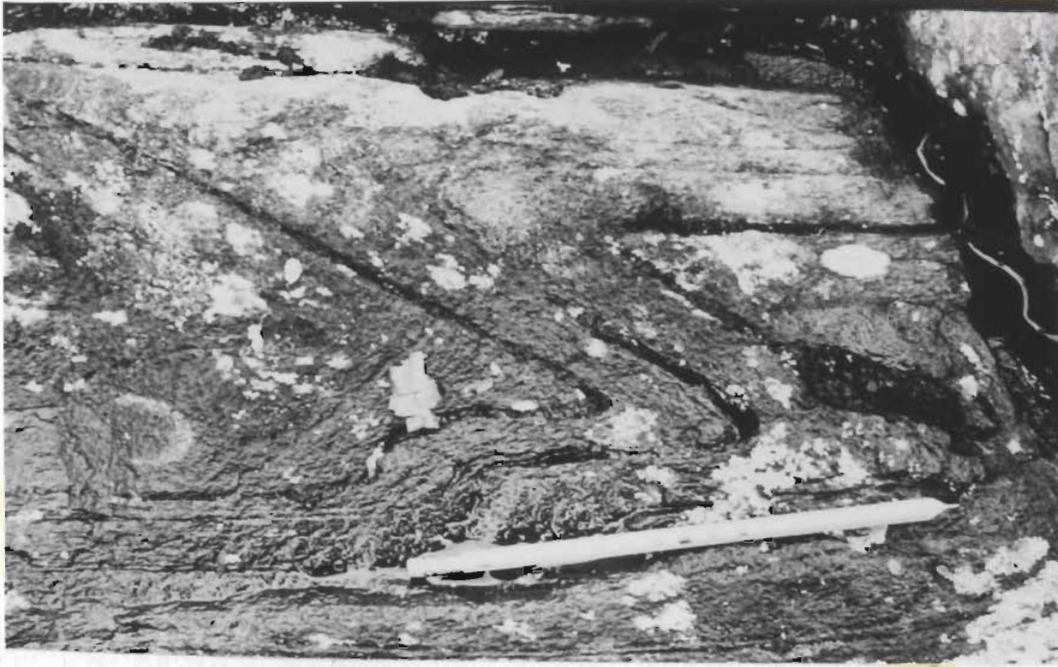


FIGURE 4.18: Mesoscopic  $F_4$  fold on eastern limb of the megascopic  $F_4$  antiform in the north.



FIGURE 4.19: Small scale elliptical dome and basin interference patterns developed in the nose of the  $F_4$  antiform.

Only faults of regional extent are included in the discussion of orientation of principle tectonic stresses. The smaller faults are considered to be of similar age, but their orientations are probably largely controlled by the attitude of the folded layering (DeSitter, 1958).

#### 4.8.1 NW-SE Trending Faults

Four major NW-SE faults are seen to transect the thesis area (Figure 4.1). The faults are near vertical in attitude (Figure 4.20) and appear to have a large strike-slip component. The geological boundaries cut by the faults are consistently offset with a sinistral sense of movement. The two large diabase dykes in the north area trend subparallel to the NW-SE set of faults, and the faults may have exerted some control on the emplacement of these mafic dykes. Shearing of the dyke-country rock margins indicates that renewed movement at least along the faults was nearly horizontal. While the total amount of movement along the faults cannot be determined, the offset  $F_3$  synform in the north suggests a minimum of 2 km sinistral strike-slip movement. The middle fault which separates the Hunt River Belt into two geographical components, probably has a much greater total displacement, as there can be no structural or lithological correlation across the fault within the confines of the map area.

The fault zones are generally quite narrow and are commonly characterized by very coarse pegmatites. In the amphibolites of the Hunt River Belt only one outcrop suffered appreciable brecciation a few metres away from the fault. Elsewhere, the layering in the country rock was reoriented by drag folds so that near the fault the layering



FIGURE 4.20: Photograph of exposure of large fault which cuts  $F_3$  synform in the northern part of the Hunt River Belt.

is sub-parallel to the plane of the fault. In some areas the quartz-feldspathic gneisses appear to have behaved in a ductile manner so that the deformation along the fault zones approached shear belt deformation as described by Ramsay and Graham (1970).

#### 4.8.2 NE-SW Trending Faults

In Figure 4.1 the NE-SW trending faults clearly offset the NW-SE faults with a dextral strike-slip sense of displacement. In the south splay faults are developed obliquely to the main NE-SW direction. Figure 4.21 is a composite diagram showing the orientations and relative sense of displacement inferred from offset geological features observed in the field.

The NE-SW fault system has also served as structural control for diabase dyke emplacement. In the north area a dyke emplaced along a NE-SW fault clearly cross-cuts dykes which are parallel to the NW-SE fault system. The NE-SW dykes contrast with the older set of NW-SE dykes in that they do not show associated deformational features, nor are they associated with ductile deformation of the quartz-feldspathic gneisses.

#### 4.9 POST-D<sub>3</sub> METAMORPHISM

This discussion is concerned with metamorphic conditions associated with the D<sub>4</sub> phase of deformation as well as the subsequent faulting. It is necessary to group these events together because many of the mineralogical changes which occurred during these last two tectonic episodes cannot, on microstructural criteria, be correlated specifically with D<sub>4</sub>. Most of the mineralogical changes involved

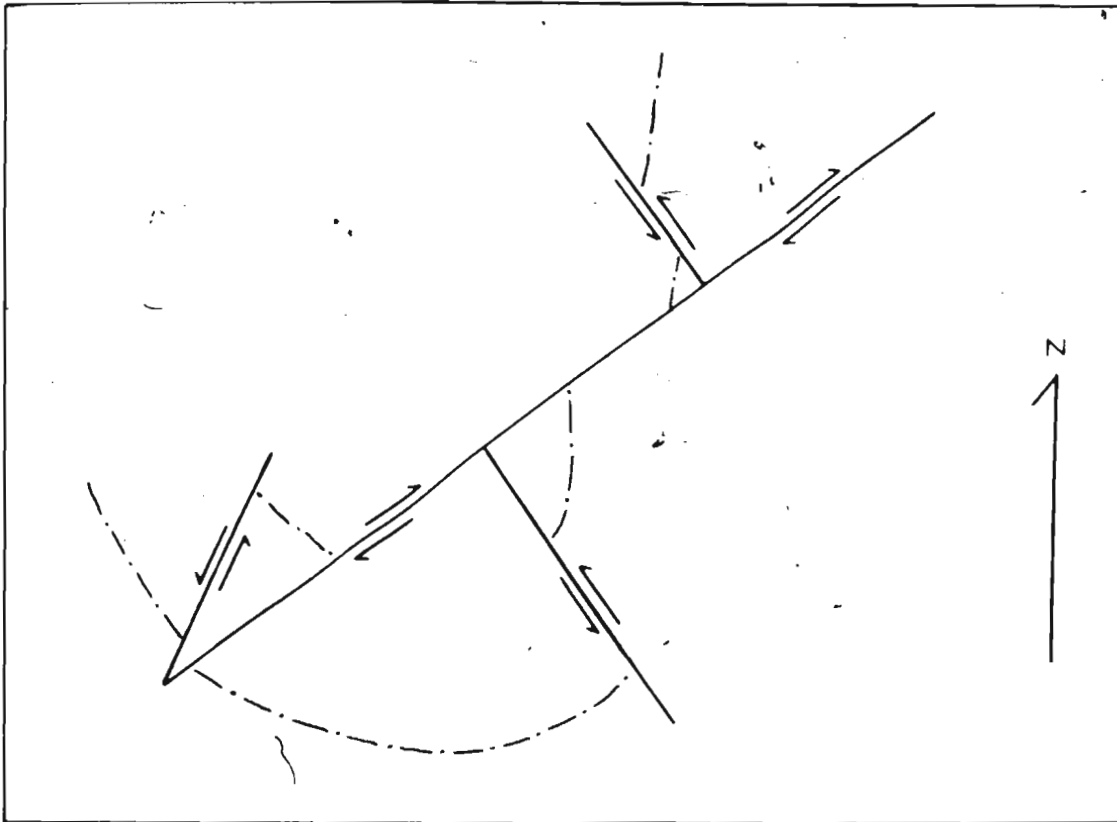


FIGURE 4.21: Schematic representation of the major fault orientations in the thesis area with their relative sense of displacement. The dotted line shows how a simple fold may be complexly dissected by late stage faulting.

retrogressive alteration of plagioclase, hornblende and biotite.

The  $F_4$  folding, open and upright in style, consists of megascopic, moderately plunging folds with common co-axial mesoscopic parasitic folds. Nowhere, either in the field or in thin section, was there evidence of a penetrative  $D_4$  fabric cross-cutting folded  $F_3$  or  $F_2$  linear and planar structural elements. The intensity of  $F_4$  folding appears to be stronger in the northern area (Figure 4.1). It may be significant that biotite as an alteration product of hornblende and garnet was found in thin sections only from the northern area. Studies of thin sections also revealed more widespread saussuritization of the plagioclases in the amphibolite schists and the quartzofeldspathic gneisses from the southern area. These mineralogical changes are representative of greenschist facies metamorphism, as the  $D_4$  tectonic environment did not lend itself to extensive recrystallization of pre-existing mineral components.

Chlorite and epidote which are also typical of greenschist facies metamorphism are widespread alteration minerals as well. Epidote is a common alteration product of biotite, hornblende and allanite. It is also commonly found along small fractures paralleling the major fault systems. Chlorite is always found as an alteration product of biotite, including both primary and secondary biotite.

As mentioned in Section 4.6.5, the changing styles of deformation episodes are interpreted to be the result of varying stages of crustal uplift. Petrographic studies show that the rocks in the thesis area were subjected to amphibolite facies metamorphism from  $D_1$  to  $D_3$ . During  $D_4$ , however, very shallow level deformation occurred,

followed closely by brittle faulting. Mineralogical evidence shows that the metamorphic conditions accompanying  $D_4$  were at the greenschist facies grade.

CHAPTER 5  
DISCUSSION AND SUMMARY

## 5.1 DISCUSSION

It is interesting to evaluate the results of this study in the southern Nain Province in conjunction with recent research near Saglek, Labrador in the northern part of the Nain Province, and to see how certain geological elements of the Labrador rocks fit into adjacent Archean crustal blocks and surrounding Precambrian mobile belts.

The Archean block that extends through south-central Greenland is actually an extension of the Nain Province, and together they form a major portion of the North Atlantic Craton (Figure 1.1). In southwestern Greenland radiometric dating shows that the gneissic terrain becomes progressively younger when traced from the north to the south (Bridgwater et al., 1973c). McGregor's (1973) studies also show that the north is composed of old rocks and this is substantiated by radiometric dating by Moorbath et al. (1972, 1973), and Pankhurst et al. (1973).

Interestingly enough, the Superior Province of Archean age, to the west, although thought to be generally younger in age than the North Atlantic Craton (Windley, 1973), is comprised of a series of east-west trending linear belts which also become younger towards the south (Goodwin, 1972; Goodwin and West, 1974). While radiometric dating of rocks along the Labrador seaboard has just begun, results so far point to a similar trend of rocks becoming younger to the south. Hurst et al. (1975) recorded a Rb/Sr age of  $\approx 3622$  m.y. for the Uivak gneisses at Saglek. Progressively younger ages have been found to the south; 3600 m.y. at Hebron (Barton, 1975b) and

3400 m.y. at Lost Channel (Hurst, 1974).

Two basic theories which might explain why the rocks become younger to the south in the Nain Province include:

1. the North Atlantic Craton developed by successive addition of younger rock to the south by lateral accretion, or
2. the present level of erosion transects a tilted stratigraphic section exposing older rocks from the lower portions of the stratigraphic sequence in the north, and younger rocks in the upper section of the stratigraphic sequence in the south.

Neither of these explanations, however, can account for the complexity of the lithological, structural and metamorphic relations in the Nain Province.

Based on the results of this thesis, an alternative theory explaining the crustal evolution of the North Atlantic Craton and its subsequent effects on bordering terrain is proposed.

Throughout the North Atlantic Craton there is evidence that a very early deformation caused an intercalation of gneisses and supracrustals of widely varying ages (Bridgwater et al., 1975; this thesis, Chapter 5, Section 4.3). This event is generally interpreted to have occurred in a horizontal tectonic regime in Greenland (Bridgwater et al., 1974) and resulted in considerable early crustal thickening. Therefore, subsequent deformations throughout Archean time affected a thick crustal block which was composed of chronologically mixed lithologies.

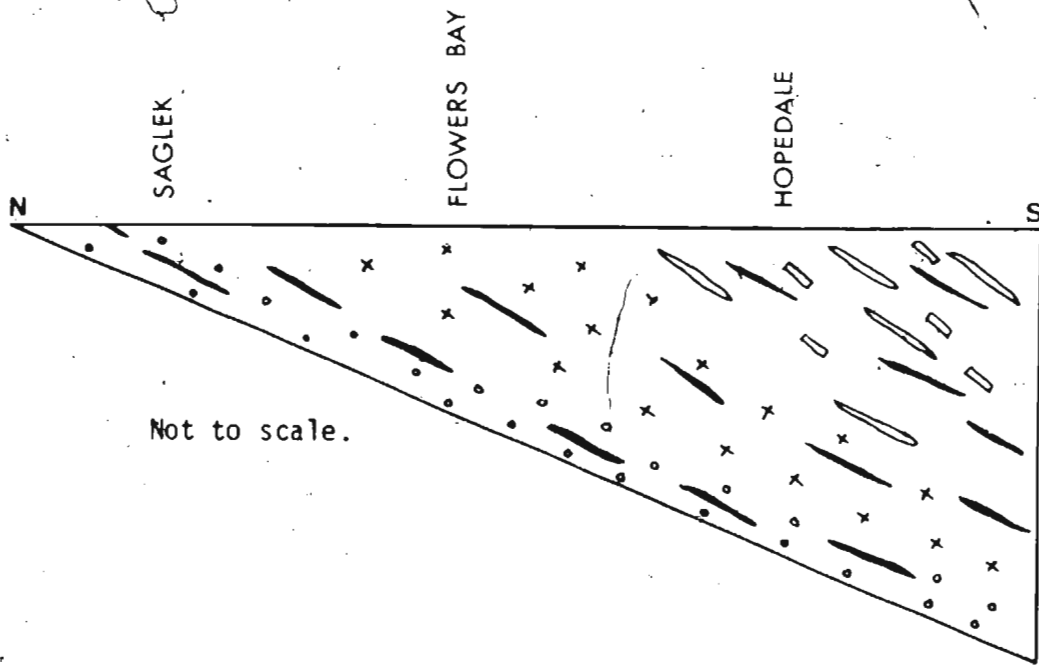
The question remains, however, that if rocks of old ages were distributed randomly (?) throughout the North Atlantic crustal block, then why are they seemingly preserved in only the northern area.

A study of the structural style and other geological features may provide some insight into this problem.

Once the horizontal tectonic event ceased, further deformations would deform the crustal block into a metamorphically horizontally layered section. In other words, the lower portions of the crust would be metamorphosed under granulite facies metamorphism, the middle portions of the crust would undergo considerable anatexis under amphibolite facies metamorphism, and the upper portions of the crust would possibly receive rising melted fractions forming extensive agmatites. J. Watson (1973) suggests a similar theoretical relationship in a polycyclic province of high grade gneisses. Successive deformations would also be accompanied by the deposition and intrusion of younger granitic fractions.

What is ultimately formed, then, is a crustal block comprised of a heterogeneous intercalation of rocks of varying ages. This crustal block is subsequently overprinted by a metamorphic differential megascopic layering. Deposition of younger rocks would also accompany subsequent deformational events and a true stratigraphic sequence of younger rocks would develop throughout geological time.

The North Atlantic Craton provides us with a cross-section through this very complex situation, with lower portions of the crust exposed in the north and upper portions of the crust exposed in the south (Figure 5.1). Thus, the overall structural style varies from north to south. The structures to the north in the North Atlantic Craton are characterized by a highly intricate, non-linear pattern (Windley, 1969b), and only in the south does the non-directional



Not to scale.

-  Old rocks intercalated with younger rocks during major horizontal tectonic regime to form thick crustal pile.
-  Successively younger supracrustal sequences deposited during deformation of crustal pile.
-  Granulite facies metamorphism near base of crust.
-  Anatexis of gneisses under amphibolite facies metamorphism.
-  Agmatites formed from rising leucosome from underlying anatectic melts.

FIGURE 5.1: Schematic cross-section through the North Atlantic Craton from north to south. The effects of folding are not shown.

structural style diminish and a linear trend (although still polydeformed) persist. This may be due to nothing more than heterogeneous deformation, but it could also reflect an original difference in competence between an older, thinner crust in the north and a somewhat younger, thicker crust in the south.

Extensive outcrops of granulite facies gneisses in the Labrador north also indicate that portions of the lowermost layers of the crust are exposed. Ryan (1974) reports extensive anatexis and migmatization of gneisses under amphibolite facies from Flowers Bay, and in the south near Hopedale (this thesis, Chapter 4, Section 4.6) agmatites are found.

All the evidence discussed thus far suggests that the Nain Province comprises a wedge-shaped section of continental crust which thins to the north (Figure 5.1). The presence of such a wedge-shaped crustal segment raises two questions. How in the first place did this particular geometrical configuration develop, and what geological implications can be predicted from such an obviously isostatic imbalance? The first question will not be dealt with at this time, although it is pointed out that there are many significant geological events (Engel et al., 1974) which could have contributed to such an imbalance.

The second question is quite intriguing. As represented in Figure 5.1, the wedge-shape is in imbalance with isostatic equilibrium and should, under natural physical laws, adjust itself. This adjustment would best be made if the southern end of the wedge floated upwards. Figure 5.2 is a diagrammatic representation which

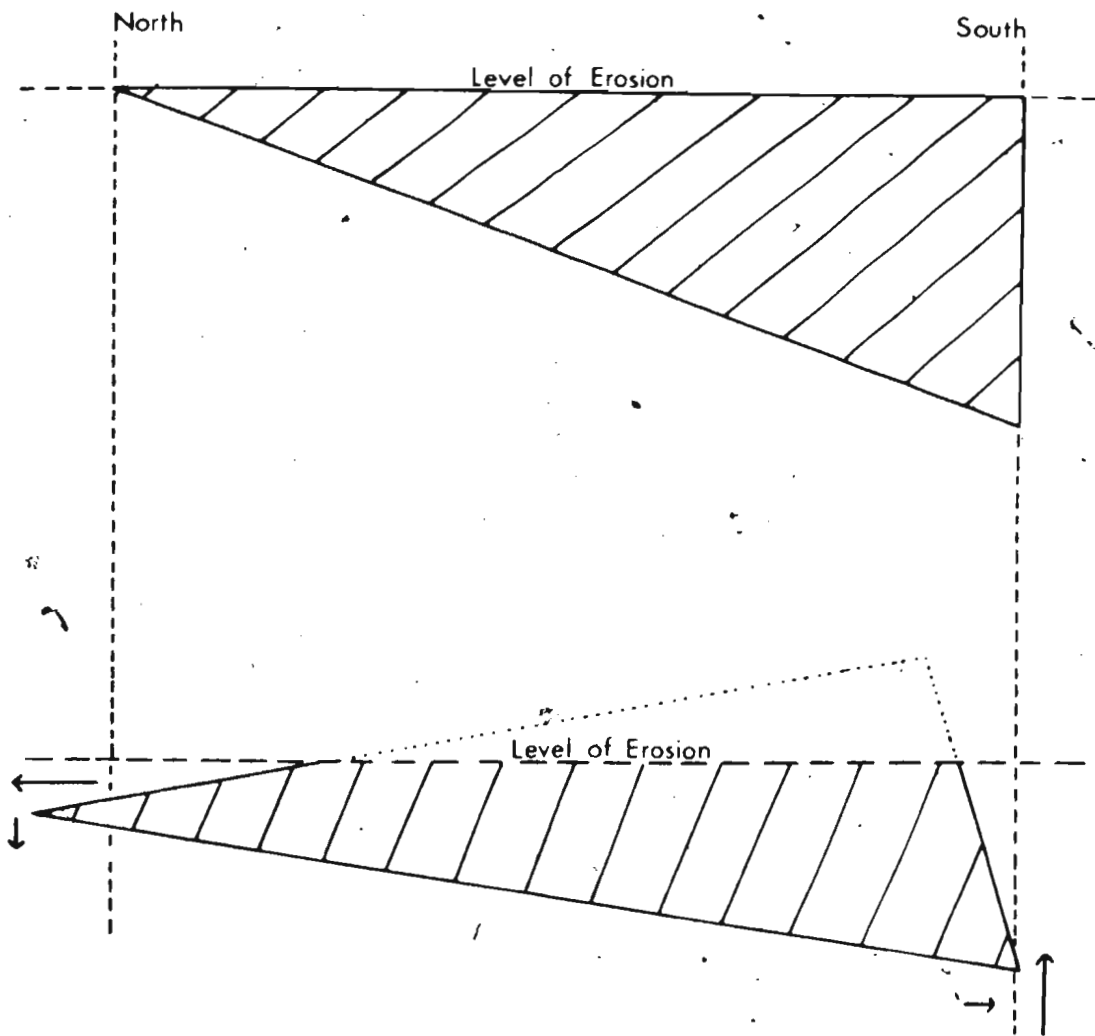


FIGURE 5.2: Diagrammatic representation of the distribution of forces resulting from the crustal wedge (shown in Figure 5.1) attaining isostatic equilibrium.

attempts to show the distribution of stress that would occur if such an imbalance were to equilibrate.

In the south (Figure 5.2) it is shown that the largest component of movement would be vertical, although some compression towards the south would be expected due to partial rotation of the crustal wedge. The geometrical dimensions of the wedge mean that if the southern end rises, then the northern end must move also. It is highly unlikely that this movement in the north would go down, into the mantle. It is more realistic to envision a predominantly horizontal movement to the north.

If the geological boundaries of the North Atlantic Craton are examined, it can be shown that the movements predicted above are actually evident in the field. The North Atlantic Craton is bounded in the north by the Nagssugtoqidian mobile belt. The Nagssugtoqidian is characterized by considerable crustal shortening, very limited igneous activity, and high pressure regional metamorphism. The main deformation boundary is sub-horizontal (Bridgwater et al., 1973b).

The North Atlantic Craton is bounded in the south by the Ketilidian mobile belt. The Ketilidian is characterized by widespread igneous activity. Evidence suggests that vertical as well as possible transcurrent movements are important, and there is little evidence of crustal shortening (Bridgwater et al., 1973b).

Figure 5.2 shows that isostatic rebound in the south would leave room for considerable plutonic emplacement, and the rising crust would also provide detrital material contributing to the Ketilidian

sedimentary rocks.

## 5.2 SUMMARY

In conclusion, petrological, geochemical, structural and metamorphic studies of the thesis area (located in the southern part of the Archean Nain Province) reveal the following characteristics. The area is basically made up of a predominantly mafic supracrustal belt (the Hunt River Belt) which has been highly deformed and infolded into a high grade quartzofeldspathic gneiss complex.

Lithologically, the Hunt River Belt comprises massive to schistose amphibolites, a series of ultramafic lenses, and minor meta-sediments. The amphibolites (meta-tholeiitic volcanics) include garnetiferous and pyroxeniferous varieties as well as thinly layered felsic-enriched varieties. When compared chemically to other basic volcanic rocks the Hunt River amphibolites are significantly lower in titanium and have lower K/Rb ratios than modern oceanic tholeiites. Modern island arc tholeiites have lower nickel and chromium contents than the Hunt River meta-volcanics. The amphibolites from the thesis area compare most favourably with meta-basalts associated with ultramafics in the lower parts of volcanic cycles from Archean greenstone belts.

The ultramafics include locally discordant units of hornblende schist, concordant layers of tremolite schist, and a series of lenses of serpentinite schist. In certain of the serpentinite lenses preserved hartzburgite patches retain coarse textures involving elongate olivine and interstitial enstatite. Microstructures, rock and

mineral chemical analyses all suggest that the textures may represent igneous harbitic textures. The ultramafics appear to have originated as a series of early intrusive sheets into a developing volcanic sequence.

Meta-sediments are represented by a variety of garnet-staurolite-cordierite-bearing schists, biotite-garnet rusty zones, and grey feldspar-biotite schists. The pelitic schist displays anomalously high nickel and chromium concentrations, similar to values found at Saglek in the northern Nain Province. It is suggested that the provenance contained a high proportion of ultramafic material which contributed detrital matter rich in nickel and chromium.

The deformational history of the thesis area is very complex. The first deformation event ( $D_1$ ) recognized on a regional scale involved intense thrusting and rotational shearing ( $k = 1$ ) which formed the dominant layering in the banded gneisses. The transposition and intercalation of quartzofeldspathic gneiss and schlieren of mafic material from the Hunt River Belt almost completely obliterated the pre- $D_1$  character of the rocks. Locally, in small zones of low intensity deformation, pre- $D_1$  diabase dykes retained their discordant character. The  $D_1$  phase of deformation reflects an intense period of deformation apparently associated with a megascopic scale sub-horizontal simple shear component. This is in agreement with theories postulating horizontal tectonism for early Archean crustal deformation of high grade gneiss terrains (Condie, 1972; Talbot, 1973; Bridgwater *et al.*, 1974).

The second major deformational event ( $D_2$ ) involved the intrusion of large sheets of trondhjemitic and granitic rock, followed by isoclinal

folding and the formation of a strong planar fabric. Bowes (1975) suggests that Archean gneisses in northwestern Britain developed a gneissic banding followed by progressive flattening of rather plastic deep crust against the sub-horizontal crust-mantle or lower crust-upper crust interface. This deep level flattening could possibly be correlated with  $D_2$ . In the thesis area a marked pure shear component of flattening ( $k = 0$ ) is indicated by the development of a well-defined schistosity, disc-shaped boudings of pegmatites lying at high angles to the main compressive stress, and disharmonic pygmatic folding of pegmatites which were oriented at a low angle to the main compressive stress.

Bowes (1975, author's abstract) suggests two further periods of crustal deformation, the first of which "deformed the flat-lying metamorphic foliation, and marks the initiation of the structural control of uprising gas and magma ... with pegmatites situated in the fold hinge zones." This agrees quite well with the heterogeneous character of the  $D_3$  phase of deformation during which time pegmatite developed in cores of the  $F_3$  synforms. Bowes continues to state that "crustal uplift towards the close of Archaean times ... is indicated by the successive development of upright open folds ... and little or no related mineral growth." This describes almost exactly the style and metamorphic character of the  $D_4$  phase of deformation in the thesis area.

The structural history, then, may be summarized as follows:

1. A highly active tectonic sub-horizontal subduction and crustal buildup ( $D_1$ ) was followed by a period of relatively acquiescent deep level plastic flattening ( $D_2$ ).

2. A final period of highly active tectonism ( $D_3$ ) resulted in an uplift of the rocks with associated upwelling of magma to shallow crustal levels where the tectonic activity died out with a period of low deformation folding ( $D_4$ ) and faulting.
3. Post tectonic diabase dykes intruded along major fault systems.

In the amphibolite schists and the quartzofeldspathic gneisses, the mineral assemblages which display microstructural evidence of equilibrium for each phase of deformation indicate that  $D_1$ ,  $D_2$  and  $D_3$  all occurred within the amphibolite facies of metamorphism.  $D_4$  and subsequent faulting occurred within the greenschist facies of metamorphism.

REFERENCES

## REFERENCES

- Anderson, L.S. and Friend, C. 1973. Structure of the Ravns Storo amphibolite belt in the Fiskenaasset region. Rapp. Gronlands geol. Unders. 51, pp. 37-40.
- Anhaeusser, C.R. 1973. The evolution of the early Precambrian crust of Southern Africa. Phil. Trans. R. Soc. Lond. A 273, pp. 359-388.
- \_\_\_\_\_, Mason, R., Viljoen, M.J. and Viljoen, R.P. 1969. A reappraisal of some aspects of Precambrian Shield geology. Bull. Geol. Soc. Am. 80, pp. 2175-2200.
- Baragar, W.R.A. 1966. Geochemistry of the Yellowknife volcanic rocks. Can. J. Earth Sci. 3, pp. 9-30.
- \_\_\_\_\_. 1968. Major-element geochemistry of the Noranda Volcanic Belt. Can. J. Earth Sci. 5, pp. 773-790.
- \_\_\_\_\_ and Goodwin, A.M. 1971. Andesites and Archean volcanism of the Canadian Shield. In: Andesite Conference, Proceedings, Oreg. Dept. Geol. Miner., Ind. Bull. 65, pp. 121-141.
- Barton, J.M. Jr. 1975a. The Mugford Group volcanics of Labrador: age, geochemistry, and tectonic setting. Can. J. Earth Sci. 12, pp. 1196-1208.
- \_\_\_\_\_. 1975b. Rb-Sr isotopic characteristics and chemistry of the 3.6 b.y. Hebron gneiss, Labrador. Earth Planet. Sci. Lett. 27, pp. 427-435.

Behr, H.J., Den Tex, E., DeWaard, D., Mehnert, K.R., Scharbert, H.G., Sobolev, S. St., Watznauer, A., Winkler, G.H.F., Wynne-Edwards, H.R., Zoubek, U. and Zwart, H.J. 1971. Granulites, results of a discussion. *Neues. Jb. Miner. Mh.* 1971, pp. 97-123.

Berg, J.H. 1974. Mineral assemblages in the contact aureole of the Hettasch intrusion and some P-T estimates for the emplacement of the Nain Complex, coastal Labrador. *Abstr., Geol. Assoc. Can., Prog., St. John's, Newfoundland.*

Binns, R.A. 1964. Zones of progressive regional metamorphism in the Willyama Complex, Broken Hill, N.S.W.. *J. Geol. Soc. Aust.* 11, pp. 283-320.

\_\_\_\_\_ 1965. The mineralogy of metamorphosed basic rocks from the Willyama Complex, Broken Hill district, New South Wales. Part 1: Hornblendes. *Miner. Mag.* 35, pp. 306-326.

\_\_\_\_\_ 1969. Ferromagnesian minerals in high grade metamorphic rock. *Spec. Publs. Geol. Soc. Aust.* 2, pp. 323-332.

Bowes, D.R. 1975. Archaean crustal history in northwestern Britain. *Unpubl. Author's Abstr., Dept. Geol., University of Glasgow, Scot., For: NATO conference "Early History of the Earth", University of Leicester, England, 1975.*

Bridgwater, D. 1970. Observations on the Precambrian rocks of Scandinavia and Labrador and their implications for the interpretation of the Precambrian of Greenland. *Rapp. Gronlands geol. Unders.* 28, pp. 43-47.

Bridgwater, D., Escher, A., Jackson, G.D., Taylor, F.C. and Windley, B.F.

1973a. Development of the Precambrian Shield in West Greenland, Labrador, and Baffin Island. *Am. Assoc. Petrol. Geol. Mem.* 19, pp. 99-116.

\_\_\_\_\_, Escher, A. and Watterson, J. 1973b. Tectonic displacements and thermal activity in two contrasting Proterozoic mobile belts from Greenland. *Phil. Trans. R. Soc. Lond.* A 273, pp. 513-533.

\_\_\_\_\_, Watson, J. and Windley, B.F. 1973c. The Archean of the North Atlantic region. *Phil. Trans. R. Soc. Lond.* A 273, pp. 493-512.

\_\_\_\_\_ and Fyfe, W.S. 1974. The pre-3b.y. crust: fact-fiction-fantasy. *Geoscience Can.* 3, pp. 7-11.

\_\_\_\_\_, McGregor, V.R. and Myers, J.S. 1974. A horizontal tectonic regime in the Archean of Greenland and its implications for early crustal thickening. *Precamb. Res.* 1, pp. 179-197.

\_\_\_\_\_, Collerson, K.D., Hurst, R.W. and Jesseau, C.W. 1975. Field characters of the early Precambrian rocks from Saglek, coast of Labrador. *Geol. Sur. Can. Paper* 75-1, Part A, pp. 287-296.

Carmichael, I.S.E., Turner, F.J. and Verhoogen, J. 1974. *Igneous Petrology*. McGraw-Hill.

Chatterjee, N.D. 1971. Phase equilibria in the Alpine metamorphic rocks of the Dora-Maira Massif, Western Italian Alps. *N. Jb. Miner. Abh.* 114, pp. 181-210.

- Clifford, P.M. and McNutt, R.H. 1971. Evolution of Mt. St. Joseph - an Archean volcano. *Can. J. Earth Sci.* 8, pp. 150-161.
- Collerson, K.D. 1974. Descriptive microstructural terminology for high-grade tectonites. *Geol. Mag.* 4, pp. 313-318.
- \_\_\_\_\_ and Ethridge, M.A. 1972. A contribution to the discussion of granulite terminology. *Nues. Jb. Miner.* 4, pp. 159-162.
- \_\_\_\_\_, Jesseau, C.W. and Bridgwater, D. 1976 (in press). Crustal development of the Archean gneiss complex: eastern Labrador. *In: Early History of the Earth*. Ed. B.F. Windley. Wiley, London.
- Condie, K.C. 1972. A plate tectonics evolutionary model of the South Pass Archean greenstone belt, southwestern Wyoming. 24th I.G.C., Section 1, pp. 104-112.
- \_\_\_\_\_ 1975. Trace element distributions in Archean greenstone belts. Author's Abst. NATO conference "Early History of the Earth", University of Leicester, England, 1975.
- Coward, M.P. 1973. Heterogeneous deformation in the development of the Laxfordian Complex of South Dist, Outer Hebrides. *J. Geol. Soc. Lond.* 129, pp. 137-160.
- Dawes, P.R. 1970. Bedrock geology of the nunataks and semi-nunataks in the Frederikshabs Isblink area of southern West Greenland. *Rapp. Gronlands geol. Unders.* 29, pp. 1-60.

- Deer, W.A., Howie, R.A. and Zussman, J. 1966. An Introduction to the Rock Forming Minerals. Longman Group Ltd., London, 528 p.
- DeSitter, L.U. 1958. Structural Geology. McGraw-Hill, New York.
- DeWaard, D. 1971. Country-rock of the anorthosite massif and anorthosite contacts in the Ford Harbour region. In: The Nain Anorthosite Project: Field Report. S.A. Morse (Ed.), Geol. Dept., U. Mass., Amherst, Mass. 9, pp. 15-56.
- Donaldson, C.H. 1974. Olivine crystal types in harrisitic rocks of the Rhum pluton and in Archean spinifex rocks. Geol. Soc. Amer. Bull. 85, pp. 1721-1726.
- Engel, A.E.J. and Engel C.G. 1962. Hornblendes formed during progressive metamorphism of amphibolite, northwest Adirondack Mountains, New York. Bull. Geol. Soc. Am. 73, pp. 1499-1514.
- \_\_\_\_\_, Engel, C.G. and Havens, R.G. 1965. Chemical characteristics of oceanic basalts and upper mantle. Geol. Soc. Amer. Bull. 76, pp. 719-734.
- \_\_\_\_\_, Itson, S.P., Engel, C.G., Stickney, D.M. and Cray, E.J.Jr. 1974. Crustal evolution and global tectonics: a petrogenetic view. Geol. Soc. Amer. Bull. 85, pp. 843-858.
- Escher, A. and Watterson, J. 1974. Stretching fabrics, folds and crustal shortening. Tectonophysics 22, pp. 223-231.

- Eskola, P. 1939. Die metamorphen gesteine. In: Die Entstehung der Geskin (T.F.W. Barth, C.W. Correns, P. Eskola), Springer, Berlin.
- Evans, B.W. and Trommsdorff, V. 1974. On elongate olivine of metamorphic origin. Geology 2, pp. 131-132.
- Fahrig, W.F. and Eade, K.E. 1968. The chemical evolution of the Canadian Shield. Can. J. Earth Sci. 5, pp. 1247 - 1258.
- Fleuty, M.J. 1964. The description of folds. Geol. Assoc. Proc. 75, pp. 461-492.
- Flinn, D. 1962. On folding during three-dimensional progressive deformation. Q. J. geol. Soc. Lond. 118, pp. 385-433.
- Glikson, A.Y. 1970. Geosynclinal evolution and geochemical affinities of early Precambrian systems. Tectonophysics 9, pp. 397-433.
- \_\_\_\_\_ 1971. Primitive Archean element distribution patterns: chemical evidence and geotectonic significance. Earth Planet. Sci. Lett. 12, pp. 309-320.
- \_\_\_\_\_ 1975. Volcanic stratigraphy greenstone suites. Author's Abst. NATO conference "Early History of the Earth", University of Leicester, England, 1975.
- Goodwin, A.M. 1972. The Superior Province. In: Variations in Tectonic Styles in Canada. Geo. Ass. Can. Spec. Paper 11, pp. 527-623.

- Goodwin, A.M. and Ridler, R.H. 1972. The Abitibi orogenic belt. In:  
Symposium on Basins and Geosynclines of the Canadian Shield.  
Geol. Surv. Can. Paper 70-40, A. J. Baer (Ed.), pp. 1-30.
- \_\_\_\_\_ and West, G.F. 1974. The Superior geotraverse project.  
Geoscience Canada 3, pp. 21-29.
- Greene, B.A. 1974. An outline of the geology of Labrador. Information  
Circular No. 15, Min. Develop. Div., Dept. of Mines and Energy,  
Prov. of Nfld., 64 p.
- Gunn, B.M. 1975. A comparison of modern and Archean sea-floor and  
island arc petrochemistry and alteration processes. Author's Abst.  
NATO conference "Early History of the Earth", University of  
Leicester, England, 1975.
- Hallberg, J.A. 1972. Geochemistry of Archean volcanic belts in the  
Eastern Goldfields region of Western Australia. J. Petrol. 13,  
pp. 45-46.
- \_\_\_\_\_ and Williams, D.A.C. 1972. Archean mafic and ultramafic rock  
associations in the Eastern Goldfields region, Western Australia.  
Earth Planet. Sci. Lett. 15, pp. 191-200.
- Heier, K.S. 1965. Metamorphism and the chemical differentiation of the  
crust. Geol. For. Stockh. Forh. 87, pp. 249-256.
- \_\_\_\_\_ 1973. Geochemistry of granulite facies rocks and problems of  
their origin. Phil. Trans. R. Soc. Lond. A 273, pp. 429-442.

Heier, K.S. and Adams, J.A.S. 1964. Concentration of radioactive elements in deep crustal material. *Geochim. Cosmochim Acta* 29, pp. 53-61.

\_\_\_\_\_ and Thoresen, K. 1971. Geochemistry of high grade metamorphic rocks, Lofoten-Vesteralen, north Norway. *Geochim. Cosmochim Acta* 35, pp. 89-99.

Hietanen, A. 1973. Co-existing cummingtonite and aluminous hornblende from garnet amphibolite, Boehls Bute area, Idaho, U.S.A. *Lithos* 6, pp. 261-264.

Higgins, A.K. 1968. The Tartoq Group on Nuna Qaqortoq and in the Iterdlak area, South-West Greenland. *Rapp. Gronlands geol. Unders.* 17, pp. 1-17.

\_\_\_\_\_ and Bondsen, E. 1966. A pre-Ketilidian supracrustal series ( the Tartoq Group) and its relations to Ketilidian supracrustals in the Ivigtut region, South-West Greenland. *Rapp. Gronlands geol. Unders.* 8, pp. 1-17.

Holland, J.J. and Lambert, R.St.J. 1972. Major element chemical composition of shields and the continental crust. *Geochim. Cosmochim Acta* 36, pp. 673-683.

Hubregtse, J.J.M.W. 1975. Volcanism in the western Superior Province in Manitoba. Author's Abst. NATO conference "Early History of the Earth", University of Leicester, England, 1975.

- Hunter, D.R. 1974. Crustal development in the Kaapvaal craton  
1. The Archaean. *Precambrian Research* 1, pp. 259-294.
- Hurst, R.W. 1974. The early Archean of coastal Labrador. In: *The Main Anorthosite Project: Field Report*. S.A. Morse (Ed.), Geol. Dept., U. Mass., Amherst, Mass. 13, pp. 29-32.
- \_\_\_\_\_, Bridgwater, D., Collerson, K.D. and Wetherill, G.W. 1975. Rb-Sr systematics in very early Archaean gneisses from Saglek Fiord, Labrador. *Earth Planet. Sci. Lett.* (in press).
- Irvine, T.N. and Baragar, W.R.A. 1971. A guide to the chemical classification of the common volcanic rocks. *Can. J. Earth Sci.* 8, pp. 523-548.
- Jakes, P. 1968. Retrogressive changes of granulite-facies rocks. - An example from the Bohemian massif. *Spec. Publs. Geol. Soc. Aust.* 2.
- \_\_\_\_\_, and White, A.J.R. 1970. K/Rb ratios of rocks from island arcs. *Geochim. Cosmochim. Acta* 34, pp. 849-856.
- Jensen, S.B. 1969. Field work in the Frederikshab district. *Rapp. Gronlands geol. Unders.* 19.
- Joubert, P. 1971. The regional tectonism of the gneisses of part of Namaqualand. *Chamber of Mines, Precamb. Res. Unit, Bull.* 10, U. of Cape Town, S.A., 220 p.
- Kalsbeek, F. and Leake, B.E. 1970. The chemistry and origin of some basement amphibolites between Ivigtut and Frederikshab, South-West Greenland. *Meddr. Gronland* 90, pp. 1-36.

- Kanisawa, S. 1968. Garnet-amphibolites at Yokokawa in the Abukuma metamorphic belt, Japan. *Cont. Mineral. Petrol.* 20, pp. 164-176.
- Keto, L. and Allaart, J.H. 1975. The pre-3760m.y. old supracrustal rocks of the Isua area with their main occurrence of quartz-banded ironstone. Author's Abst. NATO conference "Early History of the Earth", University of Leicester, England, 1975.
- Kranck, E.H. 1953. Bedrock geology of the seaboard of Labrador between Domino Run and Hopedale, Newfoundland. *Geol. Surv. Can. Bull.* 26.
- Kroner, A. 1971. The origin of the southern Namaqualand gneiss complex, South Africa, in the light of geochemical data. *Lithos* 4, pp. 325-344.
- Lambert, I.B. and Heier, K.S. 1968. Geochemical investigations of deep-seated rocks in the Australian Shield. *Lithos* 1, pp. 30-53.
- \_\_\_\_\_, Holland, J.G. and Chamberlain, V.E. 1975. The geochemistry of Archean rocks. Author's Abst. NATO conference "The Early History of the Earth", University of Leicester, England, 1975.
- MacDonald, G.A. and Katsura, T. 1964. Chemical composition of Hawaiian lavas. *J. Petrol.* 5, pp. 82-133.
- Matthes, S. 1971. Die ultramafischen hornfelse insbesondere ihre phasenpetrologie. *Fortschr. Mineralogie* 48, pp. 109-127.
- Matthews, D.W. 1967. Zoned ultrabasic bodies in the Lewisian of the Moine Nappe in Skye. *Scott. J. Geol.* 3, pp. 17-33.

- Maxwell, J.A. 1968. Rock and Mineral Analysis. Interscience Publ.
- Misar, Z. 1973. Precambrian ultramafic rocks south of Sermilk, Frederikshab District, South-West Greenland. Bull. Gronlands geol. Unders. 107.
- Moorbath, S., O'Nions, R.K. and Pankhurst, R.J. 1973. An early Archean age for the Isua iron-formation. Nature Phys. Sci. 245, pp. 138-139.
- \_\_\_\_\_, O'Nions, R.K. Pankhurst, R.J., Gale, N.H. and McGregor, V.R. 1972. Further rubidium-strontium age determinations of the very early Precambrian rocks of the Godthaab district, West Greenland. Nature Phys. Sci. 240, pp. 78-82.
- Moorhouse, W.W. 1959. The Study of Rocks in Thin Section. Harper and Row, New York, 514 p.
- Myers, J.S. 1973. Field evidence concerning the origin of early Precambrian gneisses and amphibolites in part of the Fiskenasset region. Rapp. Gronlands geol. Unders. 51, pp. 19-22.
- McGregor, V.R. 1973. The early Precambrian gneisses of the Godthaab district, West Greenland. Phil. Trans. R. Soc. Lond. A 273, pp. 348-358.
- \_\_\_\_\_. 1975. The earliest granites: evidence from the Godthaab district West Greenland. Author's Abst. NATO conference "Early History of the Earth", University of Leicester, England, 1975.

- Nesbitt, R.W. 1971. Skeletal crystal forms in the ultramafic rocks of the Yilgarn Block, Western Australia: evidence for an Archaean ultramafic liquid. *Spec. Publs. Geol. Soc. Aust.* 3, pp. 331-347.
- Oliver, R.L., Nesbitt, R.W., Hansen, D.M. and Franzen, N. 1972. Metamorphic olivine in ultramafic rocks from Western Australia. *Contrib. Mineral. and Petrol.* 36, pp. 335-342.
- Pankhurst, R.J., Moorbath, S. and McGregor, V.R. 1973. Late event in the geological evolution of the Godthab district, West Greenland. *Nature Phys. Sci.* 243, pp. 24-26.
- Park, R.G. 1969. Structural correlation in metamorphic belts. *Tectonophysics* 7, pp. 323-338.
- Park, C.F. and MacDiarmid, R.A. 1970. *Ore Deposits*. W.H. Freeman & Co., 522 p.
- Pearce, J.A. 1975. Basalt geochemistry used to investigate past tectonic environments on Cyprus. *Tectonophysics* 25, pp. 41-67.
- \_\_\_\_\_ and Cann, J.R. 1971. Ophiolite origin investigated by discriminant analysis using Ti, Zr and Y. *Earth Planet. Sci. Lett.* 12, pp. 339-349.
- \_\_\_\_\_ and Cann, J.R. 1973. Tectonic setting of basic volcanic rocks determined using trace element analyses. *Earth Planet. Sci. Lett.* 19, pp. 290-300.

Pyke, D.R., Naldrett, A.J. and Extrand, D.R. 1973. Archean ultramafic flows in Munro Township, Ontario. Bull. Geol. Soc. Amer. 84, pp. 955-978.

Ramberg, H. 1966. The Scandinavian Caledonides as studied by centrifuged dynamic models. Bull. geol. Inst. Univ. Upsula 18.

Ramsay, D.M. and Sturt, B.A. 1963. A study of fold styles, their association and symmetry relationships, from Soyoy, North Norway. Norsk. Geol. Tidsskr. 43, pp. 411- 430.

Ramsay, J.G. 1960. The deformation of early linear structures in areas of repeated folding. J. Geol. 68, pp. 75-93.

\_\_\_\_\_ 1967. Folding and Fracturing of Rocks. McGraw-Hill, New York, 568 p.

\_\_\_\_\_ and Graham, R.H. 1970. Strain variation in shear belts. Can. J. Earth Sci. 7, pp. 786-813.

Ridler, R.H. 1970. Relationship of mineralization to volcanic stratigraphy in the Kirkland-Larder Lakes area, Ontario. Geol. Assoc. Can. Proc. 21, pp. 33-42.

Rivalenti, G. 1975a. Geochemistry of metavolcanic amphibolites from South West Greenland. Author's Abst. NATO conference "The Early History of the Earth", University of Leicester, England, 1975.

\_\_\_\_\_ 1975b. Chemistry and differentiation of mafic dykes in an area near Fiskenaesset, West Greenland. Can. J. Earth Sci. 12, pp. 721-730.

- Rivalenti, G. and Rossi, A. 1972. The geology and petrology of the Precambrian rocks to the north-east of the Fjord Qagssit, Frederikshab district, South West Greenland. *Meddr. Gronland* 192, pp. 1-92.
- Robins, B. 1973. Crescumulate layering in a gabbroic body on Seiland, northern Norway. *Geol. Mag.* 109, pp. 533-542.
- Robinson, D. and Leake, B.E. 1975. Sedimentary and igneous trends on AFM diagrams. *Geol. Mag.* 112, pp. 303-305.
- Ryan, A.B. 1974. Metamorphic and Structural Investigation of the Hopedale Gneiss, Flowers Bay, Labrador. Unpubl. B.Sc. (Hon.) Thesis, Memorial University of Newfoundland, St. John's, Nfld., 189 p.
- Schrijver, K. 1973. Correlated changes in mineral assemblages and in rock habit and fabric across an orthopyroxene isograd, Grenville Province, Quebec. *Amer. J. Sci.* 273, pp. 171-186.
- Shaw, D.M. 1954. Trace elements in pelitic rocks, part 1: variations during metamorphism. *Bull. Geol. Soc. Am.* 65, pp. 1151-1166.
- \_\_\_\_\_ 1956. Geochemistry of pelitic rocks, part III: major elements and general geochemistry. *Bull. Geol. Soc. Am.* 67, pp. 919-934.
- \_\_\_\_\_, Reilly, G.A., Muysson, J.R., Pattenden, G.E. and Campbell, F.E. 1967. An estimate of the chemical composition of the Canadian Precambrian Shield. *Can. J. Earth Sci.* 4, pp. 829-853.

- Sighnolfi, G.P. 1971. Investigations into deep crustal levels: fractionation effects and geochemical trends related to high grade metamorphism. *Geochim. Cosmochim Acta* 35, pp. 1005-1021.
- Smith, T.E. and Longstaffe, F.J. 1974. Archean rocks of shoshonitic affinities at Bijou Point, northwestern Ontario. *Can. J. Earth Sci.* 11, pp. 1407-1413.
- Speer, J.A. 1975. The contact metamorphic aureole of the Kiglapait intrusion. In: The Nain Anorthosite Project: Field Report 1974, S.A. Morse (Ed.), Geol. Dept., U. Mass., Amherst, Mass. 17, pp. 16-26.
- Spry, A. 1969. *Metamorphic Textures*. Pergamon Press.
- Stockwell, C.H. 1963. Third report on structural provinces, orogenies, and time classification of rocks of the Canadian Shield. *Geol. Surv. Can. Paper* 63-17 (Part 2), pp. 125-131.
- \_\_\_\_\_ 1964. Fourth report on structural provinces, orogenies and time classification of rocks of the Canadian Precambrian Shield. *Geol. Surv. Can. Paper* 64-17 (Part 2), pp. 1-21.
- Sturt, B.A. and Harris, A.L. 1961. The metamorphic history of the Loch Tummel area, Perthshire, Scotland. *Lpool. March geol. J.* 2, pp. 689-711.
- Sutton, J. 1973. Some changes in continental structure since early Precambrian time. In: Implications of Continental Drift to the Earth Sciences. D.H. Tarling and S.K. Runicorn (Eds.), 2, pp. 1070-1080.

- Sutton, J. and Watson, J. 1951. Pre-Torrionian history of the Loch Torrion and Scourie areas of the northwest Highlands. Q. J. Geol. Soc. Lond. 106, pp. 241-296.
- Sutton, J.S. 1972. The Precambrian gneisses and supracrustal rocks of the western shore of Kaipokok Bay, Labrador, Newfoundland. Can. J. Earth Sci. 9, pp. 1677-1692.
- \_\_\_\_\_, Marten, B.E., Clark, A.M.S. and Knight, I. 1972. A correlation of the Precambrian supracrustal rocks of coastal Labrador and southwestern Greenland. Nature Phys. Sci. 238, pp. 122-123.
- Talbot, C.J. 1973. A plate tectonic model for the Archean crust. Phil. Trans. R. Soc. Lond. 273, pp. 413-427.
- Taylor, F.C. 1971. A revision of Precambrian structural provinces in northwestern Quebec and northern Labrador. Can. J. Earth Sci. 8, pp. 579-584.
- \_\_\_\_\_. 1972. Reconnaissance geology of a part of the Precambrian Shield, northeastern Quebec and northern Labrador, Part III. Geol. Surv. Can. Paper 71-48.
- Taylor, S.R. 1965. The application of trace element data to problems in petrology. Physics and Chemistry of the Earth. 6, pp. 133-213.
- Thayer, T.P. 1967. Chemical and structural relations of ultramafic and feldspathic rocks in Alpine intrusive complexes. In: Ultramafic and Related Rocks. P.J. Wyllie (Ed.), John Wiley & Sons, pp. 222-239.

- Trommsdorff, V. and Evans, B.W. 1972. Progressive metamorphism of antigorite schist in the Bergell tonalite aureole (Italy). *Amer. J. Sci.* 272, pp. 423-437.
- Turner, F.J. 1968. *Metamorphic Petrology - Mineralogical and Field Aspects*. McGraw-Hill Book Co., New York, 403 p.
- \_\_\_\_\_ and Verhoogen, J. 1960. *Igneous and Metamorphic Petrology*. McGraw-Hill Book Co., New York, 694 P.
- \_\_\_\_\_ and Weiss, L.E. 1963. *Structural Analysis of Metamorphic Tectonites*. McGraw-Hill Book Co., New York, 545 p.
- Upton, B.G.J. 1974. Basic dykes in the Nain-Kiglapait region. In: *The Nain Anorthosite Project. Field Report, 1973*. S.A. Morse (Ed.), Geol. Dept., U. Mass., Amherst, Mass. 13, pp. 133-137.
- Vernon, R.H. 1968. Microstructures of high-grade metamorphic rocks at Broken Hill, Australia. *J. Petrol.* 9, pp. 1-22.
- Viljoen, M.J. and Viljoen, R.P. 1969. Evidence for the existence of a mobile extrusive peridotitic magma from the Komati Formation of the Onverwacht Group. In: *Upper Mantle Project. Geol. Soc. South Africa Spec. Pub.* 2, pp. 87-112.
- Watson, J.V. 1973. Effects of reworking on high-grade gneiss complexes. *Phil. Trans. R. Soc. Lond. A* 273, pp. 443-455.
- Watterson, J. 1968. Homogeneous deformation of the gneisses of Vesterland, South-west Greenland. *Meddr. Gronland* 175, pp. 1-72.

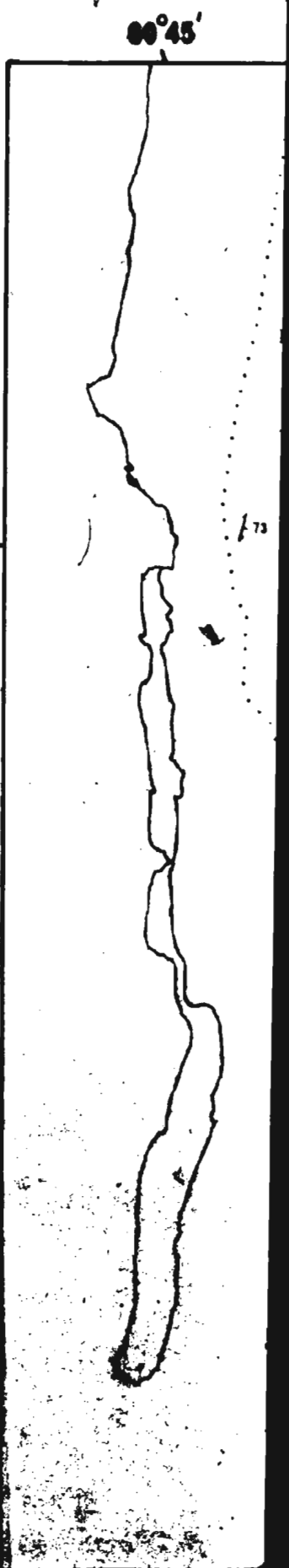
- Weiner, R.W. 1975. An Archean gabbro-anorthosite complex, Tessiuyakh Bay. In: The Nain Anorthosite Project: Field Report 1974. S.A.Morse (Ed.), Geol. Dept., U. Mass., Amherst, Mass. 17, pp. 7-15.
- Williams, D.A.C. 1972. Archaean ultramafic, mafic and associated rocks, Mt. Monger, Western Australia. J. Geol. Soc. Aust. 19, pp. 163-188.
- Williams, D.F. 1970. A criticism of the use of style in the study of deformed rocks. Bull. Geol. Soc. Am. 81, pp. 3283-3295.
- Windley, B.F. 1969a. Anorthosites of southern West Greenland. Amer. Assoc. Petrol. Geol. Mem. 12, pp. 899-915.
- \_\_\_\_\_ 1969b. Evolution of the early Precambrian basement complex of southern West Greenland. In: Age Relations in High-grade Metamorphic Terrains. Geol. Ass. Can. Spec. Paper No. 5, pp. 155-161.
- \_\_\_\_\_ 1972. Regional geology of early Precambrian high-grade metamorphic rocks in West Greenland, Part 1: Kagnaitsoq to Ameralik Fjord. Rapp. Gronlands geol. Unders. 46, pp. 1-46.
- \_\_\_\_\_ 1973. Crustal development in the Precambrian. Phil. Trans. R. Soc. Lond. A 273, pp. 321-341.
- \_\_\_\_\_ and Bridgwater, D. 1971. The evolution of Archaean low- and high-grade terrains. Spec. Publ. Geol. Soc. Aust. 3, pp. 33-46.
- \_\_\_\_\_, Hendriksen, N., Higgins, A.K., Bondsen, E. and Jensen, S.B. 1966. Some border relations between supracrustal and infracrustal rocks in South-West Greenland. Rapp. Gronlands geol. Unders. 8.

Winkler, H.G.F. 1965. Petrogenesis of Metamorphic Rocks. Springer  
Verlag, New York, 220 p.

\_\_\_\_\_, 1967. Petrogenesis of Metamorphic Rocks. Springer Verlag,  
New York, 237 p.

# LEGEND

-  Limit of outcrop
-  Post-tectonic mafic dyke
-  Outline of Hunt River Amphibolite Belt
-  Fault
-  Gneissic banding ( $S_1$ )
-  Axial plane of  $F_2$  fold
-  Plunge of  $F_2$  fold
-  Plunge of  $F_3$  fold
-  Mineral lineation parallel to plunge of  $F_2$  folds
-  Axial trace of megascopic  $F_2$  synform
-  Axial trace of megascopic  $F_2$  antiform
-  Axial plane of  $F_1$  fold
-  Plunge of  $F_1$  fold
-  Axial trace of megascopic  $F_1$  synform



Index

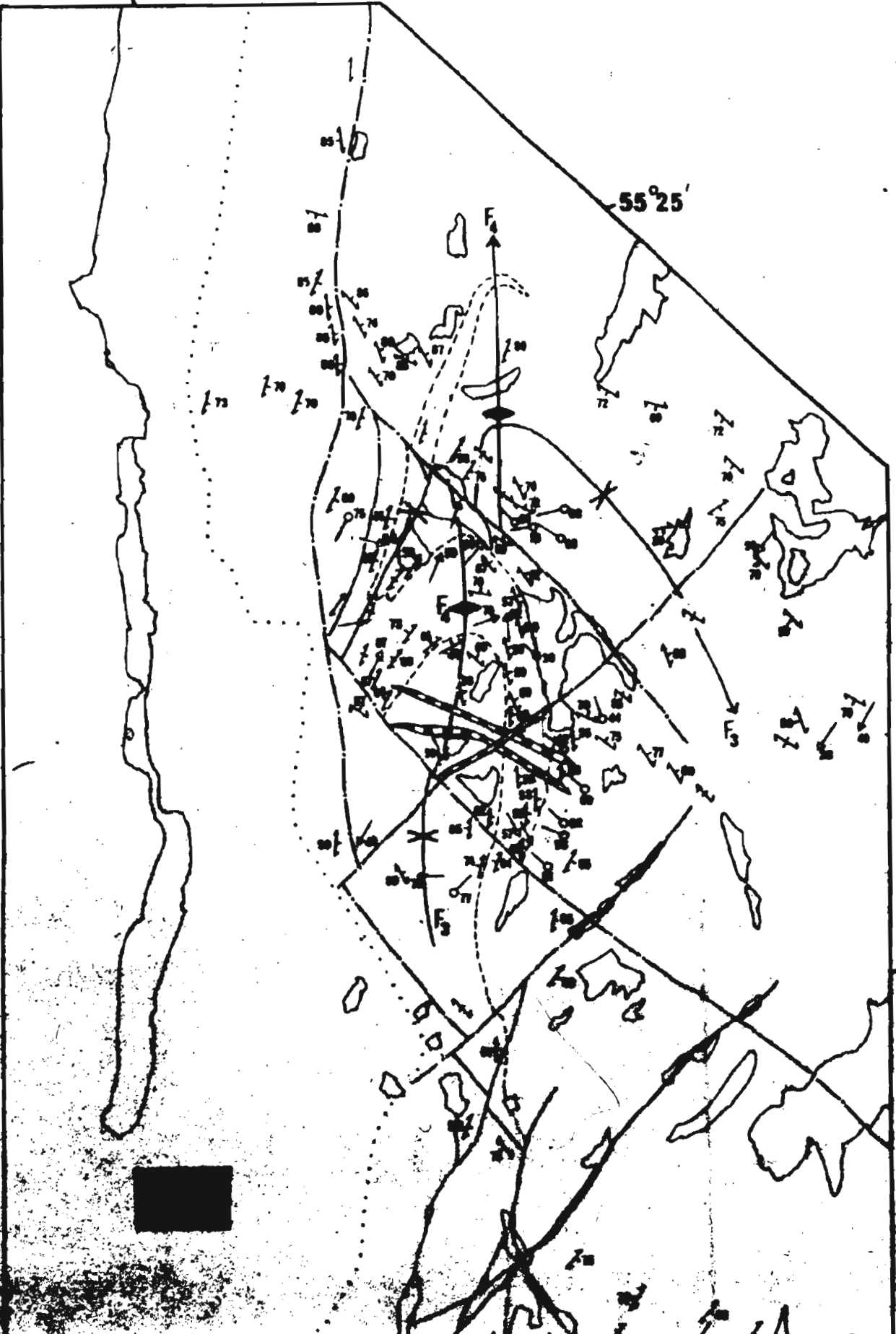


60°45'

55°25'

55°25'

F<sub>3</sub> folds



55°

-  Axial trace of megascopic  $F_3$  antiform
-  Axial plane of  $F_2$  fold
-  Plunge of  $F_2$  fold
-  Axial trace of megascopic  $F_5$  antiform

Index Map

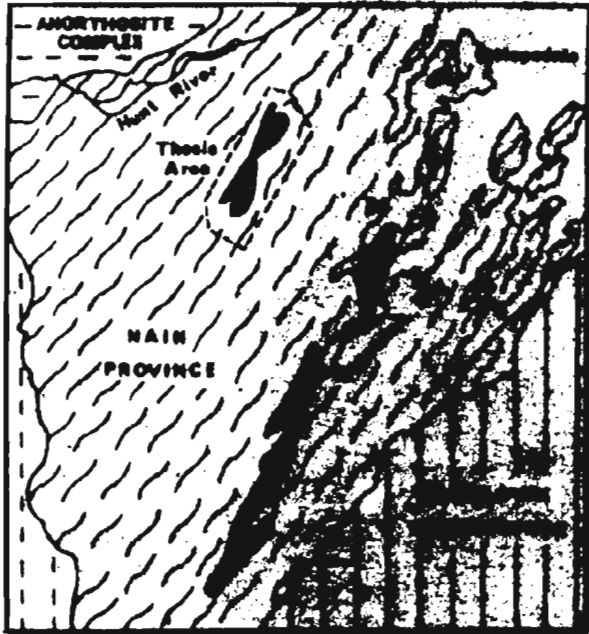
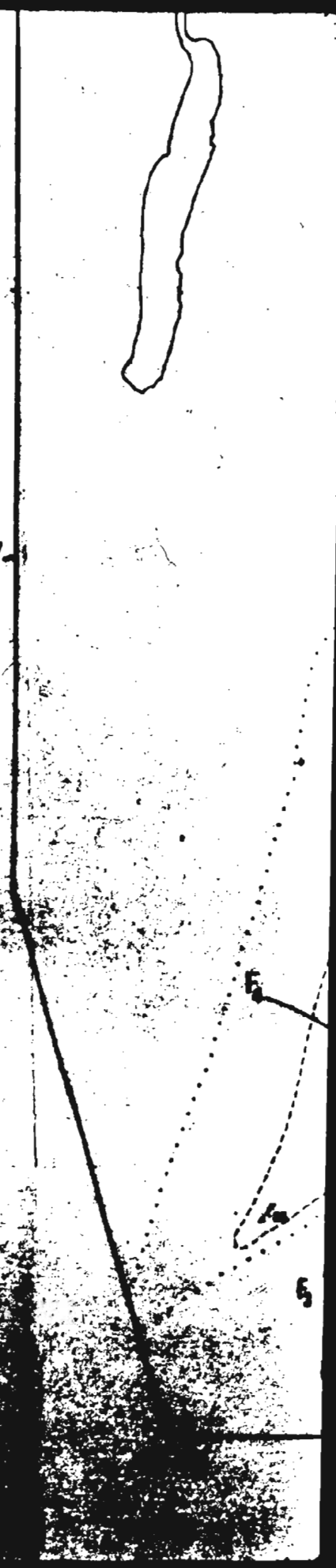
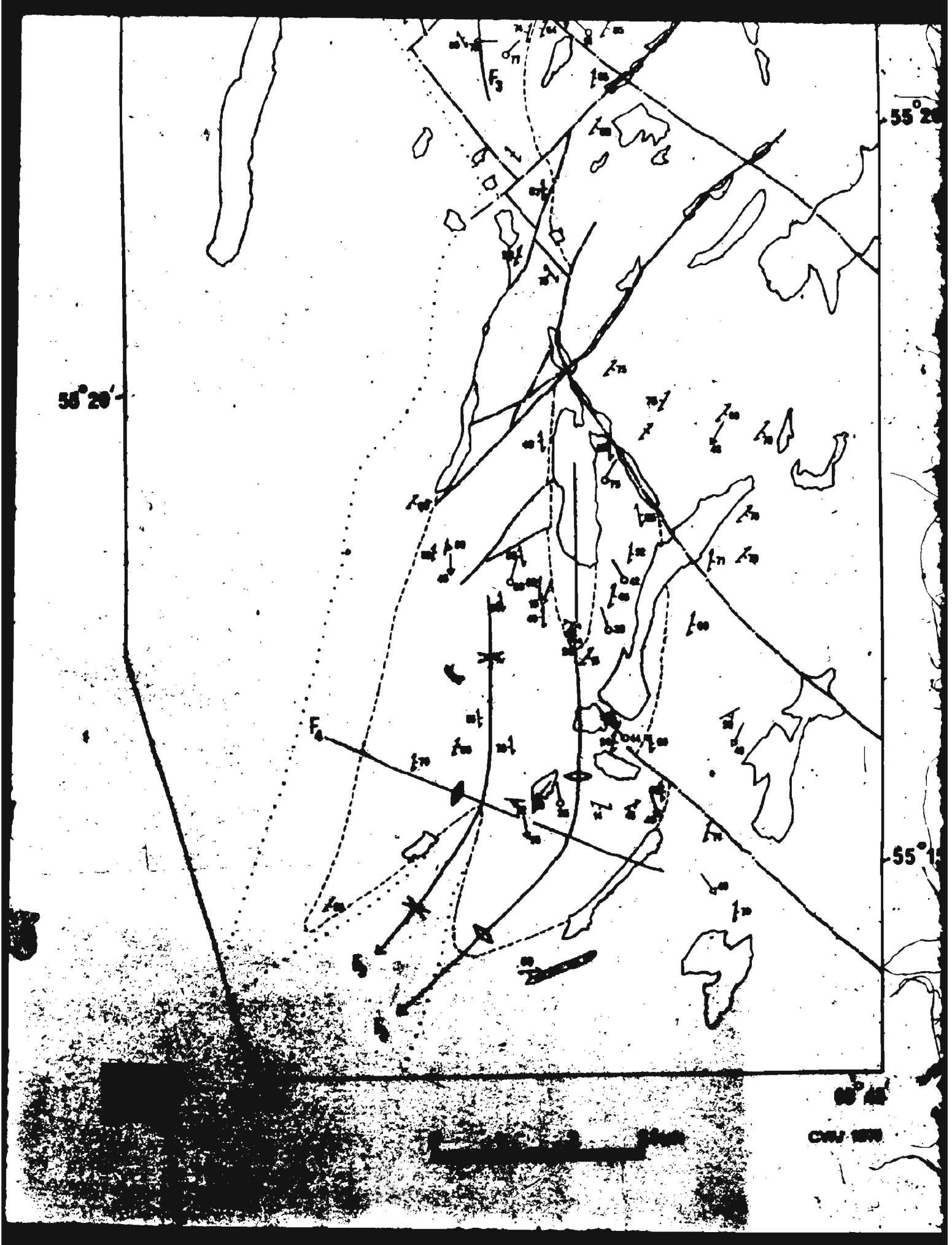


Figure 4.1 Structural Geology of the  
Hunt River - Northsibite Belt





# LEGEND

## Intrusives



DIABASE DYKES



GRANODIORITE



PEGMATITE



META-QUARTZMONZO-  
DIORITE

## Hunt River Belt



AMPHIBOLITE SCHIST



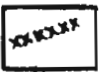
SERPENTINITE SCHIST



HORNBLENDITE SCHIST



TREMOLITE SCHIST



RUSTY ZONES



PELITIC SCHIST



GREY SCHIST

## Border Zone



VARIABLE QUARTZOFELDSPATHIC GNEISS



PINK MUSCOVITE GNEISS

## Quartzofeldspathic Gneiss Complex



AGMATITE



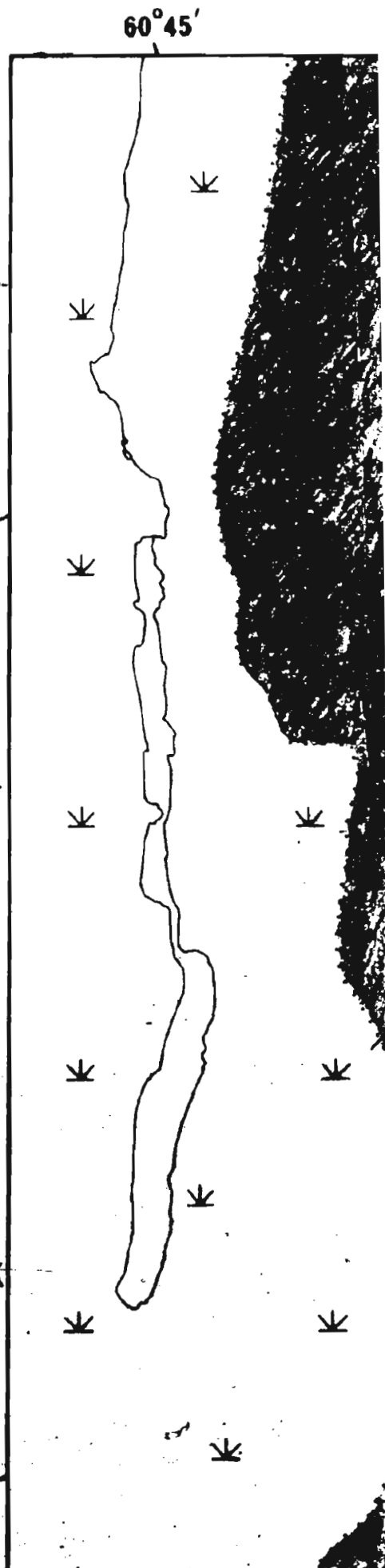
HOMOGENEOUS GNEISS



MIXED GNEISS



BANDED GNEISS



60° 45'

TE

ZMONZO

55° 25'

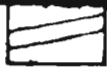
55° 25'

55° 20'

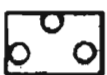
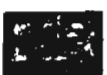
Complex

55° 20'

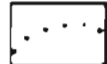
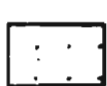
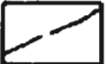
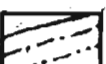


 PINK MUSCOVITE GNEISS

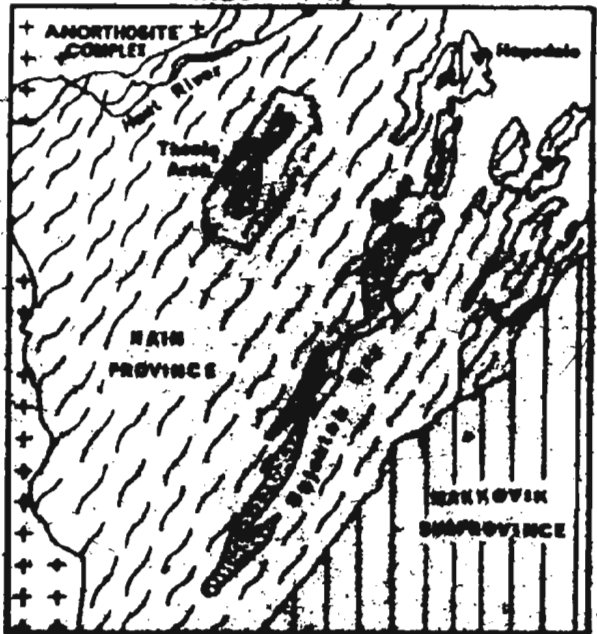
**Quartzofeldspathic Gneiss Complex**

-  AGMATITE
-  HOMOGENEOUS GNEISS
-  MIXED GNEISS
-  BANDED GNEISS
-  ANORTHOSITIC GABBRO
-  AMPHIBOLITE GNEISS

**Key**

-  LIMIT OF OUTCROP
-  SWAMPY LOWLANDS
-  GLACIAL DRIFT
-  FAULT
-  GEOLOGICAL BOUNDARY (defined, approximate, transitional)

**Index Map**



55° 20'

55° 15'

**Figure 2.2: Solid Geology of**

Complex

55°20'

55°20'

AL BOUNDARY  
(approximate,  
sitional)

55°15'

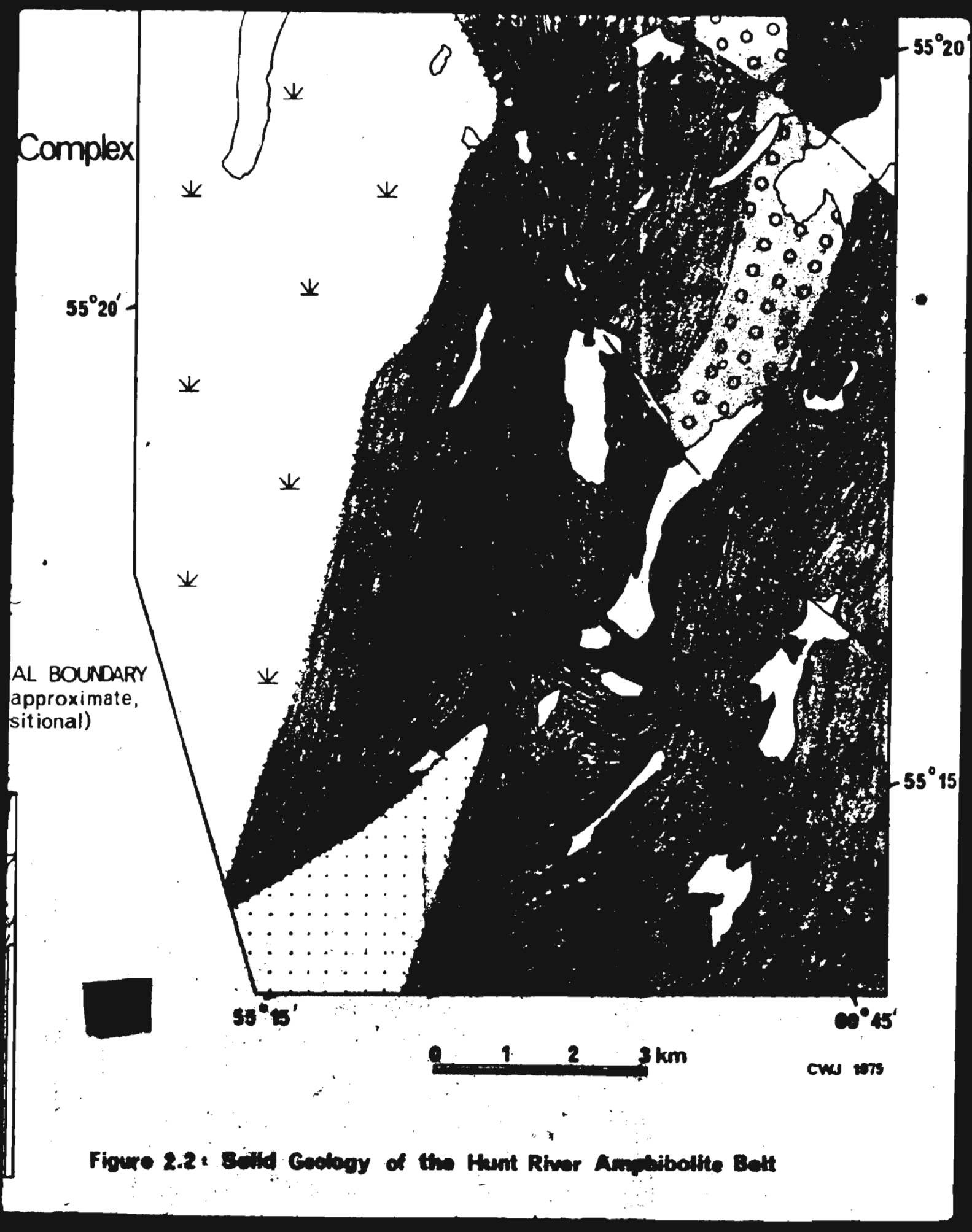
55°15'

00°45'

0 1 2 3 km

CWJ 1979

Figure 2.2: Solid Geology of the Hunt River Amphibolite Belt



33768

